

UNCLASSIFIED

AD NUMBER

AD510384

CLASSIFICATION CHANGES

TO: unclassified

FROM: confidential

LIMITATION CHANGES

TO:
Approved for public release, distribution
unlimited

FROM:
Distribution authorized to DoD only;
Administrative/Operational Use; Jun 1970.
Other requests shall be referred to
Director, Naval Research Laboratory,
Washington, DC 20390.

AUTHORITY

NRL ltr, 22 Aug 2002; NRL ltr, 22 Aug 2002

THIS PAGE IS UNCLASSIFIED

UNCLASSIFIED

| |
|--|
| |
| |
| |
| |
| AD NUMBER |
| AD510384 |
| CLASSIFICATION CHANGES |
| TO |
| confidential |
| FROM |
| secret |
| AUTHORITY |
| 30 Jun 1982, per document marking, DoDD 5200.10 |

THIS PAGE IS UNCLASSIFIED

SECRET

NRL Memorandum Report 2139

Copy No. **2** of **4** Copies

AD 510384

**Effects of Aircraft Roll
on Target Acquisition
Using Electro-Optical Sensors**
[Unclassified Title]

JOHN A. PAVCO

*Airborne Radar Branch
Radar Division*

June 1970



Aug 12 1970

NAVAL RESEARCH LABORATORY
Washington, D.C.

SECRET

Downgraded at 12 year intervals;
Not automatically declassified.

In addition to security requirements which apply to this document and must be met, each transmittal outside the Department of Defense must have prior approval of the Director, Naval Research Laboratory, Washington, D.C. 20390

Best Available Copy

SECRET

SECURITY

This document contains information affecting the national defense of the United States within the meaning of the Espionage Laws, Title 18, U.S.C., Sections 793 and 794. The transmission or revelation of its contents in any manner to an unauthorized person is prohibited by law.

SECRET

SECRET

ABSTRACT (S)

ABSTRACT

(S) The effects of aircraft roll on ground locked electro-optical sensors has been investigated with emphasis on the detection and acquisition phases of the mission. It was found that roll rates up to $5^{\circ}/\text{sec}$ were generally acceptable.

PROBLEM STATUS

This report completes the work in this phase of the problem.

AUTHORIZATION

NRL Problem 53D01-03.318
AIR A05-510-151/652-1/W11-63-000

SECRET

SECRET

TABLE OF CONTENTS

| | |
|--|-----|
| Abstract | i |
| Problem Status | i |
| Authorization | i |
| Table of Contents | ii |
| List of Figures | iii |
| Precis | vii |
| 1.0 Introduction | 1 |
| 2.0 Description of Tactics Considered | 2 |
| 3.0 The Effects of Motion on TV Resolution | 20 |
| 4.0 Derivation of Equations | 31 |
| 5.0 Sample Problem | 40 |
| 6.0 Results | 47 |
| 7.0 Conclusions | 70 |
| 8.0 Acknowledgements | 78 |
| 9.0 References | 79 |

SECRET

LIST OF FIGURES

| <u>Figure</u> | <u>Title</u> | <u>Page</u> |
|---------------|--|-------------|
| 1. | Target 1 is Detected During Tactic A (U) | 4 |
| 2. | Target 2 is Detected During Tactic A (U) | 5 |
| 3. | Target 3 is Detected During Tactic A (U) | 6 |
| 4. | Target 1 is Acquired During Tactic A (U) | 7 |
| 5. | Target 2 is Acquired During Tactic A (U) | 8 |
| 6. | Target 3 is Acquired During Tactic A (U) | 9 |
| 7. | Aircraft Roll Rate Versus Time (U) | 12 |
| 8. | Aircraft Roll Angle Versus Time (U) | 13 |
| 9. | Target 1 is Detected During Tactic C (U) | 14 |
| 10. | Target 2 is Detected During Tactic C (U) | 15 |
| 11. | Target 3 is Detected During Tactic C (U) | 16 |
| 12. | Target 1 is Acquired During Tactic C (U) | 17 |
| 13. | Target 2 is Acquired During Tactic C (U) | 18 |
| 14. | Target 3 is Acquired During Tactic C (U) | 19 |
| 15. | Modulation Transfer Function for Moving Image (\cos^2 x Distribution) (U) | 23 |
| 16. | Square Wave Response Curve for a TV System at 10^{-3} Foot Candles (S) | 24 |
| 17. | Resolution Degradation due to Linear Motion for LLTV System, 1/5 Second Integration Time (U) | 26 |
| 18. | Resolution as a Function of Motion with 1/5 Second Integration Time at 5% Aperture Response for LLLTV System (U) | 28 |

SECRET

LIST OF FIGURES (Cont'd)

| <u>Figure</u> | <u>Title</u> | <u>Page</u> |
|---------------|---|-------------|
| 19. | Apparent Lines on Target as a Function of Apparent Resolution and Resolvable Lines on Target (U) | 29 |
| 20. | Cumulative Probability of Detection as a Function of Number of Lines on Target (U) | 30 |
| 21. | Imaging System Geometry (U) | 32 |
| 22. | Tracking Geometry (U) | 33 |
| 23. | Number of Lines on Target (10' x 20' x 10') as a Function of Range Tactic A & B (U) | 41 |
| 24. | Target Motion Per Frame as a Function of Range Tactic A (U) | 43 |
| 25. | Conversion of Raster Lines to Resolvable Lines on Target for TV System Response of 590 Lines at 5% Contrast (U) | 44 |
| 26. | Apparent TV Resolution as a Function of Range Tactic A (U) | 45 |
| 27. | Apparent Lines on Target as a Function of Range Tactic A (U) | 46 |
| 28. | Cumulative Probability of Detection as a Function of Range Tactic A (S) | 48 |
| 29. | Target Motion Per Frame as a Function of Range Tactic B 1°/sec and 5°/sec Roll Rates (U) | 49 |
| 30. | Target Motion Per Frame as a Function of Range Tactic B 15°/sec and 45°/sec Roll Rates (U) | 50 |
| 31. | Apparent TV Resolution as a Function of Range Tactic B 1°/sec and 5°/sec Roll Rates (U) | 51 |
| 32. | Apparent TV Resolution as a Function of Range Tactic B 15°/sec and 45°/sec Roll Rates (U) | 52 |

LIST OF FIGURES (Cont'd)

| <u>Figure</u> | <u>Title</u> | <u>Page</u> |
|---------------|---|-------------|
| 33. | Apparent Lines on Target as a Function of Range Tactic B 1°/sec and 5°/sec Roll Rates (U) | 53 |
| 34. | Apparent Lines on Target as a Function of Range Tactic B 15°/sec and 45°/sec Roll Rates (U) | 54 |
| 35. | Cumulative Probability of Detection as a Function of Range Tactic B 1°/sec and 5°/sec Roll Rates (U) | 55 |
| 36. | Cumulative Probability of Detection as a Function of Range Tactic B 15°/sec and 45°/sec Roll Rates (U) | 56 |
| 37. | Number of Lines on Target (10' x 20' x 10') as a Function of Range Tactic C and D (U) | 57 |
| 38. | Target Motion Per Frame as a Function of Range Tactic C (U) | 58 |
| 39. | Apparent TV Resolution as a Function of Range Tactic C (U) | 59 |
| 40. | Apparent Lines on Target as a Function of Range Tactic C (U) | 60 |
| 41. | Cumulative Probability of Detection as a Function of Range Tactic C (U) | 61 |
| 42. | Target Motion Per Frame as a Function of Range Tactic D 1°/sec and 5°/sec Roll Rates (U) | 62 |
| 43. | Target Motion Per Frame as a Function of Range Tactic D 15°/sec and 45°/sec Roll Rates (U) | 63 |
| 44. | Apparent TV Resolution as a Function of Range Tactic D 1°/sec and 5°/sec Roll Rates (U) | 64 |
| 45. | Apparent TV Resolution as a Function of Range Tactic D 15°/sec and 45°/sec Roll Rates (U) | 65 |

SECRET

LIST OF FIGURES (Cont'd)

| <u>Figure</u> | <u>Title</u> | <u>Page</u> |
|---------------|---|-------------|
| 46. | Apparent Lines on Target as a Function of Range Tactic D 1°/sec and 5°/sec Roll Rates (U) | 66 |
| 47. | Apparent Lines on Target as a Function of Range Tactic D 15°/sec and 45°/sec Roll Rates (U) | 67 |
| 48. | Cumulative Probability of Detection as a Function of Range Tactic D (U) | 68 |
| 49. | Cumulative Probability of Detection as a Function of Range Tactic D (U) | 69 |
| 50. | Resolution Lines on Target as a Function of Range Tactic C and D (U) | 73 |
| 51. | Apparent IR Resolution as a Function of Range Tactic C and D (U) | 74 |
| 52. | Apparent Lines on Target as a Function of Range Tactic C and D (FLIR Sensor) (U) | 75 |
| 53. | Cumulative Probability of Detection as a Function of Range Ground Lock Mode, FLIR Sensor (U) | 76 |

SECRET

PRECIS

SUBJECT: Effects of Aircraft Roll on Target Acquisition Using
Electro-Optical Sensors

Background:

(S) The Naval Research Laboratory is participating in the Trail Roads Interdiction Multi Sensor (TRIM) program in which the night attack capabilities of the A-6A Intruder Aircraft are enhanced with electro-optical sensors. Previous experience being applied to this program is NRL's past contributions to the development of the F-4B, F-8U, F-2A, and F-111 weapon systems.

Findings:

(S) This report is specifically concerned with the effects of aircraft roll on ground locked electro-optical sensors during the target detection and acquisition phases of the mission. The analysis shows that for a low light level television (LLTV) system, moderate roll rates up to $5^{\circ}/\text{sec}$ are generally acceptable. Rates of 15 to $45^{\circ}/\text{sec}$ tend to make target detection and acquisition extremely difficult if not impossible. The resolution degradation due to roll is negligible for the forward looking infrared (FLIR) system.

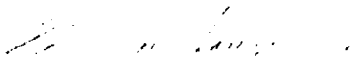
R & D Implications:

(U) Translational and rolling motions of an aircraft tend to generate image smear in a LLTV system. This is due to inability of the system to reduce image retention from one frame to the next as a result of phosphor persistence. Investigation of techniques to reduce image retention should be conducted.

SECRET

Recommended Action:

(S) In view of the finding that roll rates in excess of 5°/sec tend to produce unacceptable ILLTV presentations, it is recommended that tactics be developed to reduce aircraft roll during the target designation and acquisition phases of the TRIM mission.


Clair M. Loughmiller
Head, Tactical Analysis
Section

SECRET

1.0 INTRODUCTION

(C) The Navy, in its Trail Roads Interdiction Multi-Sensor (TRIM) program, is enhancing the night attack capabilities of the A-6A Intruder aircraft with electro-optical sensors such as Forward Looking Infrared (FLIR) and Low Light Level Television (LLLTV). These electro-optical sensors will be used first in target detection and acquisition phases of a mission. In these phases, the bombardier/navigator (B/N) has to positively detect and acquire the target of interest while the aircraft is maneuvering to follow a road or waterway. During these maneuvers, the aircraft undergoes a rolling motion which tends to degrade the resolution of the electro-optical system, thereby reducing the B/N's ability to acquire the target. Therefore, it was necessary to analyze the effects of roll on target acquisition to determine if the electro-optical sensors should be roll stabilized.

(C) This report presents a rough analytical calculation comparing the performances of two systems:

System 1 - ground-lock stabilized and roll stabilized.

System 2 - ground-lock stabilized but not roll stabilized.

In these systems the B/N has the ability to lock his electro-optical sensor on a point on the ground while he is searching for a target. System 2 is currently scheduled for installation and use in the A-6A TRIM aircraft.

(C) Only the acquisition phase is considered in this analysis since the effects of aircraft roll will be most pronounced during this phase. Once the target has been acquired and the tracking phase initiated, the B/N should have enough cues to mentally filter out the blurring effects caused by roll.

SECRET

Detection and acquisition, as used in this analysis, are defined as follows:

Detection - The B/N first becomes aware of an image on his CRT display. Although unable to identify the image, he suspects the image might be a target of interest. When the target occupies five lines of resolution, a detection is assumed to occur.*

Acquisition - The B/N definitely identifies the image as a target of interest. When the target occupies eight lines of resolution an acquisition is assumed to occur. *

Typical parameters describing the aircraft motion are given in Table 1.

Table 1 (U)

Parameters Describing Aircraft Motion

Aircraft Velocity - 350 Knots

Aircraft Altitude - 3000 Feet

| <u>Roll</u> | <u>Roll Rate (deg/sec)</u> | <u>Roll Angle (deg)</u> |
|-------------|----------------------------|-------------------------|
| Mild | 1 | 1 |
| General | 5 | 5 |
| Severe | 15 | 15 |
| Extreme | 45 | 45 |

2.0 DESCRIPTION OF TACTICS CONSIDERED

(C) In a typical TRIM mission, the aircraft will be following a road or waterway in search of a target. When the B/N detects something that might be a target, he centers it on his display with his slewstick. The computer then calculates target position and points the tracking radar antenna to this position. The point on the ground within the 1° beam width of the radar that gives the highest return, will then be tracked by the radar and the electro-optical sensors.

* The justification for these assumptions is given in Section 4.

SECRET

The B/N then tries to acquire the target with the electro-optical sensors in the ground-locked mode.

(U) The following assumptions are made to simplify the analysis:

1. The aircraft will fly at a constant altitude and velocity.
2. The roll rate remains constant during all rolling maneuvers.
3. The targets will be trucks which are 20 feet long, 10 feet high and 10 feet wide.
4. The targets will be motionless on roads directly along or parallel to the flight path.
5. The tracking radar will lock onto the target along or nearest to the flight path and this target will remain centered in the azimuth and elevation field of view (FOV) of the sensor. There will be no attempt to degrade system performance due to its inability to keep the target centered in the FOV of the sensor. Targets which are not along or nearest the flight path, will simulate the situation in which the tracking radar receives the highest return from a point on the ground other than the selected target.

(U) Four tactics will be used in this analysis. In Tactic A, the aircraft does not roll, thus simulating a roll-stabilized mode. Figures 1-6 represent various positions along the flight path during Tactic A. The targets are three trucks. The first target is on a road directly beneath the flight path, the second is on a road parallel to the flight path but offset by 250 feet, and the third is on a road parallel to the flight path but offset by 500 feet. The offsets were chosen

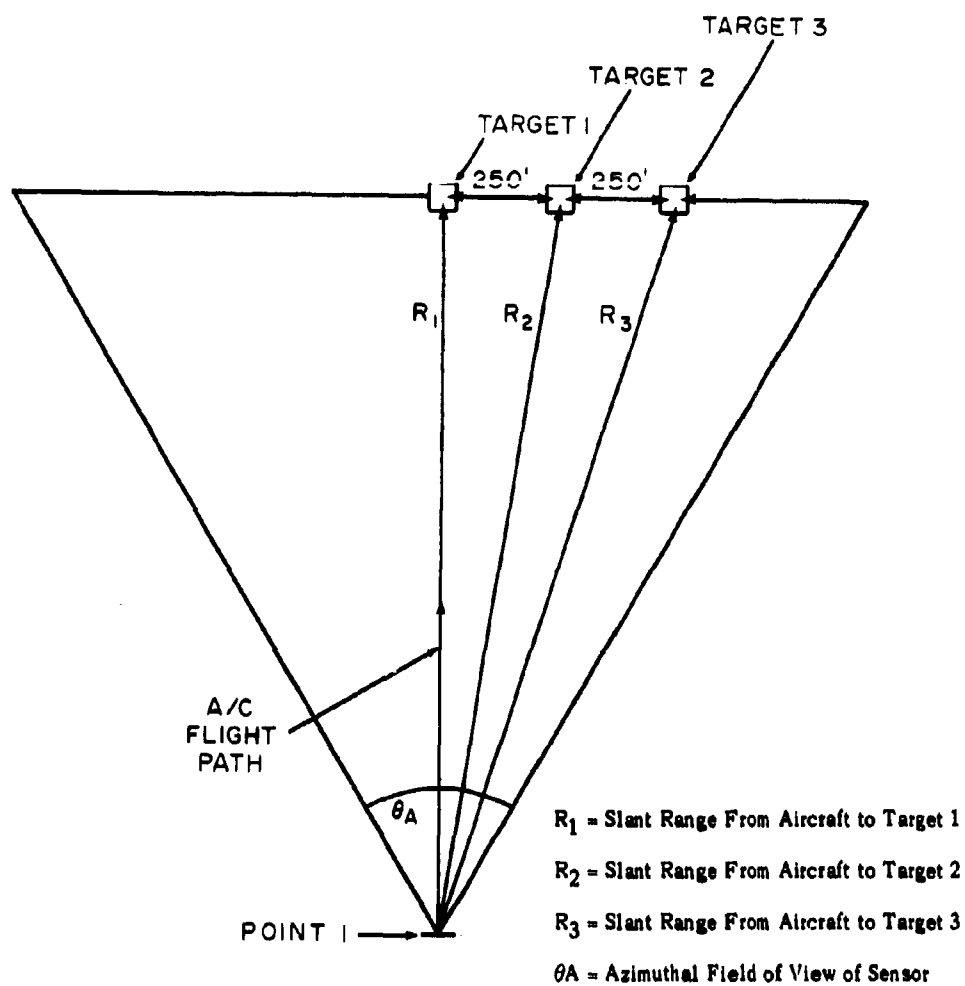


FIGURE 1 - TARGET 1 IS DETECTED DURING
TACTIC A (U)

SECRET

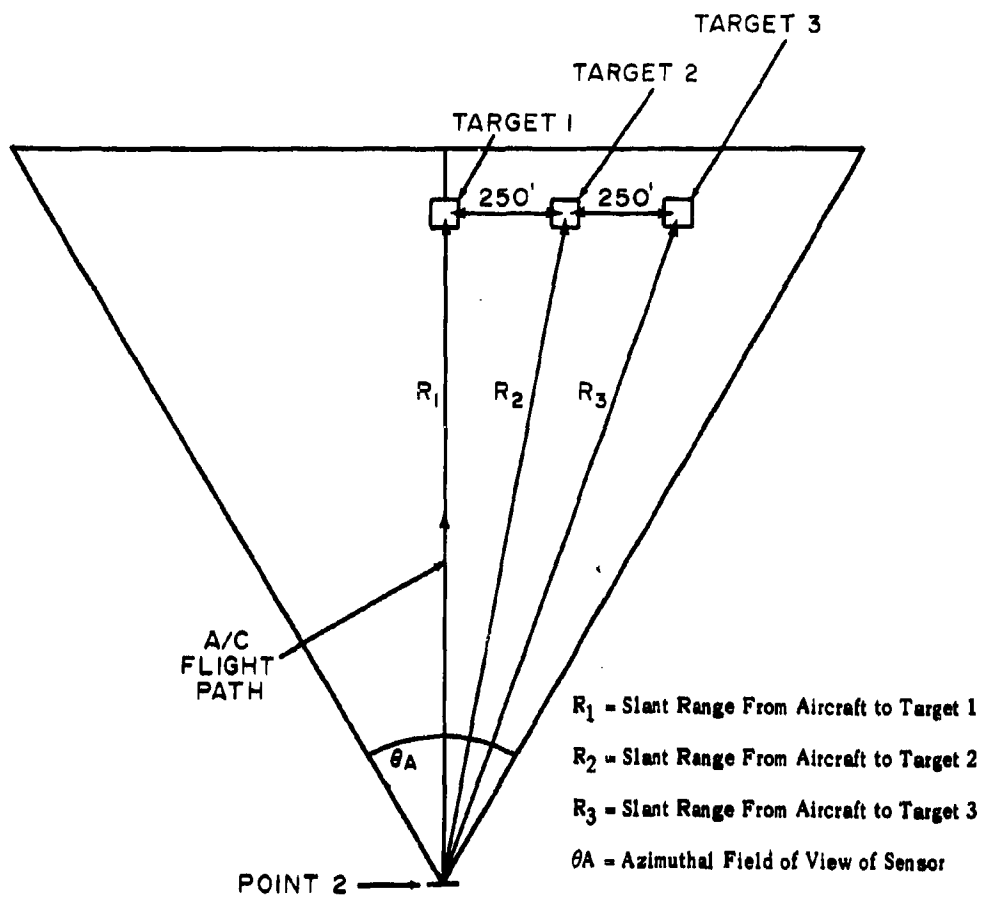


FIGURE 2 - TARGET 2 IS DETECTED DURING
TACTIC A (U)

SECRET

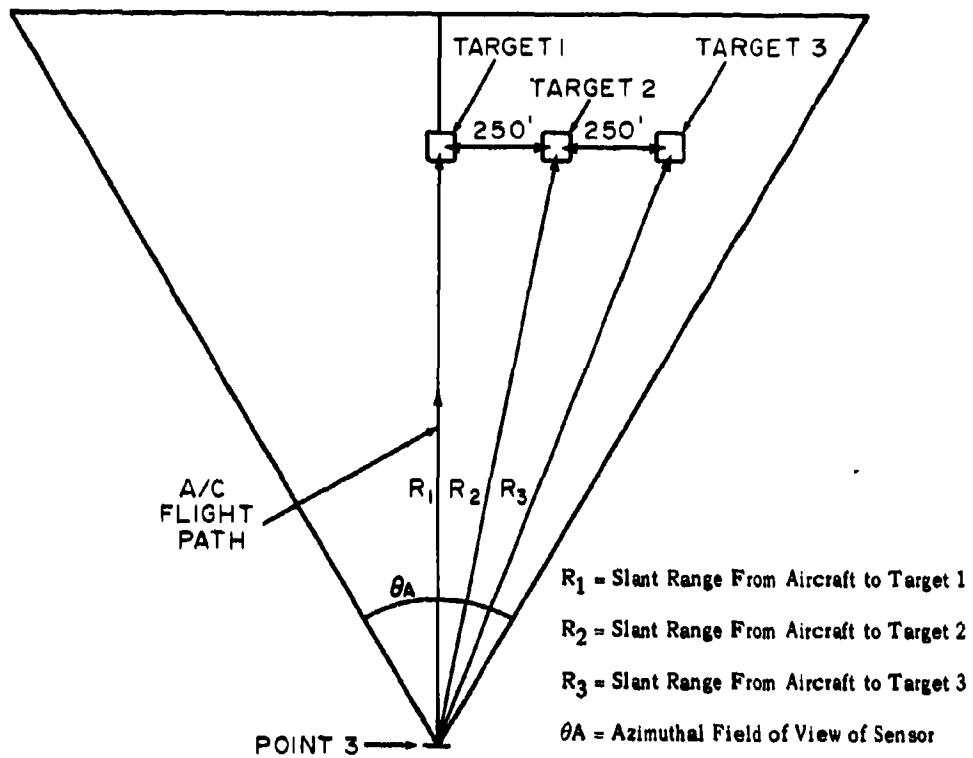


FIGURE 3 - TARGET 3 IS DETECTED DURING TACTIC A (U)

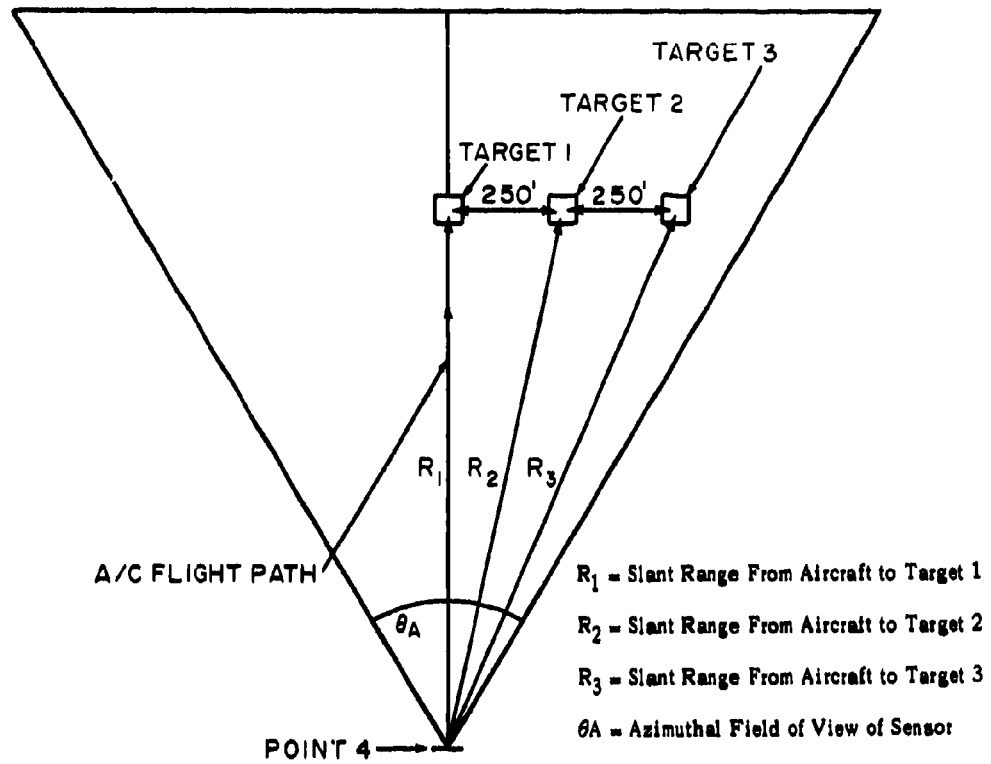


FIGURE 4 - TARGET 1 IS ACQUIRED DURING TACTIC A (U)

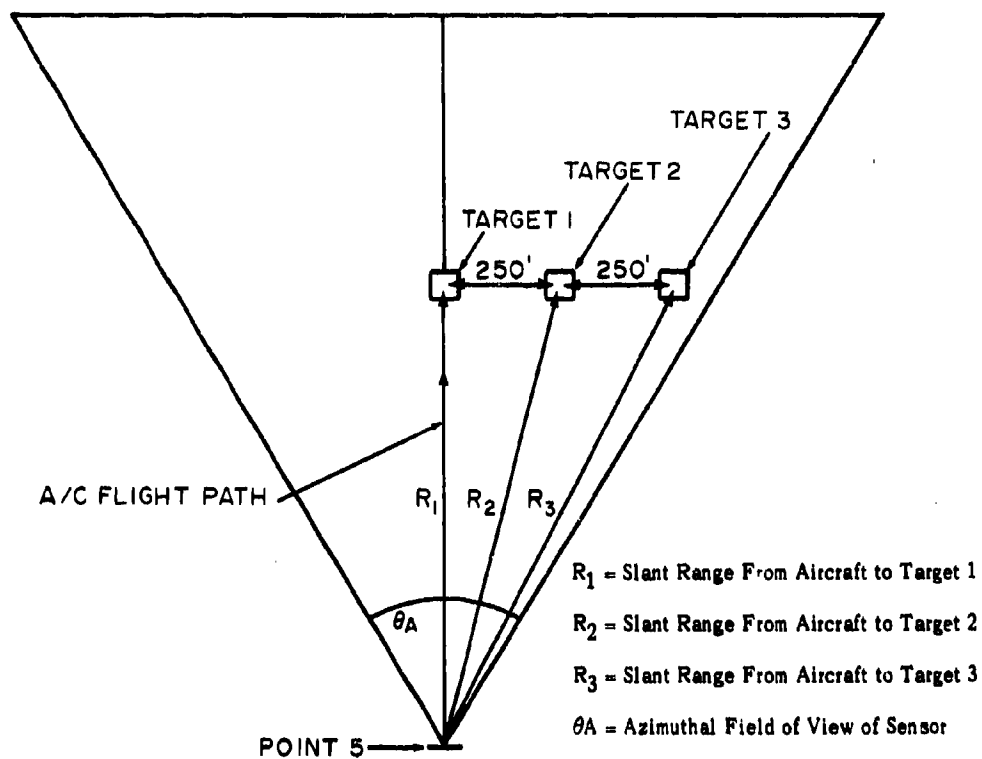


FIGURE 5 - TARGET 2 IS ACQUIRED DURING
TACTIC A (U)

SECRET

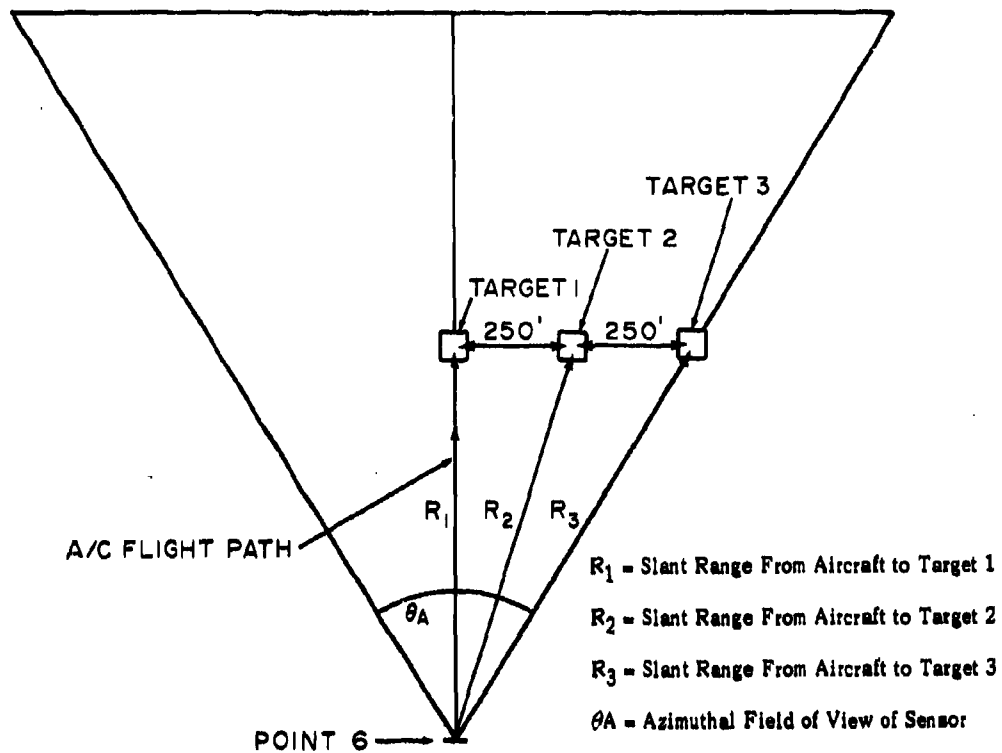


FIGURE 6 - TARGET 3 IS ACQUIRED DURING
TACTIC A (U)

SECRET

SECRET

to insure that the targets would remain in the FOV of the sensor during most of the tactic. It is assumed that the electro-optical sensor is locked on Target 1.

(U) In the following discussion P_n represents the cumulative probability of detection of Target N. In Fig. 1, Target 1 is detected when the aircraft is at Point 1 and Targets 2 and 3 have not been detected.

$$P_1 = 0.5; P_2 < 0.5; P_3 < 0.5$$

In Fig. 2, Target 2 is detected when the aircraft is at Point 2, Target 1 has been detected but not acquired, and Target 3 has not been detected.

$$.5 < P_1 < 1.0; P_2 = 0.5; P_3 < 0.5$$

In Fig. 3, Target 3 is detected when the aircraft is at Point 3, and Targets 1 and 2 have been detected but not acquired.

$$0.5 < P_1 < 1.0; 0.5 < P_2 < 1.0; P_3 = 0.5$$

In Fig. 4, Target 1 is acquired when the aircraft is at Point 4, and Targets 2 and 3 have been detected but not acquired.

$$P_1 = 1.0; .5 < P_2 < 1.0; .5 < P_3 < 1.0$$

In Fig. 5, Target 2 is acquired when the aircraft is at Point 5, and Target 1 has been acquired, and Target 3 has been detected but not acquired.

$$P_1 = 1.0; P_2 = 1.0; .5 < P_3 < 1.0$$

In Fig. 6, Target 3 is acquired when the aircraft is at Point 6, and Targets 1 and 2 have been acquired.

$$P_1 = 1.0; P_2 = 1.0; P_3 = 1.0$$

(U) Tactic B, which is similar to Tactic A except the aircraft undergoes a rolling motion, represents the situation in which the sensor is not roll

SECRET

stabilized. A simple model of aircraft roll was selected in which the roll rate was expressed by the square wave shown in Fig. 7. Figure 7 indicates that infinite roll accelerations were assumed at the reversal points. The absolute value of roll amplitude is set equal to the desired maximum roll angle at the reversal points. For example, a $1^\circ/\text{sec}$ roll rate implies a 1° maximum roll angle at a reversal point. Likewise a $45^\circ/\text{sec}$ roll rate implies a 45° maximum roll angle at a reversal point. Figure 8 shows roll angle versus time corresponding to the roll rate given in Fig. 7.

(U) Tactic C is a roll-stabilized mode similar to Tactic A except that the targets will be off the aircraft's flight path. Figures 9-14 show various positions along the flight path. Again the targets are three trucks. The first target is on a road parallel to the flight path but offset a distance of 2500 feet. The second and third targets are on roads parallel to the flight path but offset at distances of 2750 feet and 3000 feet respectively. The electro-optical sensor will again lock on Target 1.

(U) In Fig. 9, Target 1 is detected when the aircraft is at Point 1 and Targets 2 and 3 have not been detected.

$$P_1 = 0.5, P_2 < 0.5; P_3 < 0.5$$

In Fig. 10, Target 2 is detected when the aircraft is at Point 2, Target 1 has been detected and Target 3 has not been detected.

$$.5 < P_1 < 1.0; P_2 = 0.5; P_3 < 0.5$$

In Fig. 11, Target 3 is detected when the aircraft is at Point 3, and Targets 1 and 2 have been detected.

$$.5 < P_1 < 1.0; .5 < P_2 < 1.0; P_3 = 0.5$$

SECRET

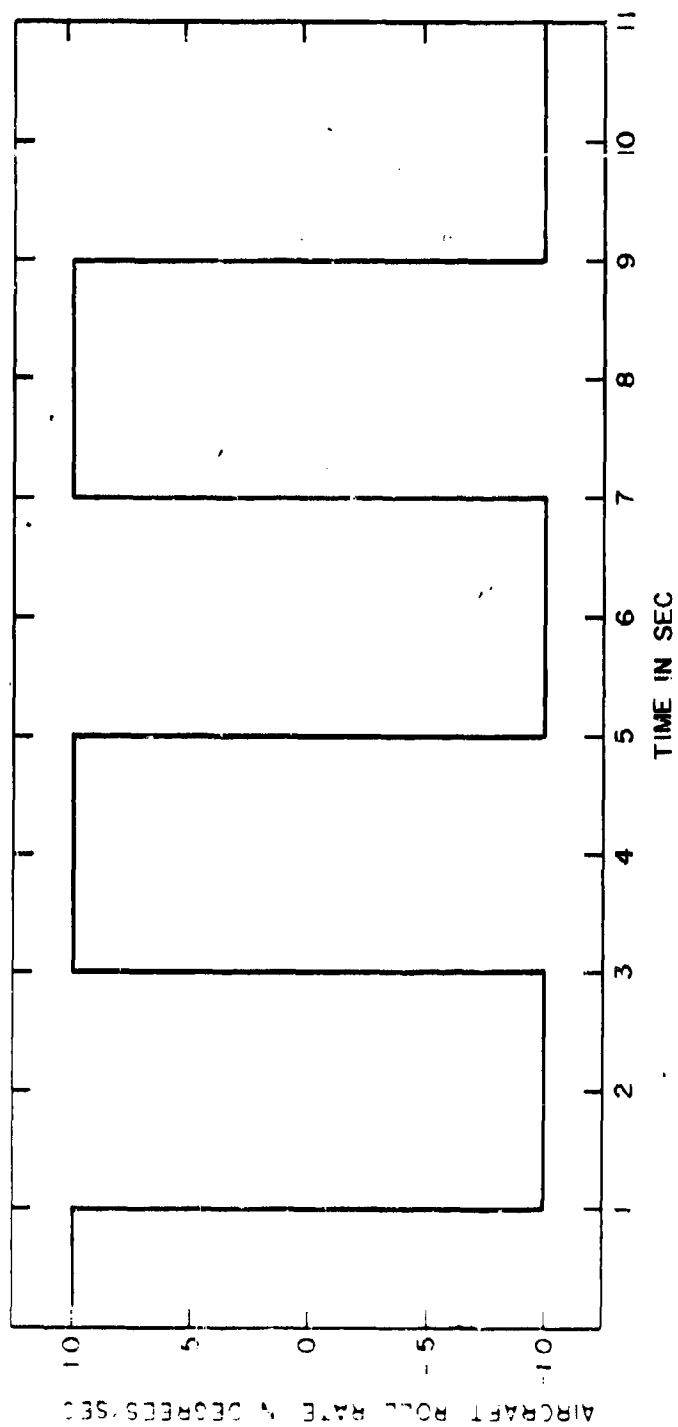


FIGURE 7 - AIRCRAFT ROLL RATE VS. TIME (U)

SECRET

SECRET

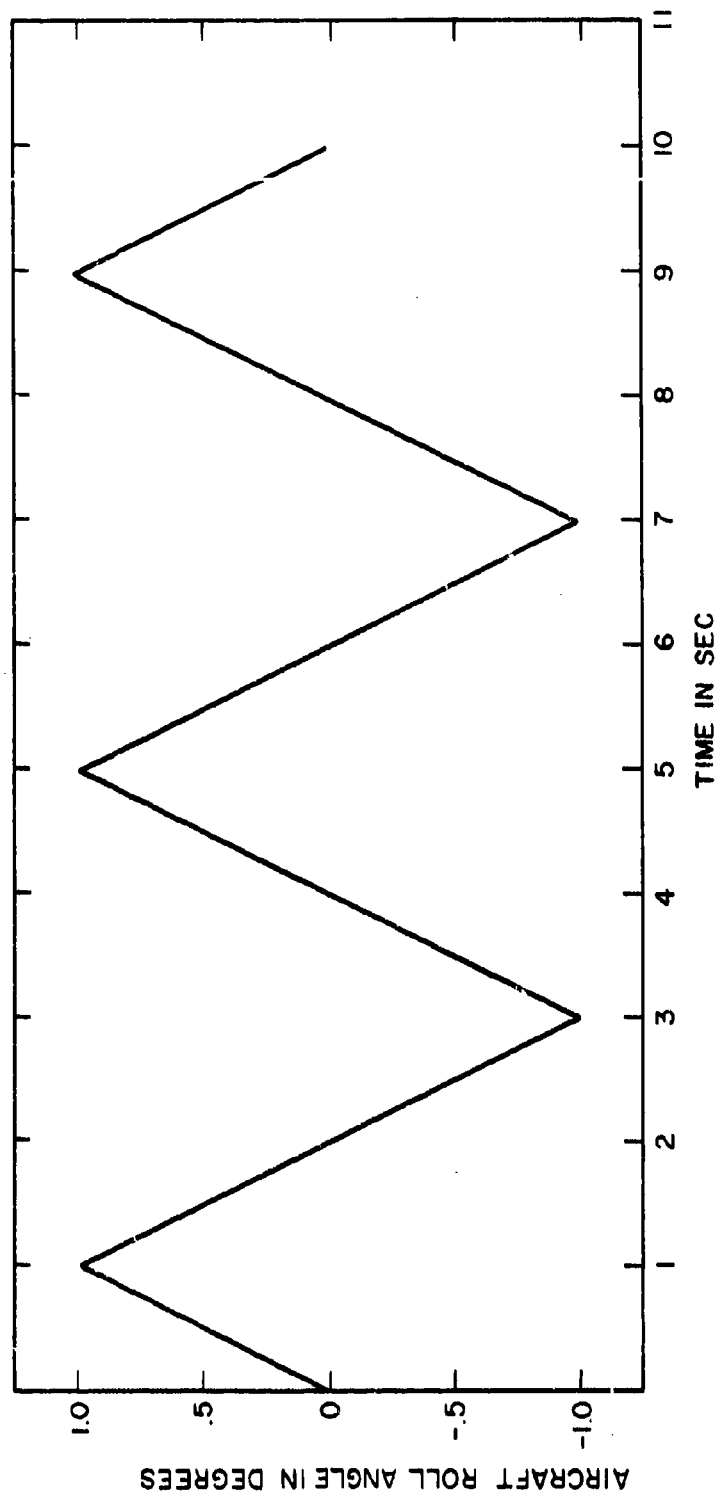


FIGURE 8 - AIRCRAFT ROLL ANGLE VS. TIME (U)

SECRET

SECRET

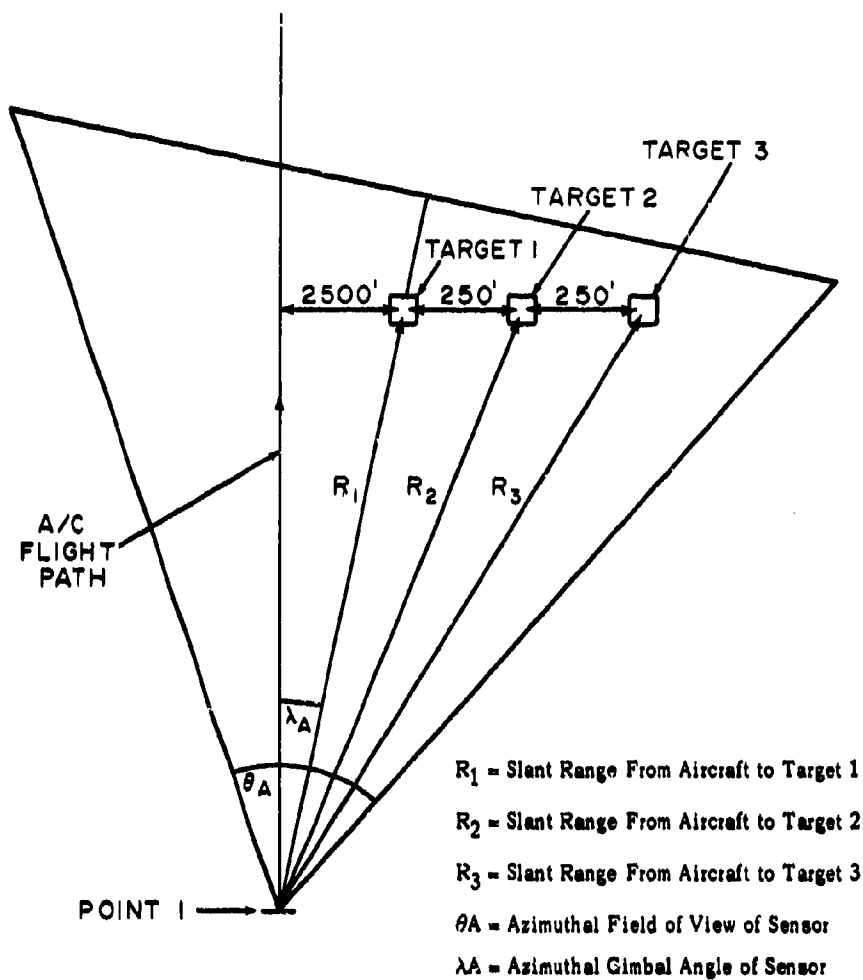


FIGURE 9 - TARGET 1 IS DETECTED DURING TACTIC C (U)

SECRET

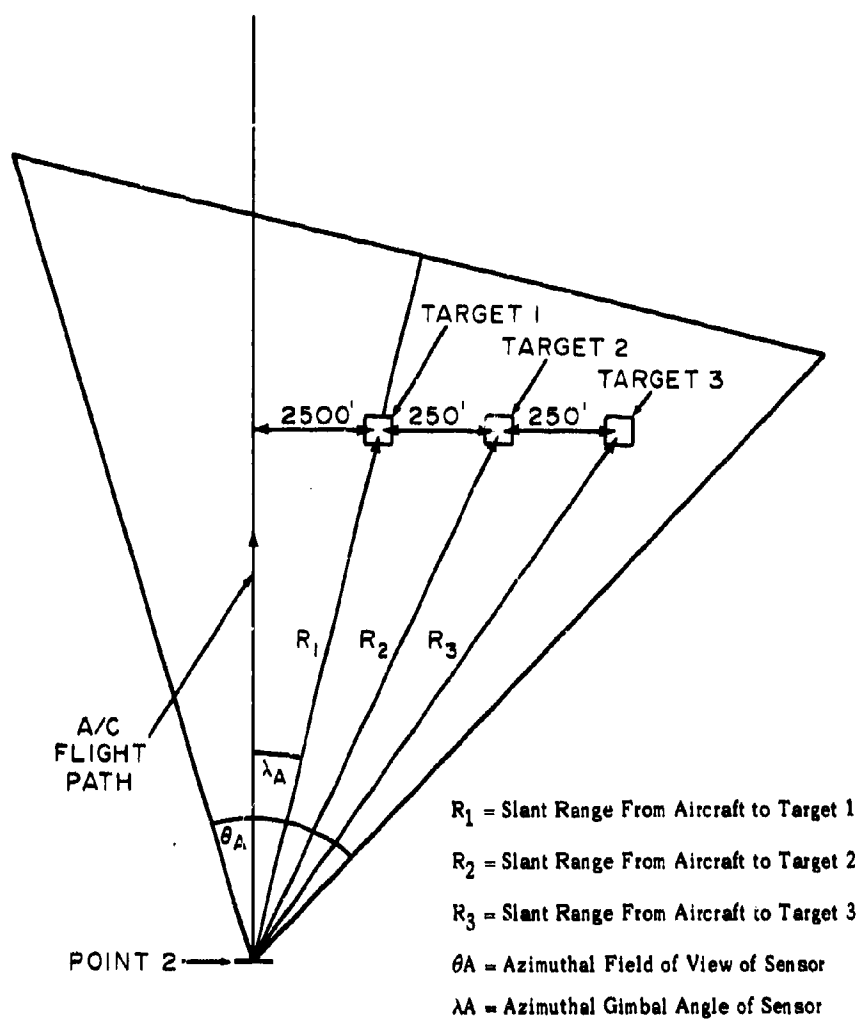


FIGURE 10 - TARGET 2 IS DETECTED DURING TACTIC C (U)

SECRET

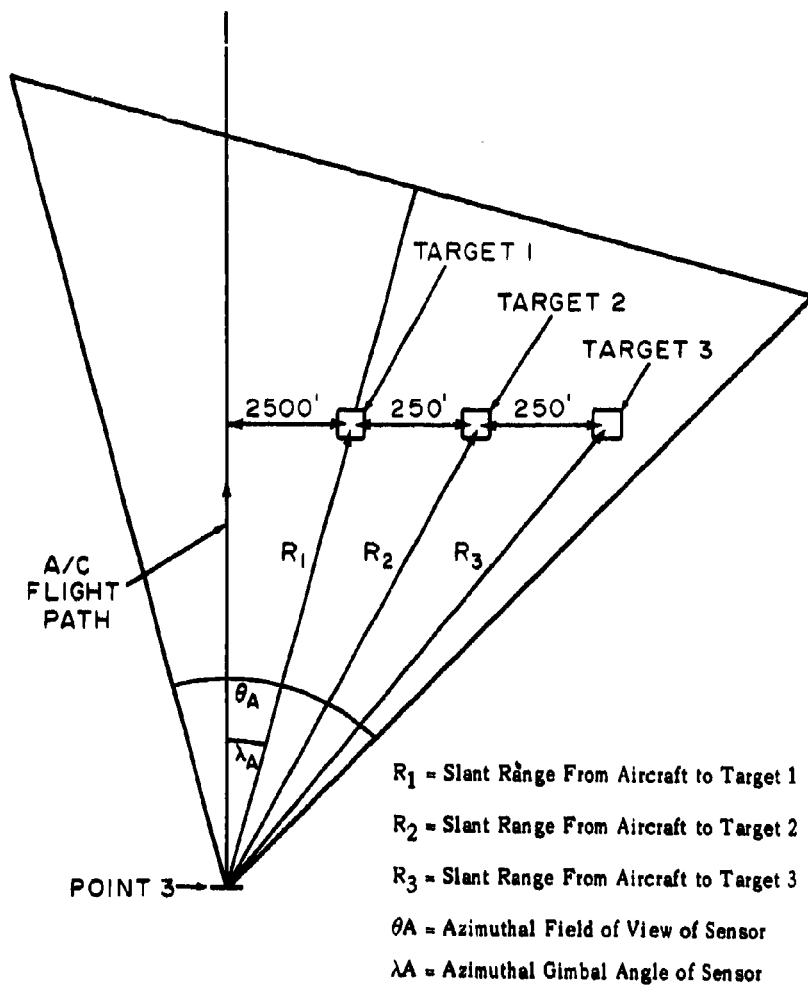


FIGURE 11 - TARGET 3 IS DETECTED DURING TACTIC C (U)

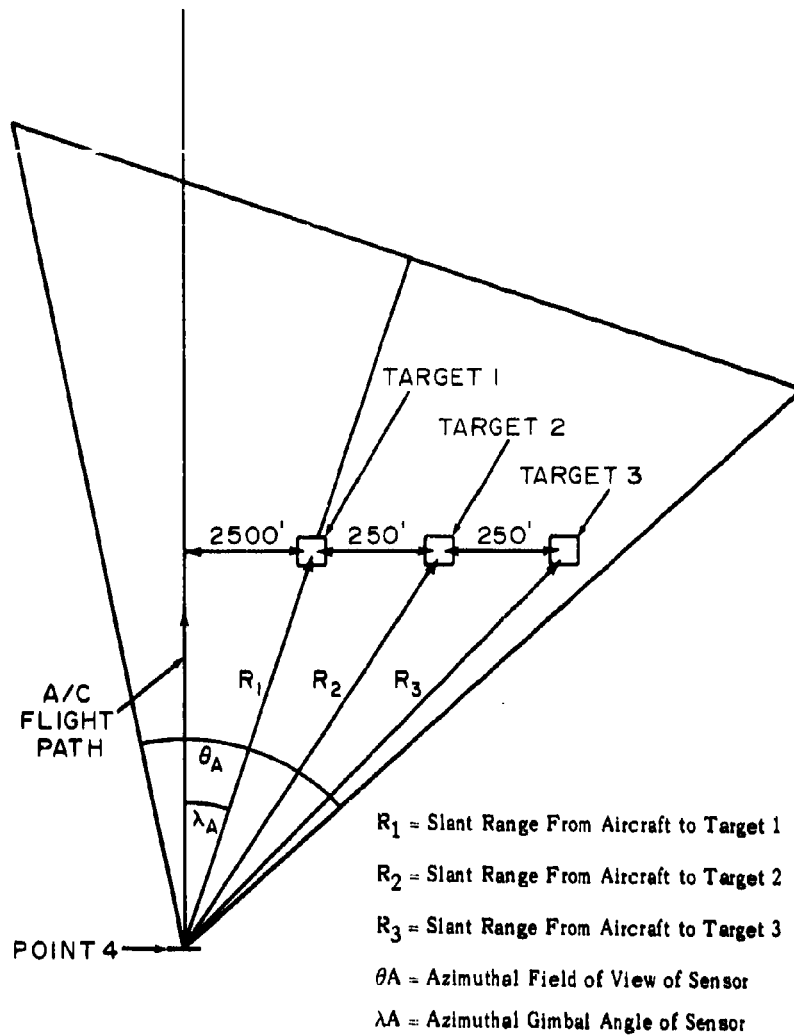


FIGURE 12 - TARGET 1 IS ACQUIRED DURING TACTIC C (U)

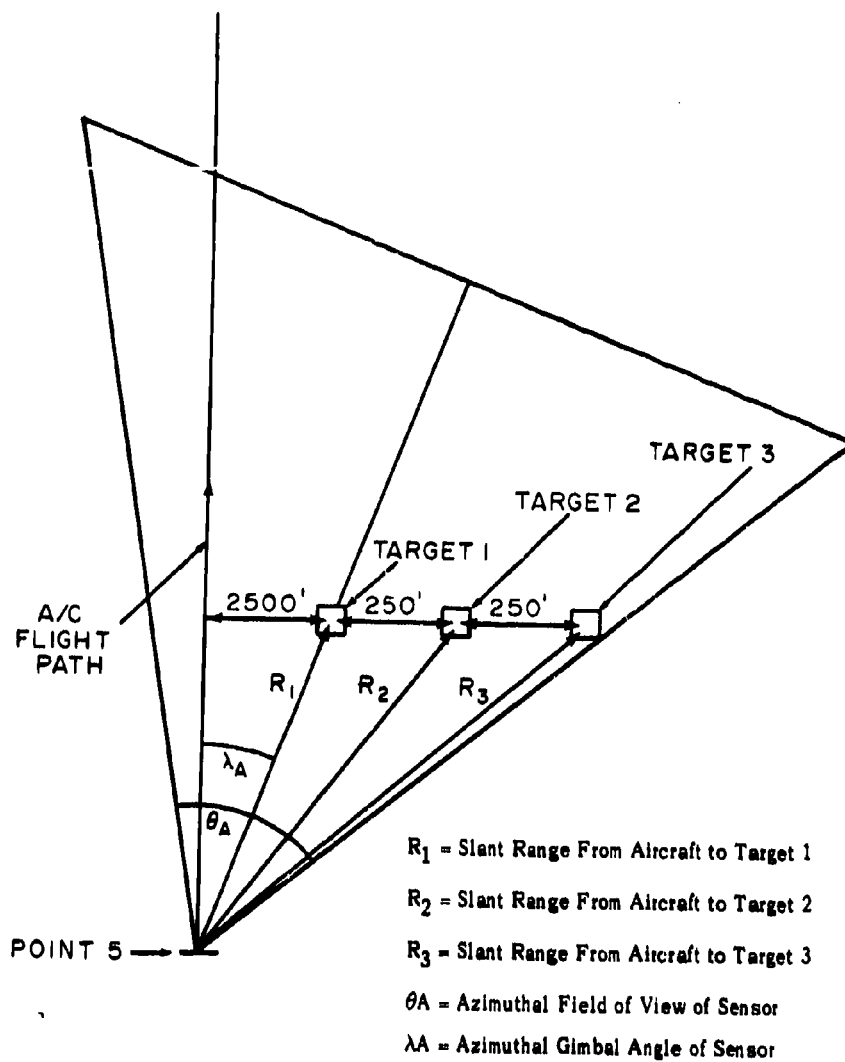


FIGURE 13 - TARGET 2 IS ACQUIRED DURING
TACTIC C (U)

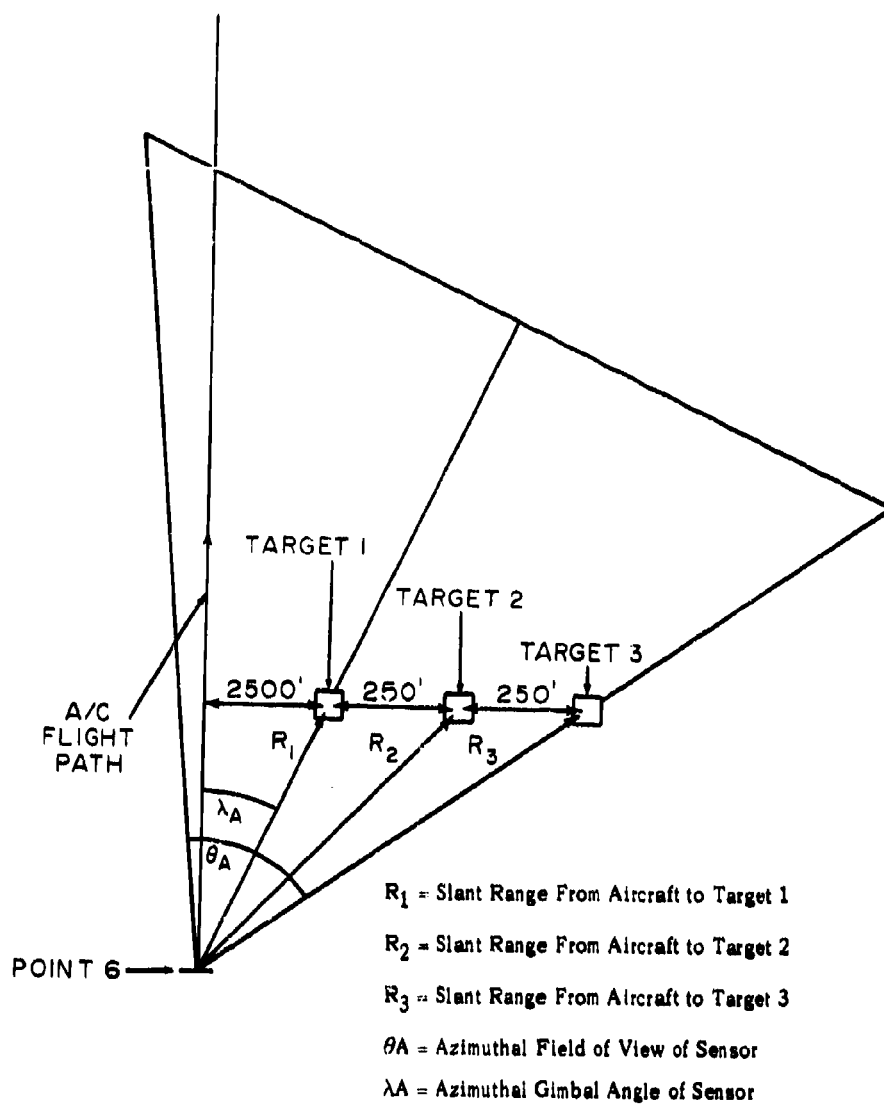


FIGURE 14 - TARGET 3 IS ACQUIRED DURING TACTIC C (U)

SECRET

In Fig. 12, Target 1 is acquired when the aircraft is at Point 4, and Targets 2 and 3 have been detected but not acquired.

$$P_1 = 1.0; 0.5 < P_2 < 1.0; 0.5 < P_3 < 1.0$$

In Fig. 13, Target 2 is acquired when the aircraft is at Point 5, Target 1 has been acquired, and Target 3 has not been acquired.

$$P_1 = 1.0; P_2 = 1.0; 0.5 < P_3 < 1.0$$

In Fig. 14, Target 3 is acquired when the aircraft is at Point 6, and Targets 1 and 2 have been acquired.

$$P_1 = 1.0; P_2 = 1.0; P_3 = 1.0$$

(U) Tactic D is similar to Tactic C, except the aircraft undergoes a rolling motion as illustrated in Figs. 7 and 8. Therefore, Tactic D represents the case for large target offsets with no roll stabilization.

3.0 THE EFFECTS OF MOTION ON TV RESOLUTION

(U) When a moving scene is viewed with a TV system, the image is smeared resulting in a loss of resolution. The extent of smear depends upon image velocity, system characteristics, and the nature of the viewed scene. The modulation given by Trott [1] for the resolution of a bar pattern experiencing linear motion as:

$$Y = \frac{\sin \pi X}{\pi X} \quad 1)$$

where, Y = modulation (Dimensionless)

X = cycles of linear motion per integration interval

Modulation as defined here is a function of image smear due to motion. The image

SECRET

smear tends to reduce system resolution by the relationship:

$$\begin{aligned} & \text{(System resolution before motion) (Modulation)} \\ & = \text{(System resolution after Motion)} \end{aligned} \quad 2)$$

(U) During an image motion equal to a bar spacing, (1) indicates a total loss of resolution. However, for an irregular pattern, as represented by an isolated target in a cluttered background, the resolution does not actually go to zero at motions equal to one resolution element. In fact, studies by Spink [2], of aerial photographs viewed with various magnitudes and frequencies of vertical linear motion, show that image motion does not appreciably affect resolution until the excursion exceeds 4 TV lines per frame. Even when the excursions were considerably greater than 4 lines, targets were observed. However, size and contrast requirements increase as image excursions per frame increase to the limit of comfortable visual tracking.

(U) It is apparent that (1) is rather pessimistic for an isolated target since it cuts off sharply at motion equal to one resolution line. A more realistic relationship for isolated targets, with linear and oscillatory motion as given by Donelan [3], is:

$$Y = \frac{1}{\pi} \int_0^a \cos^2 x \, dx \quad 3)$$

where,

$$a = \frac{\text{Image Motion per Integration Time}}{\text{Image Size}}$$

It is seen from (3) that the image width for constant exposure time varies inversely with Y since Y is a measure of resolution.

SECRET

(U) When the target is considered as an isolated point with a $\cos^2 x$ distribution, which decreases in amplitude in proportion to its velocity until lost in noise when moving in the image field, the real detection problem of discerning a target with some contrast out of the basic noise level of background clutter is more nearly synthesized. The greater the motion of the target, both oscillatory and linear, the more nearly it approaches the level of the background. It is assumed that the target is of good contrast with its surroundings and that the system has a relatively good signal-to-noise ratio. There are conditions in which both of these assumptions are invalid but their consideration in this study would be an unnecessary complication.

(U) The $\cos^2 x$ considerations compare favorably with the work of Trott [1] in his study of the effects of linear and vibratory image motion on the resolution of aerial cameras. Thus, it appears to be both expedient and accurate to utilize the $\cos^2 x$ relationships when considering the effects of aircraft roll on image resolution. By allowing the image size to vary from the minimum resolvable image to the full picture size, the modulation may be plotted as a function of target motion. Using (3), this relationship is plotted in Fig. 15 in which the image size is tagged as the width of a resolution element since it was assumed that target size was always equal to the width of a resolution element.

(U) The system transfer function describes the ability of the LLLTV system to respond to a range of input frequencies. Coltman [4] has shown that image properties may be specified by response measurements to sine wave inputs. Furthermore, this sine wave response may be calculated from bar pattern data. Thus, through laboratory tests, a response curve for the TV system determines the static characteristics.

SECRET

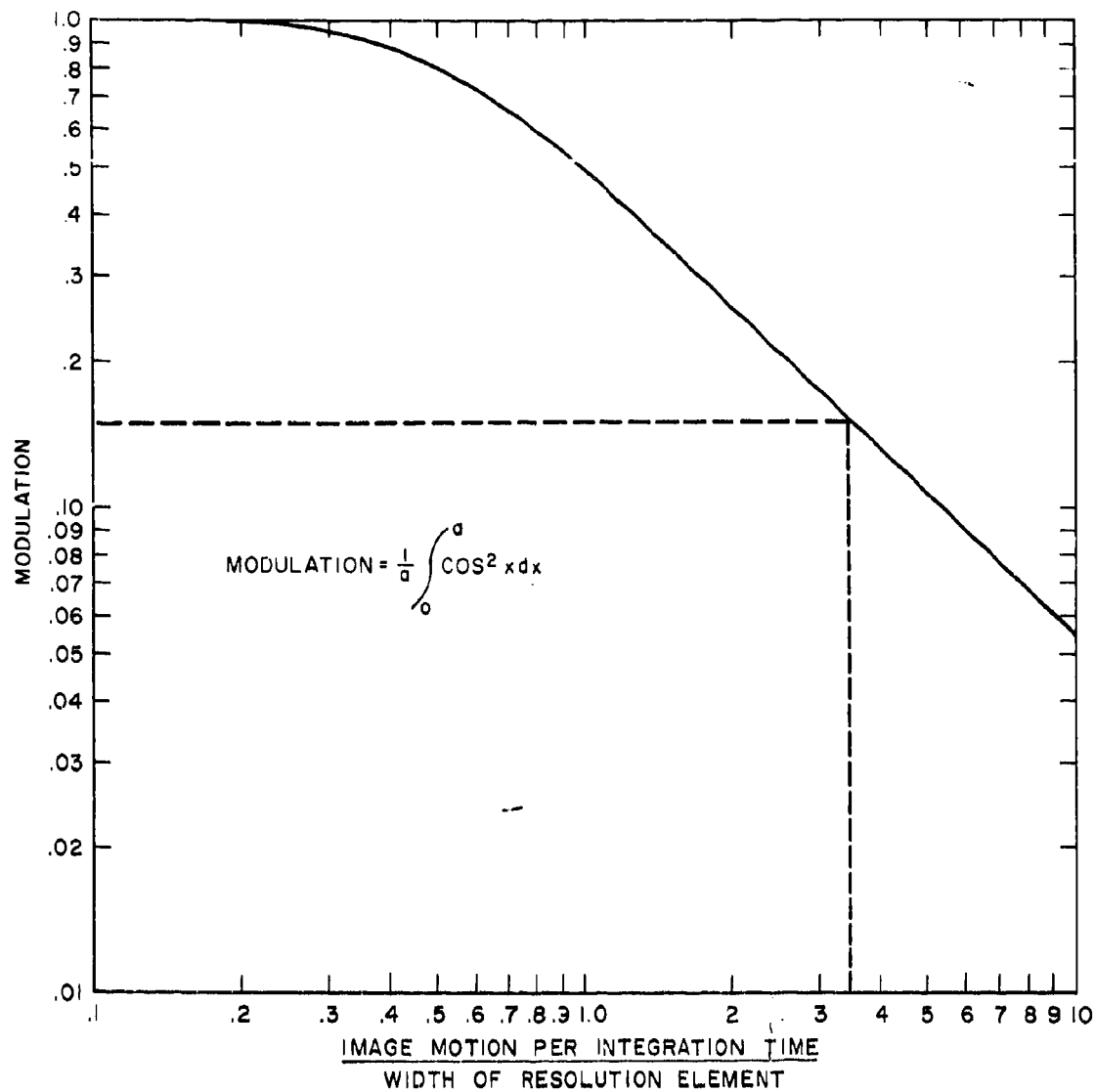


FIGURE 15 - MODULATION TRANSFER FUNCTION FOR
MOVING IMAGE ($\cos^2 x$ DISTRIBUTION) (U)

Best Available Copy

The dynamic response curve from Fig. 15 as generated by the sensor system manual response given in Fig. 15 is defined by the relationship:

$$\text{Dynamic Response} = \frac{\text{Desired Resolution}}{\text{Actual Resolution}} \quad 4)$$

The dynamic response curve is generated by having a knowledge of the effects of the dynamic response curve to generate a dynamic response curve as shown in Fig. 16. The dynamic response curve is generated by Fig. 17 from Figs. 15 and 16. The dynamic response curve is generated by Fig. 17 from Figs. 15 and 16. The dynamic response curve is generated by Fig. 17 from Figs. 15 and 16. The dynamic response curve is generated by Fig. 17 from Figs. 15 and 16.

$$\text{Dynamic Response} = \frac{\text{Desired Resolution}}{\text{Actual Resolution}} \quad 5)$$

The dynamic response curve is generated by Fig. 17 from Figs. 15 and 16. The dynamic response curve is generated by Fig. 17 from Figs. 15 and 16. The dynamic response curve is generated by Fig. 17 from Figs. 15 and 16.

$$\text{Dynamic Response} = \frac{\text{Desired Resolution}}{\text{Actual Resolution}} \quad 6)$$

The dynamic response curve is generated by Fig. 17 from Figs. 15 and 16. The dynamic response curve is generated by Fig. 17 from Figs. 15 and 16. The dynamic response curve is generated by Fig. 17 from Figs. 15 and 16.

The dynamic response curve is generated by Fig. 17 from Figs. 15 and 16. The dynamic response curve is generated by Fig. 17 from Figs. 15 and 16. The dynamic response curve is generated by Fig. 17 from Figs. 15 and 16.

The dynamic response curve is generated by Fig. 17 from Figs. 15 and 16. The dynamic response curve is generated by Fig. 17 from Figs. 15 and 16. The dynamic response curve is generated by Fig. 17 from Figs. 15 and 16.

The dynamic response curve is generated by Fig. 17 from Figs. 15 and 16. The dynamic response curve is generated by Fig. 17 from Figs. 15 and 16. The dynamic response curve is generated by Fig. 17 from Figs. 15 and 16.

The dynamic response curve is generated by Fig. 17 from Figs. 15 and 16. The dynamic response curve is generated by Fig. 17 from Figs. 15 and 16. The dynamic response curve is generated by Fig. 17 from Figs. 15 and 16.

The dynamic response curve is generated by Fig. 17 from Figs. 15 and 16. The dynamic response curve is generated by Fig. 17 from Figs. 15 and 16. The dynamic response curve is generated by Fig. 17 from Figs. 15 and 16.

The dynamic response curve is generated by Fig. 17 from Figs. 15 and 16. The dynamic response curve is generated by Fig. 17 from Figs. 15 and 16. The dynamic response curve is generated by Fig. 17 from Figs. 15 and 16.

The dynamic response curve is generated by Fig. 17 from Figs. 15 and 16. The dynamic response curve is generated by Fig. 17 from Figs. 15 and 16. The dynamic response curve is generated by Fig. 17 from Figs. 15 and 16.

The dynamic response curve is generated by Fig. 17 from Figs. 15 and 16. The dynamic response curve is generated by Fig. 17 from Figs. 15 and 16. The dynamic response curve is generated by Fig. 17 from Figs. 15 and 16.

SECRET

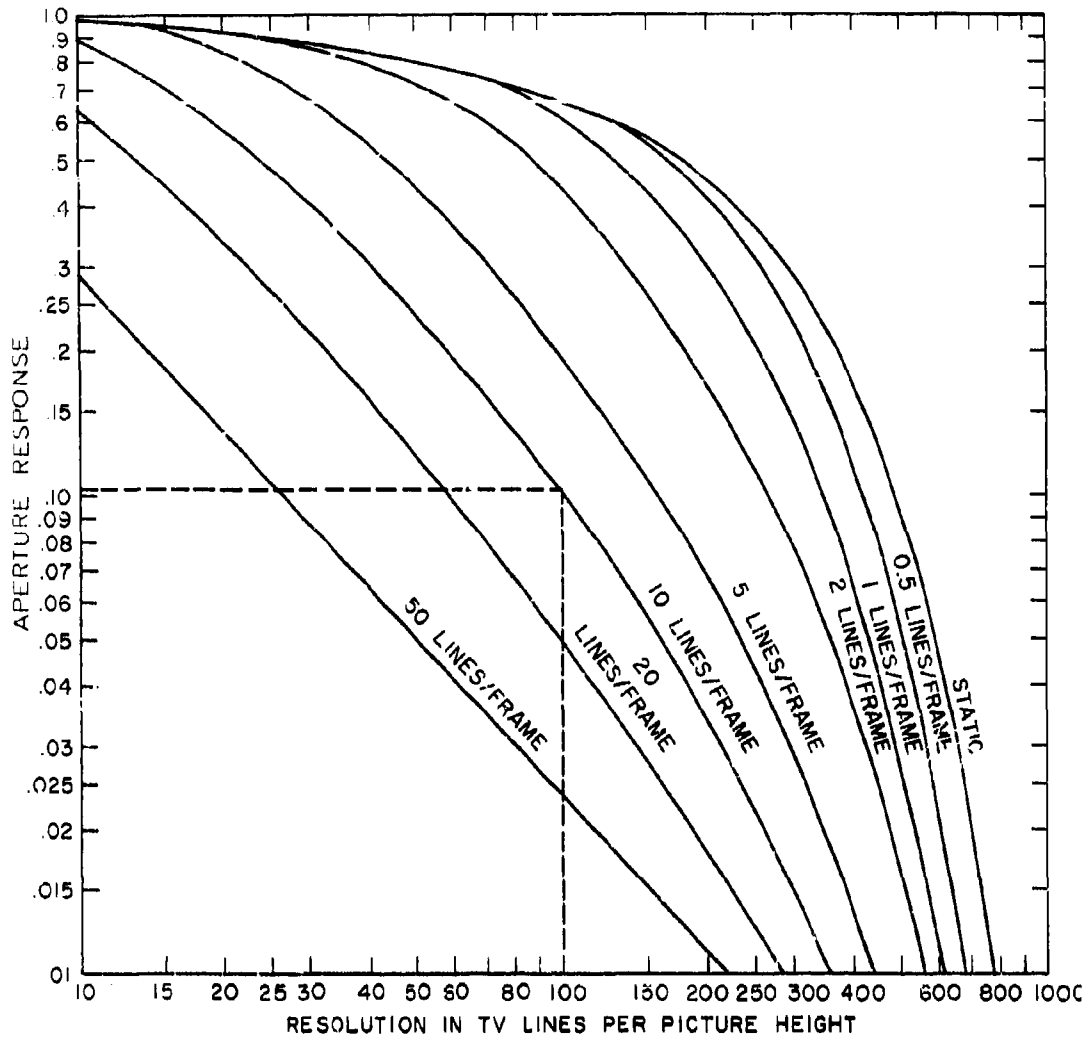


FIGURE 17 - RESOLUTION DEGRADATION DUE TO LINEAR MOTION FOR LLLTV SYSTEM, 1/5 SECOND INTEGRATION TIME (U)

SECRET

response for a 100 line system resolution due to a motion degradation of 10 lines/frame as plotted on Fig. 17 is given by:

$$\text{Aperture Response} = (0.735) (0.146) = 0.106 \text{ (Dimensionless)} \quad 9)$$

Similar calculations were made to generate the family of curves given on Fig. 17.

(U) Figure 18, which is a plot of lines of motion per frame versus the apparent resolution in TV lines, is calculated from Fig. 17. An aperture response of 5% was chosen, and the various TV resolutions for the corresponding values of image motion were taken from Fig. 17 and plotted on Fig. 18.

(S) Figure 19 is a plot of Apparent Lines on Target versus Resolution Lines on Target. Figure 19 was generated by the following equation:

$$\text{Apparent Lines} \times \frac{590}{\text{Apparent Resolution}} = \text{Resolution Lines} \quad 10)$$

where,

Apparent Lines - lines on target after consideration of motion.

Resolution Lines - lines on target before considering motion.

Apparent Resolution - apparent system resolution is 590 lines.

Note: At 5% aperture response, resolution is 590 lines.

(C) Actual flight test data from LLLTV systems [6] has shown that the minimum detection level ($P_d = 0.5$) for a high contrast stationary target is about five lines, while acquisition ($P_a = 0.95$) occurs at eight lines. From such tests, a curve of probability of detection as a function of lines on target was developed and plotted in Fig. 20. This curve is used to determine the probability of detection as a function of apparent lines on the target and the slant range to the target.

(U) To completely describe the detectability of targets during aircraft maneuvers,

SECRET

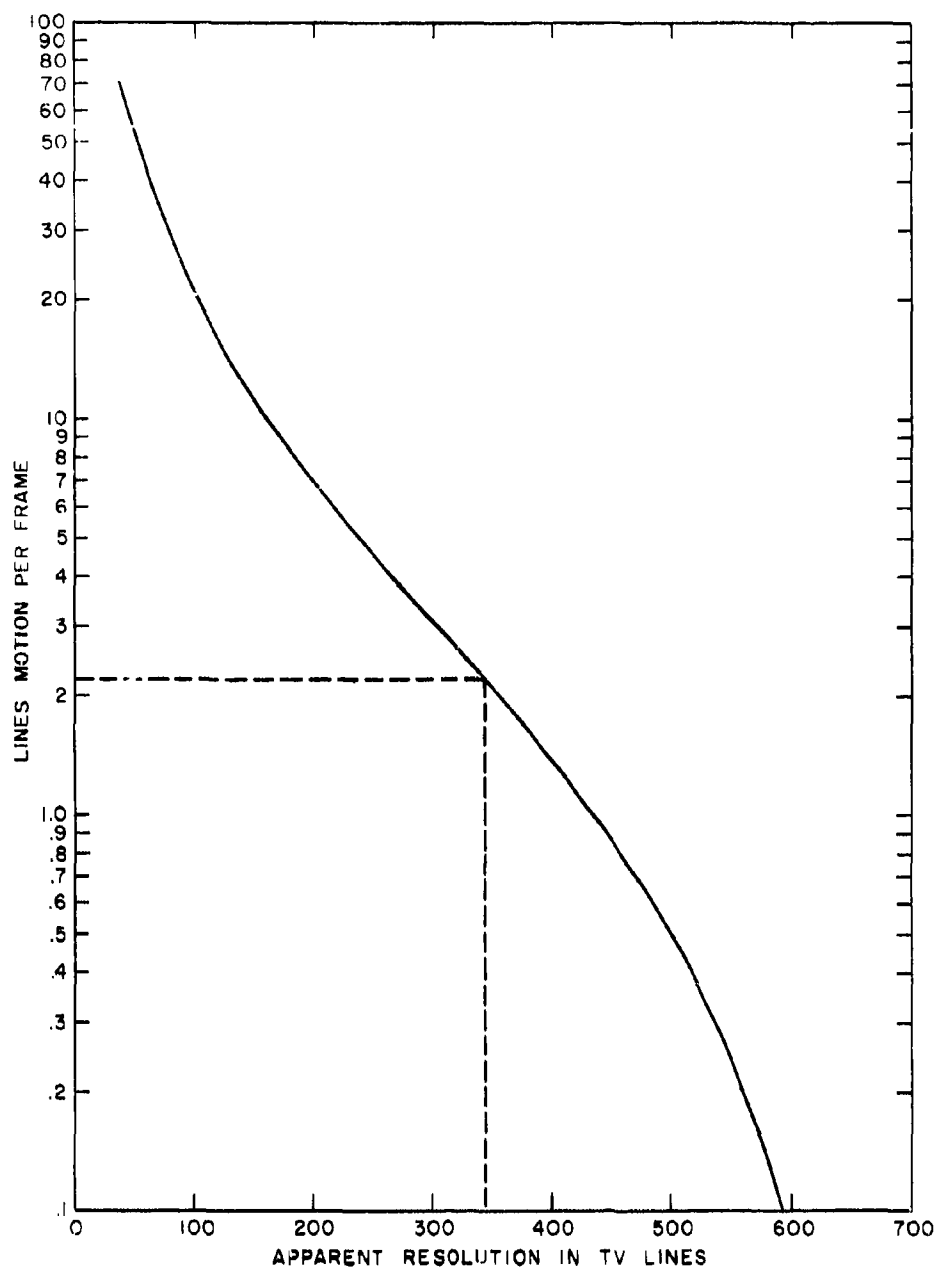


FIGURE 18 - RESOLUTION AS A FUNCTION OF MOTION
WITH 1/5 SECOND INTEGRATION TIME
AT 5% APERTURE RESPONSE FOR LLLTV
SYSTEM (U)

SECRET

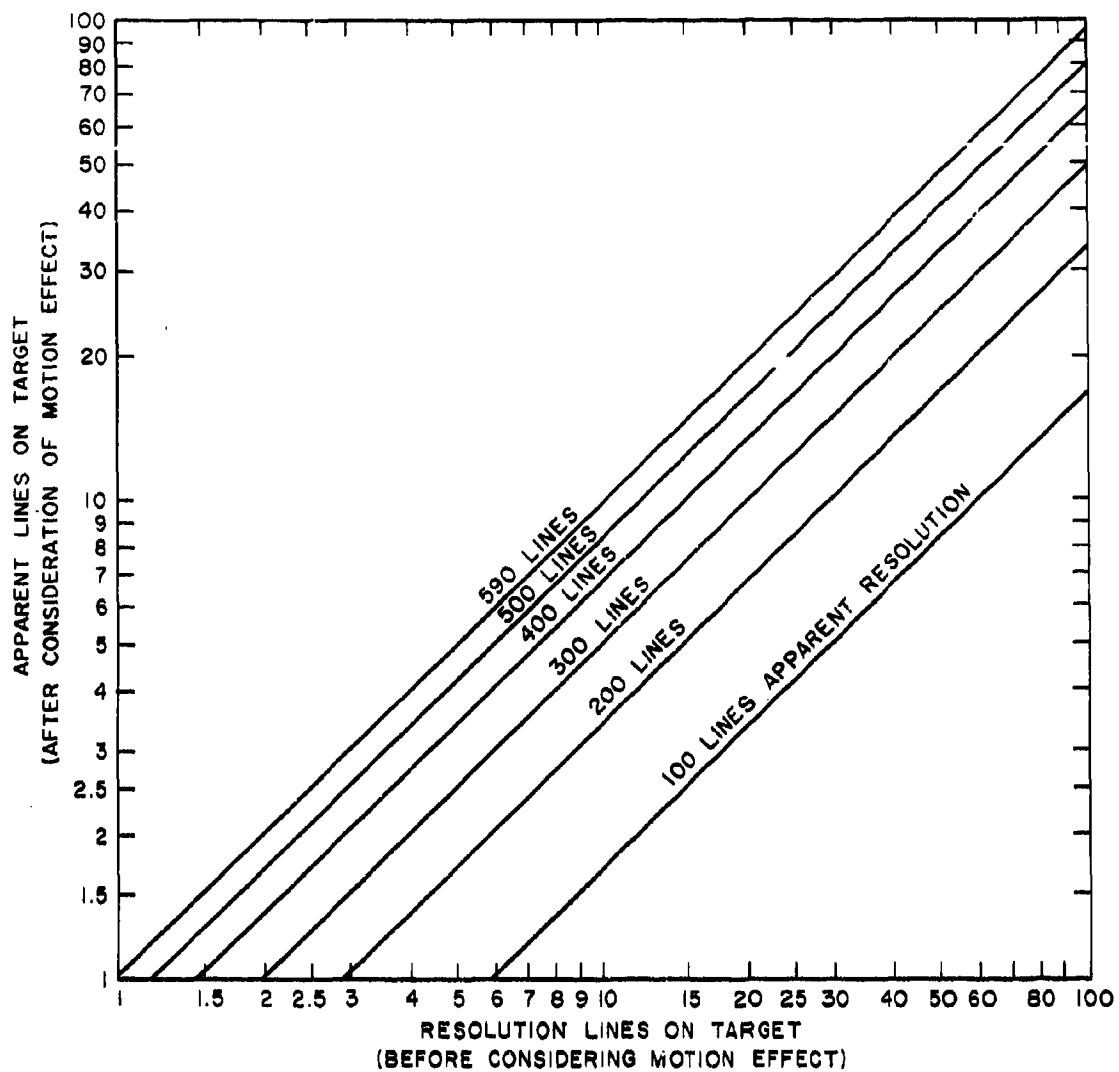


FIGURE 19 - APPARENT LINES ON TARGET AS A FUNCTION OF APPARENT RESOLUTION AND RESOLVABLE LINES ON TARGET (U)

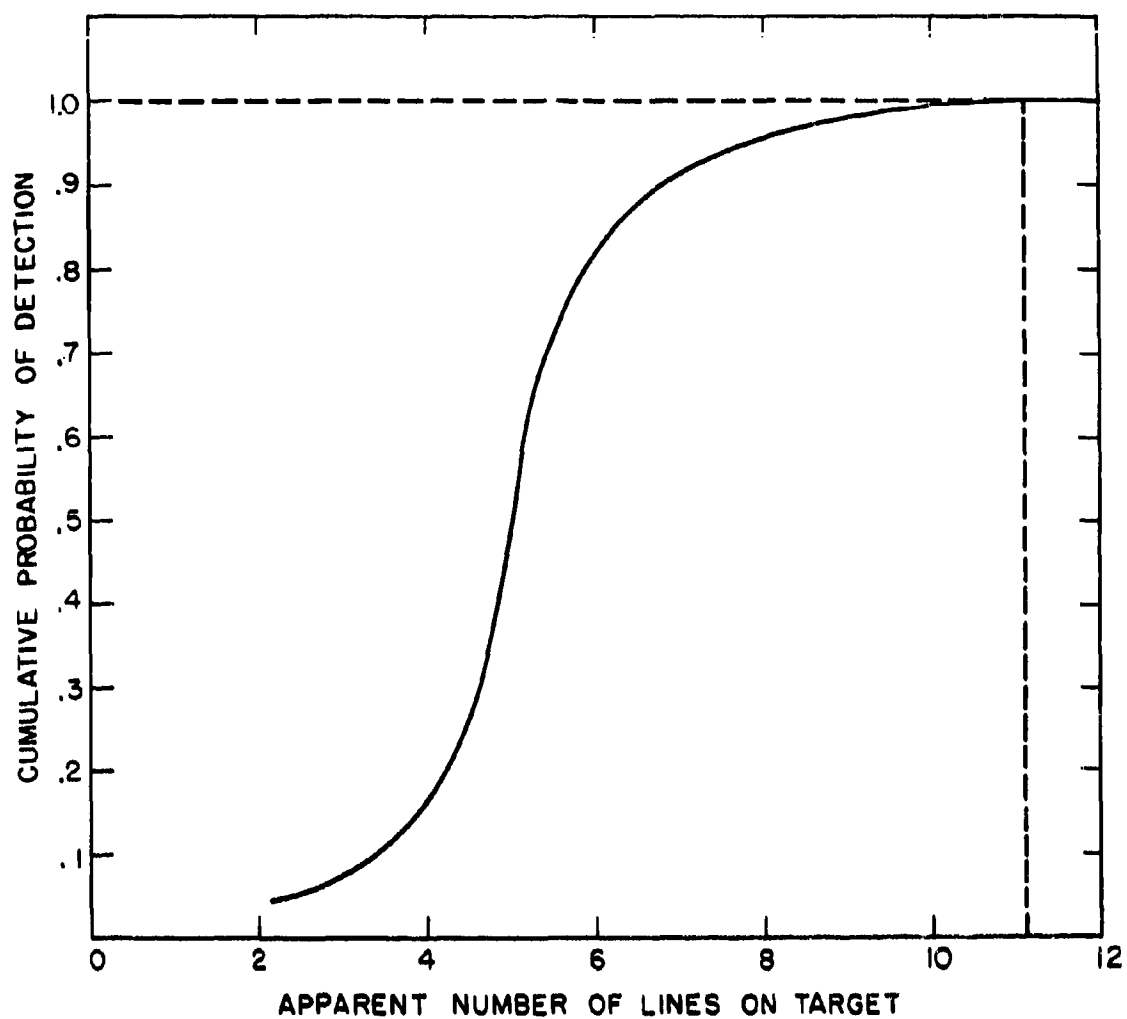


FIGURE 20 - CUMULATIVE PROBABILITY OF DETECTION AS
A FUNCTION OF NUMBER OF LINES ON TARGET (U)

SECRET

it would be necessary to describe the contrast of the target with respect to its background, scene illumination, illumination angle, terrain masking, atmospheric distortion, degradation, and other factors which affect viewing either with an electro-optical sensor or with the naked eye. These determinations are beyond the scope of this study, and it has been assumed that the target has high contrast with no obstructions or degradations. A comparison of maneuvering and non-maneuvering situations under these ideal conditions will permit a reasonable assessment of the problem under other conditions.

4.0 DERIVATION OF EQUATIONS

(U) Consider an aircraft flying at a constant velocity and altitude with an on-board electro-optical system searching the ground below for a fixed target. Assume further that the aircraft can roll about its velocity vector, while a fixed point on ground is tracked in azimuth and elevation but not in roll.

(U) A simple imaging optical system, representative of the sensor optics, is shown in Fig. 21. Point P, an arbitrary point within the sensor's field of view has coordinates R_i , R_j , and R_k . The i axis is along the boresight of the system and the j and k axes form an orthogonal set on the display. The coordinates R_i , R_j and R_k may be related to the range and display coordinate (A , E) of the point P on the ground.

(U) Figure 22 shows the aircraft and electro-optical tracking system geometry. λ_E and λ_A represent the gimbal angles in elevation and azimuth, respectively, of the electro-optical system with respect to point O on the ground. A and E represent the azimuth and elevation coordinates of Point P on the display.

(U) The point O has coordinates X , Y and Z with respect to the aircraft.

SECRET

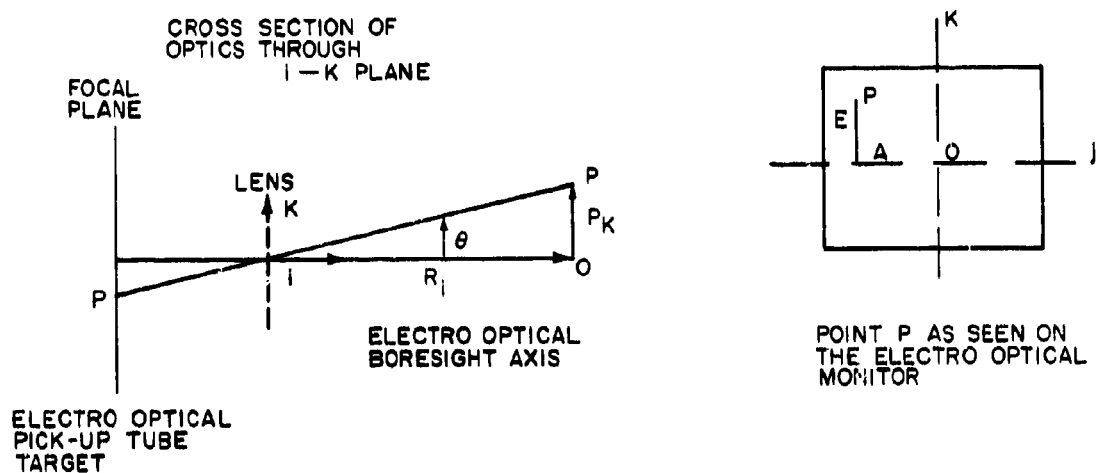


FIGURE 21 - IMAGING SYSTEM GEOMETRY

SECRET

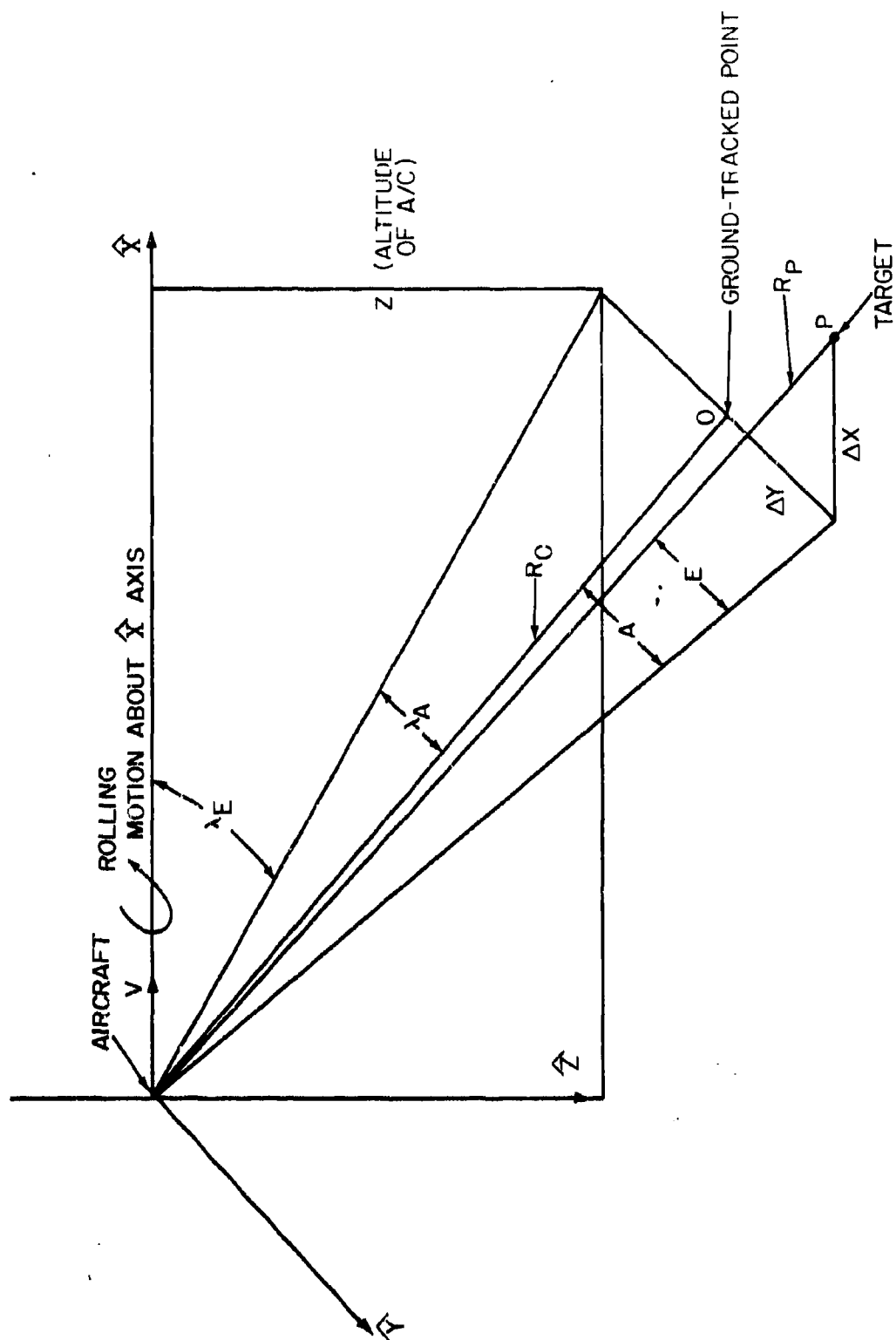


FIGURE 22 - TRACKING GEOMETRY (U)

SECRET

The point P is displaced by X, Y from point O. The aircraft velocity is equal to V. Therefore, the coordinates of point O at any time, t, are given by:

$$X(t) = X_0 - Vt \quad 11)$$

$$Y(t) = Y_0 \quad 12)$$

$$Z(t) = Z_0 \quad 13)$$

(U) The range to Point O in a coordinate system along the electro-optical bore-sight axis is given by:

$$\begin{bmatrix} R_0 \\ 0 \\ 0 \end{bmatrix} = \begin{bmatrix} \lambda_A \\ \lambda_E \\ \phi \end{bmatrix} \begin{bmatrix} X \\ Y \\ Z \end{bmatrix} \quad 14)$$

where,

$$\begin{bmatrix} \lambda_A \end{bmatrix} = \begin{bmatrix} \cos \lambda_A & \sin \lambda_A & 0 \\ -\sin \lambda_A & \cos \lambda_A & 0 \\ 0 & 0 & \phi \end{bmatrix}$$

$$\begin{bmatrix} \lambda_E \end{bmatrix} = \begin{bmatrix} \cos \lambda_E & 0 & -\sin \lambda_E \\ 0 & 1 & 0 \\ \sin \lambda_E & 0 & \cos \lambda_E \end{bmatrix}$$

$$\begin{bmatrix} \phi \end{bmatrix} = \begin{bmatrix} 1 & 0 & 0 \\ 0 & \cos \phi & \sin \phi \\ 0 & -\sin \phi & \cos \phi \end{bmatrix}$$

= Roll Angle of the Aircraft

14) is inverted to obtain:

$$\begin{bmatrix} \lambda_E \end{bmatrix}^{-1} \begin{bmatrix} \lambda_A \end{bmatrix}^{-1} \begin{bmatrix} R_0 \\ 0 \\ 0 \end{bmatrix} = \begin{bmatrix} \phi \end{bmatrix} \begin{bmatrix} X \\ Y \\ Z \end{bmatrix} \quad 15)$$

SECRET

Expanding 15) and simplifying:

$$\tan \lambda_E = \frac{Y \sin \phi - Z \cos \phi}{X} \quad 16)$$

$$\sin \lambda_A = \frac{Y \cos \phi + Z \sin \phi}{R} \quad 17)$$

$$R = (X^2 + Y^2 + Z^2)^{\frac{1}{2}} \quad 18)$$

The range, R_p , to point P with coordinates $X + \Delta X$, $Y + \Delta Y$, Z is given by:

$$\begin{bmatrix} R_p \\ 0 \\ 0 \end{bmatrix} = [E] [A] [\lambda_A] [\lambda_E] [\phi] \begin{bmatrix} X + \Delta X \\ Y + \Delta Y \\ Z \end{bmatrix} \quad 19)$$

Where:

$$[E] = \begin{bmatrix} \cos E & 0 & -\sin E \\ 0 & 1 & 0 \\ \sin E & 0 & \cos E \end{bmatrix}$$

$$[A] = \begin{bmatrix} \cos A & \sin A & 0 \\ -\sin A & \cos A & 0 \\ 0 & 0 & 1 \end{bmatrix}$$

19) is inverted to obtain:

$$[A]^{-1} [E]^{-1} \begin{bmatrix} R_p \\ 0 \\ 0 \end{bmatrix} = [M] \begin{bmatrix} X + \Delta X \\ Y + \Delta Y \\ Z \end{bmatrix} \quad 20)$$

Best Available Copy

36

Best Available Copy

air 215

... .. indicates A, E, the line of sight

Best Available Con

38

SECRET

The angles subtended by the target on the display in azimuth and elevation respectively are determined by differentiating 20) with respect to A and E as a function of X, Y, and Z. This yields:

$$R_p \begin{bmatrix} -(\sin E \cos A) \Delta E - (\cos E \sin A) \Delta A \\ -(\sin E \sin A) \Delta E + (\cos E \cos A) \Delta A \\ -\cos E \Delta E \end{bmatrix} = [M] \begin{bmatrix} X_t \\ Y_t \\ Z_t \end{bmatrix} \quad 37)$$

Where:

X_t = the size of the target in the X-direction

Y_t = the size of the target in the Y-direction

Z_t = the size of the target in the Z-direction

Simplifying 37):

$$\Delta E \left[\frac{|M_{21}|^2 X_t^2 + |M_{32}|^2 Y_t^2 + |M_{33}|^2 Z_t^2}{\cos E} \right]^{\frac{1}{2}} \quad 38)$$

$$\Delta A \left[\frac{|M_{11}|^2 X_t^2 + |M_{22}|^2 Y_t^2 + |M_{23}|^2 Z_t^2 - (\sin E \sin A \Delta E)^2}{\cos E \cos A} \right]^{\frac{1}{2}} \quad 39)$$

The error in the target in azimuth and elevation is then given by:

$$\frac{\Delta A}{\Delta E} \quad 40)$$

$$\frac{\Delta E}{\Delta A} \quad 41)$$

The error in the target in azimuth

SECRET

NTE = number of lines on the target in elevation

θ_A = field of view in azimuth

θ_E = field of view in elevation

NA = resolution (in lines) in azimuth

NE = resolution (in lines) in elevation

The number of lines of target motion per frame time in azimuth and elevation is given by:

$$VTA = \frac{\dot{A} NA}{\theta_A} FT \quad 42)$$

$$VTE = \frac{\dot{E} NE}{\theta_E} FT \quad 43)$$

Where:

VTA = lines of target motion per frame time in azimuth

VTE = lines of target motion per frame time in elevation

FT = frame time

5.0 SAMPLE PROBLEM

(U) The calculations to relate the probability of acquisition of a ground target to image motion may be demonstrated by a sample problem. From 40) and 41), the number of TV raster lines subtended by a representative target were calculated as a function of range and plotted on Fig. 23 which assumes three targets offset at distances of 0, 250 or 500 feet respectively from the aircraft ground track and that the electro-optical sensor tracks a point on the flight

SECRET

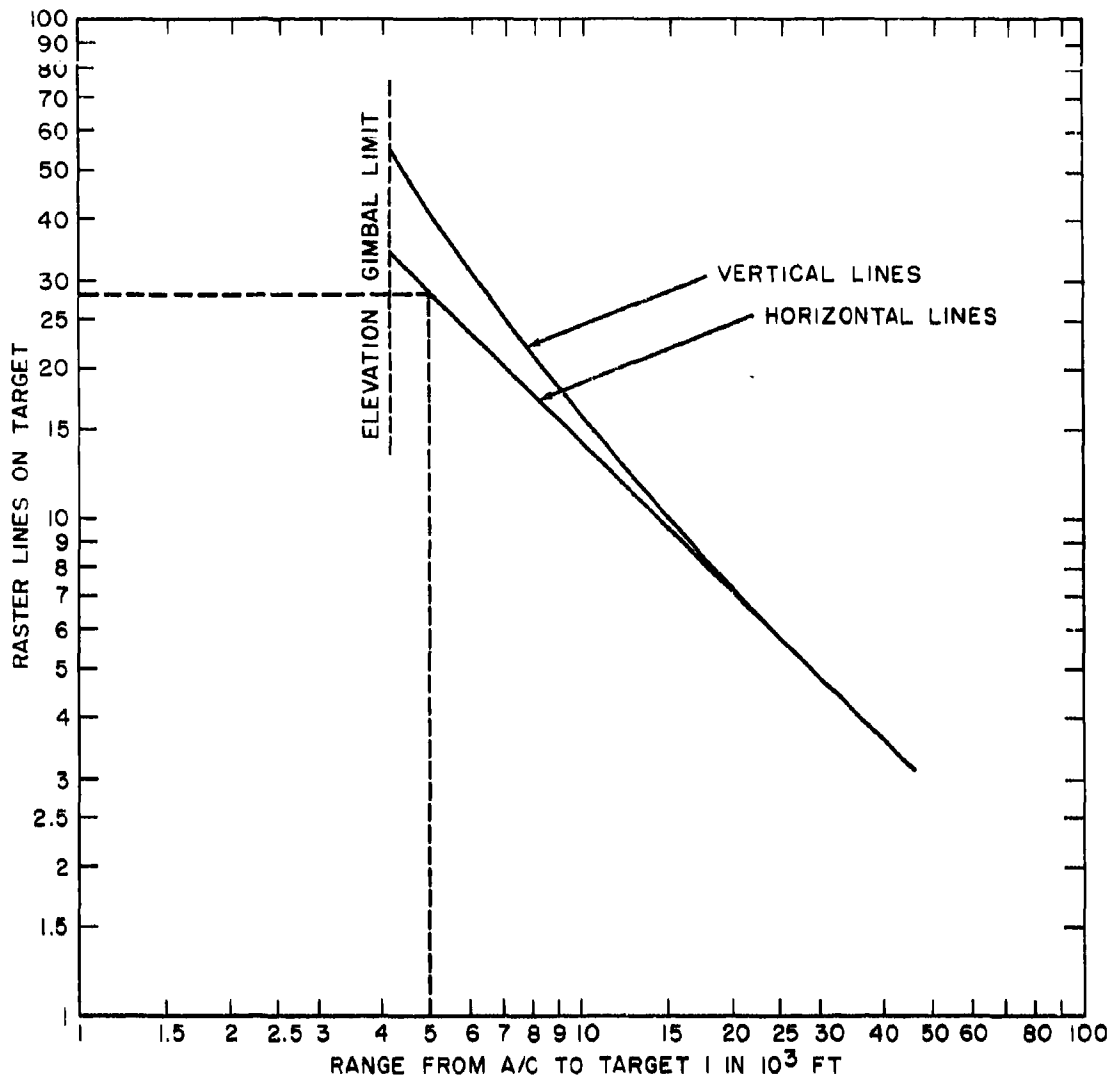


FIGURE 23 - NUMBER OF LINES ON TARGET (10' x 20' x 10') AS
A FUNCTION OF RANGE
TARGET OFFSET = 0,250 and 500 FEET
TACTIC A AND B (TV SENSOR) (U)

SECRET

path at the same range as the first target. The data shown in Fig. 23 were calculated for Tactics A and B which were described earlier. For this sample calculation, assume a LLTV system is employed and the target of interest is offset a distance of 250 feet from the flight path. From Fig. 23, it is observed that the target subtends 28 raster lines at a range of 5,000 feet.

(S) From 39), the target motion in TV raster lines per TV frame time was calculated and plotted in Fig. 24, which represents the maneuvers of Tactic A. At a range of 5,000 feet, the image motion is determined to be 3.3 lines/frame time. Figure 25, which relates TV raster lines to TV resolution lines, is generated by:

$$\text{Raster line} = \frac{875}{590} \text{ Resolvable line} \quad 44)$$

Note: System Resolution = 875 lines

System Resolution at 5% Aperture response = 590 lines

(S) The raster lines subtended by the target, and the image motion in raster lines per frame time, can be related to system resolution lines and resolution lines/frame time respectively by employing Fig. 25. As an example, at a range of 5,000 feet, the target subtends 19 resolution lines, and the image motion in resolution lines per frame time is determined to be 2.25 lines as shown on Fig. 25.

(S) Figure 18 relates lines of image motion per frame to apparent resolution in TV lines. Therefore, for an image motion of 2.25 resolution lines/frame time, the apparent TV resolution is reduced to 345 lines. Figure 26 shows the apparent system resolution as a function of range for Tactic A. It was derived from Figs. 18 and 24. Figure 27, which relates the apparent number of lines on the

SECRET

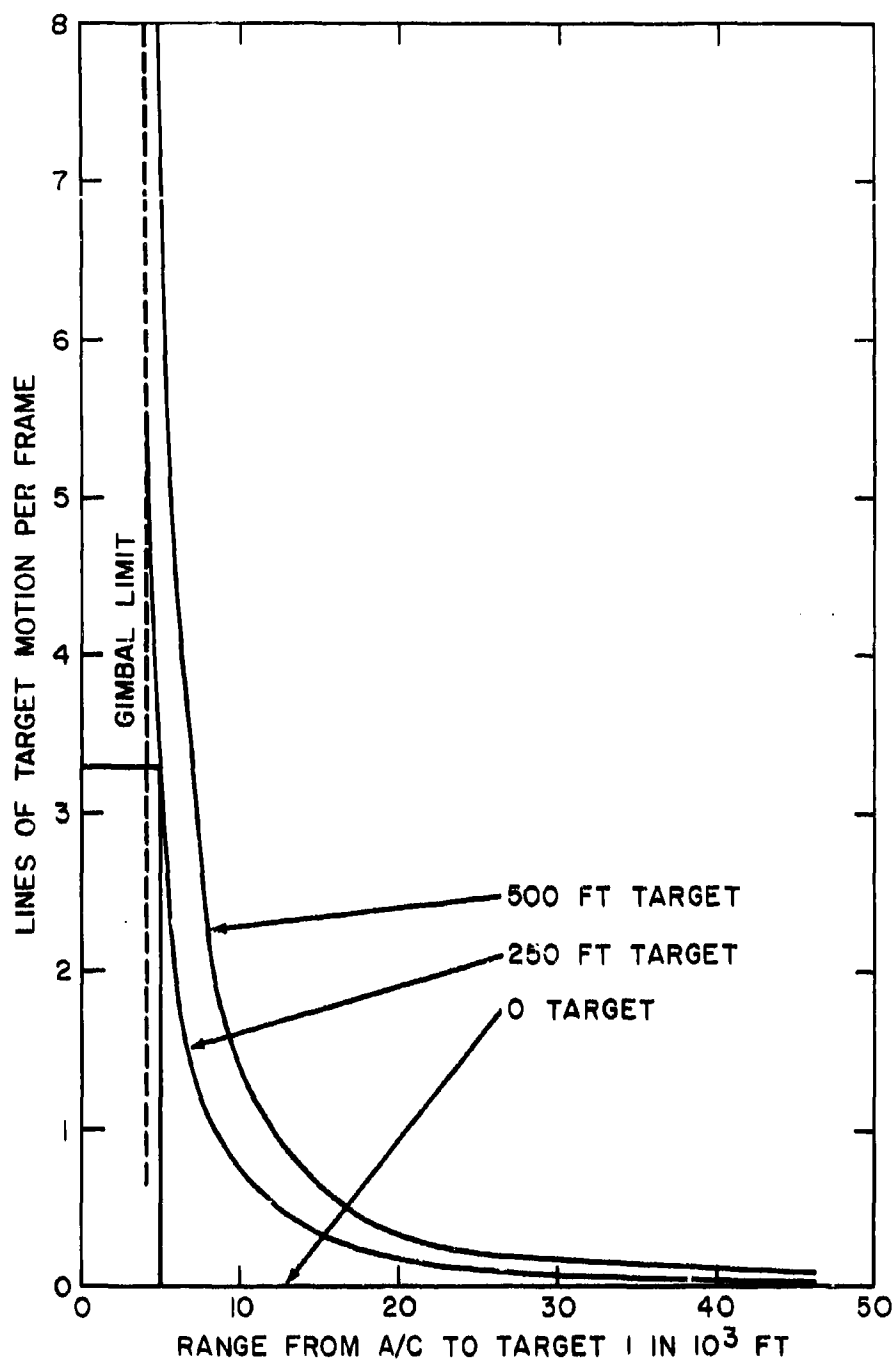


FIGURE 24 - TARGET MOTION PER FRAME AS A FUNCTION
OF RANGE
TARGET OFFSET - 0, 250, 500 FEET
TACTIC A (GROUND LOCK MODE)
(TV SENSOR) (U)

SECRET

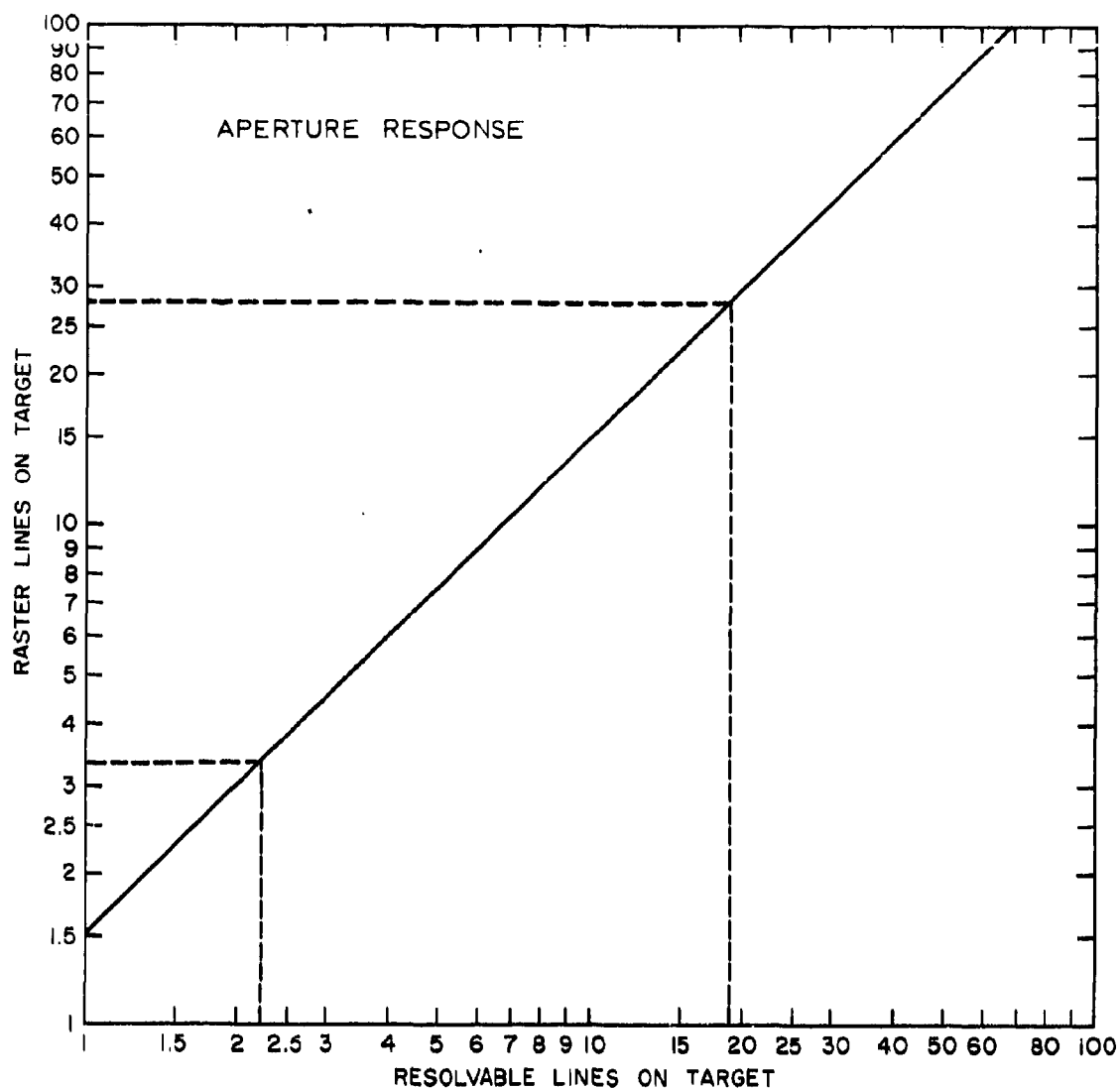


FIGURE 25 - CONVERSION OF RASTER LINES TO RESOLVABLE LINES ON TARGET FOR TV SYSTEM RESPONSE OF 590 LINES AT 5% CONTRAST (U)

SECRET

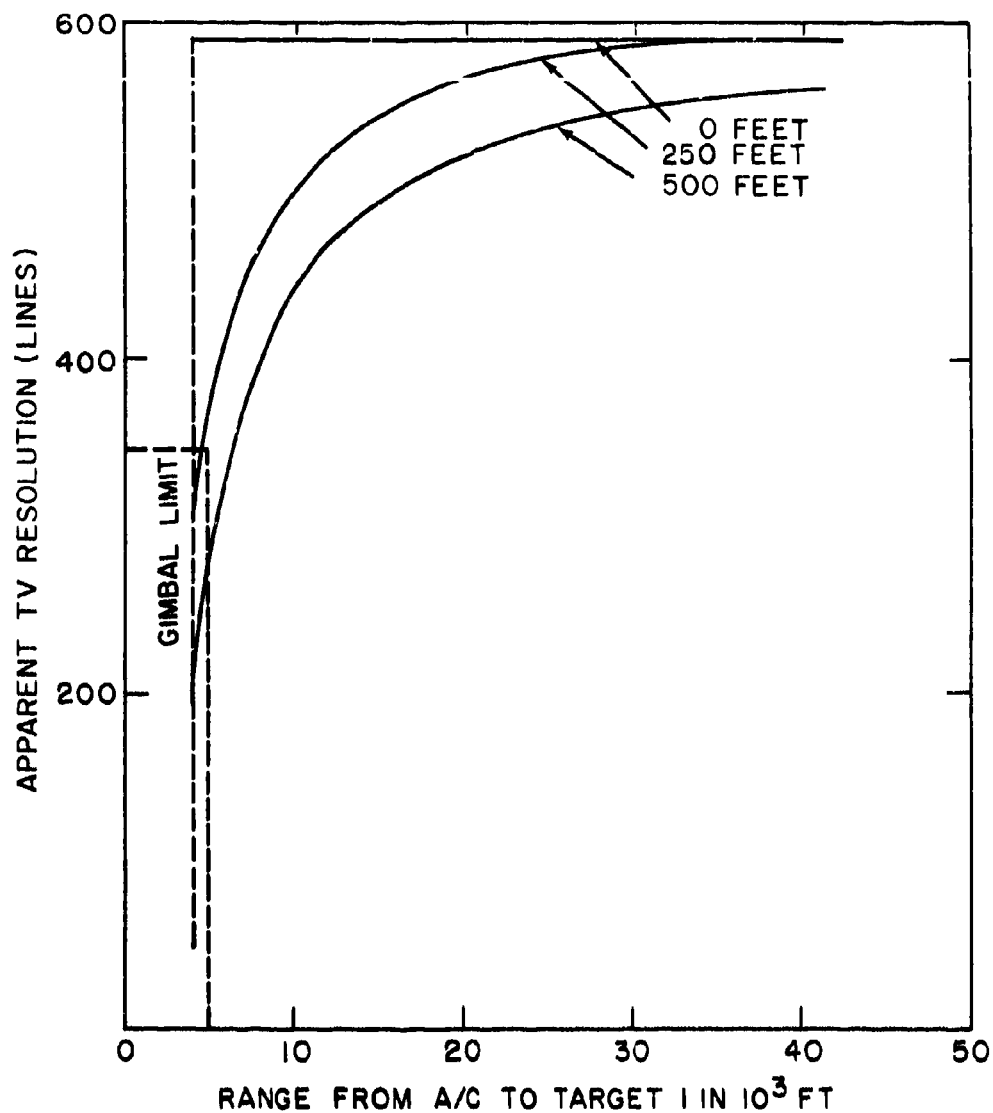


FIGURE 26 - APPARENT TV RESOLUTION AS A FUNCTION OF RANGE
TACTIC A GROUND LOCK MODE (TV SENSOR)
TARGET OFFSET 0, 250, 500 FEET (U)

SECRET

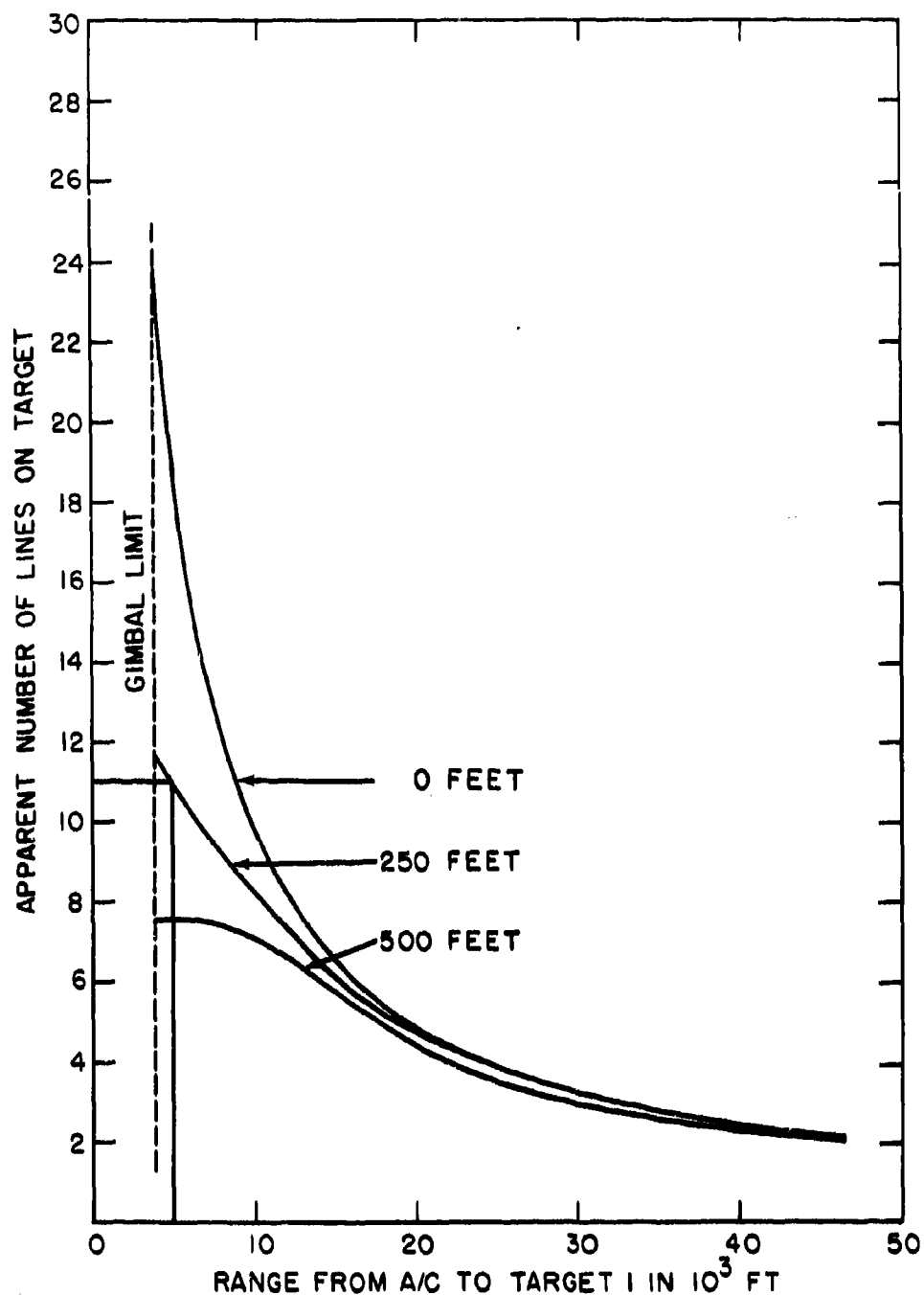


FIGURE 27 - APPARENT LINES ON TARGET AS A FUNCTION OF RANGE
TACTIC A GROUND LOCK MODE, TV SENSOR,
TARGET OFFSET 0, 250, 500 FEET (U)

SECRET

target to the range takes into account the resolution degradation due to image motion. It was generated from 45) using the data from Fig. 17, 18 and 26.

Apparent Lines on Target

Apparent TV Resolution x Resolvable Lines on Target
TV Resolution at 5% Response

45)

From Fig. 27, it can be seen that the number of apparent lines subtended by the target at a range of 5,000 feet is reduced to 11.1 lines.

(S) Figure 20 showed the cumulative probability of acquisition as a function of the number of resolution lines subtended by the target. Figure 28, which relates the cumulative probability of detection to range was derived from Figs. 20 and 27. From Fig. 28, it is observed that at a range of 5000 feet, the probability of target acquisition is 1.0 for the target offset at 250 feet.

(U) The above explanation indicates the procedure involved in developing the data shown in Section VII, the final output being the cumulative probability of target detection as a function of range.

6.0 RESULTS

(U) Plots of resolution degradation due to aircraft motion for Tactic A are given in Figs. 23-28. Figures 29-34 relate target motion to resolution degradation for Tactic B. Figures 35 and 36 are plots of the cumulative probability of detection versus range for the various roll rates and target offsets defined by Tactic B. Figures 37-40 describe resolution degradation for Tactic C, while Fig. 41 presents plots of the cumulative probability of detection for Tactic C. The resolution degradation plots for Tactic D are given in Figs. 42-47, while the cumulative probability plots for Tactic D are given in Figs. 48-49.

(U) In the figures listed above, it was assumed that the sensor was locked onto

SECRET

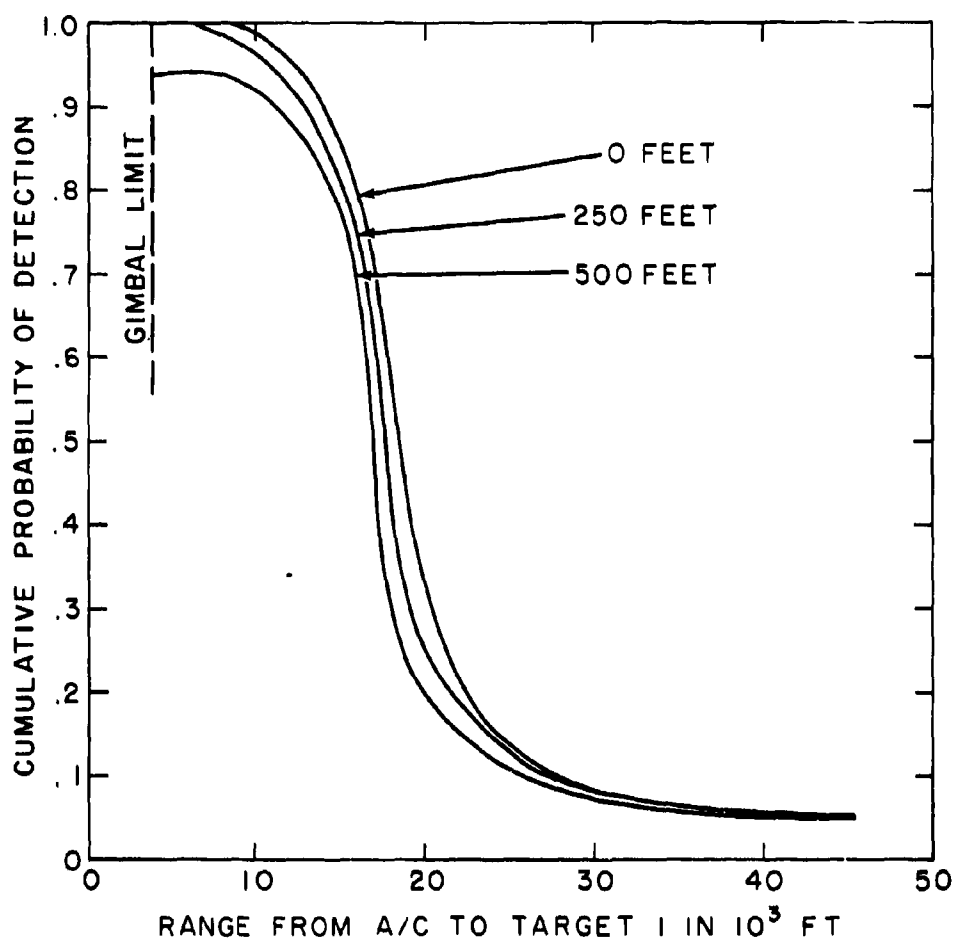


FIGURE 28 - CUMULATIVE PROBABILITY OF DETECTION AS A
FUNCTION OF RANGE
TACTIC A GROUND LOCK MODE, TV SENSOR,
TARGET OFFSET 0, 250, 500 FEET (S)

SECRET

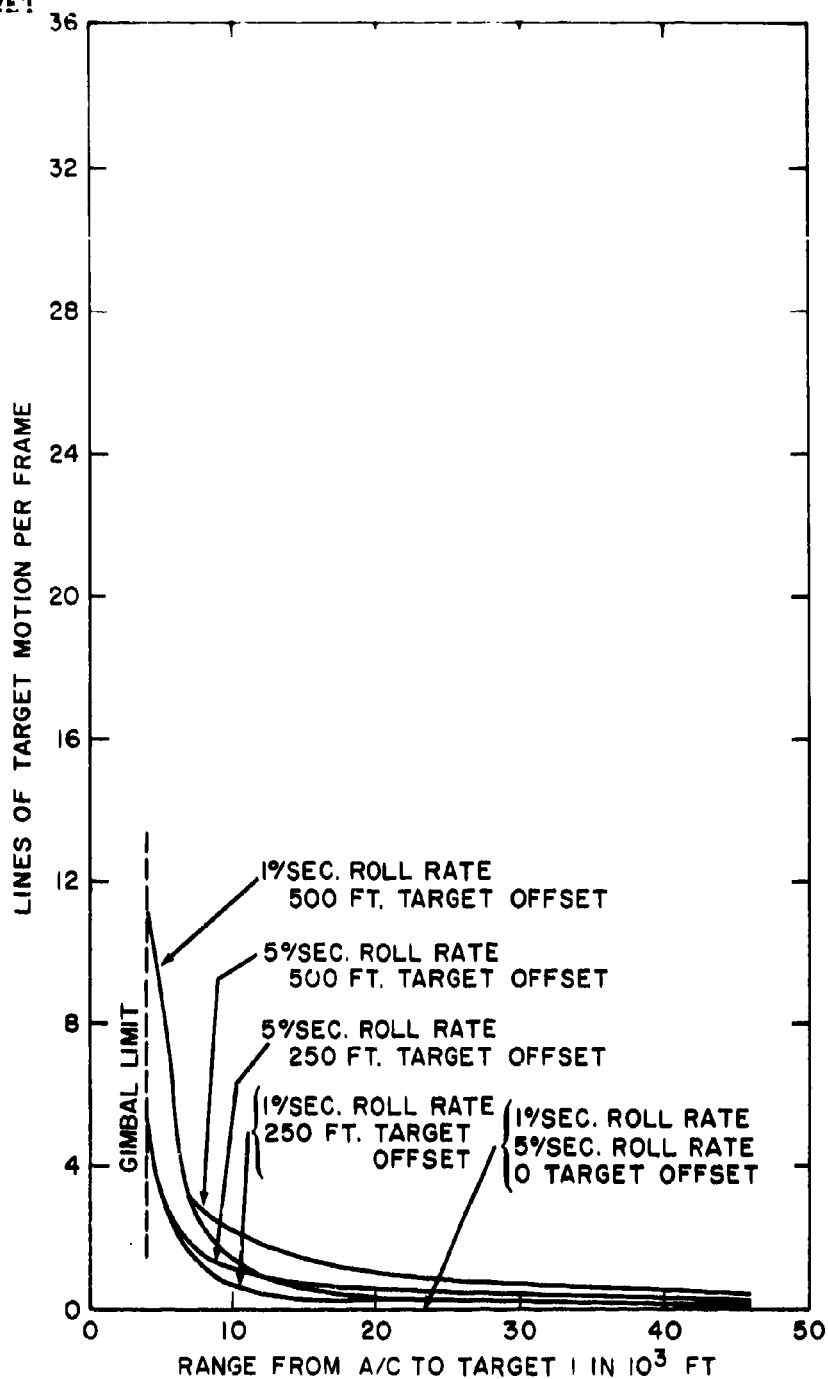


FIGURE 29 - TARGET MOTION PER FRAME AS A FUNCTION OF RANGE
TACTIC B GROUND LOCK MODE, TV SENSOR
1°/SEC AND 5°/SEC ROLL RATES (U)

SECRET

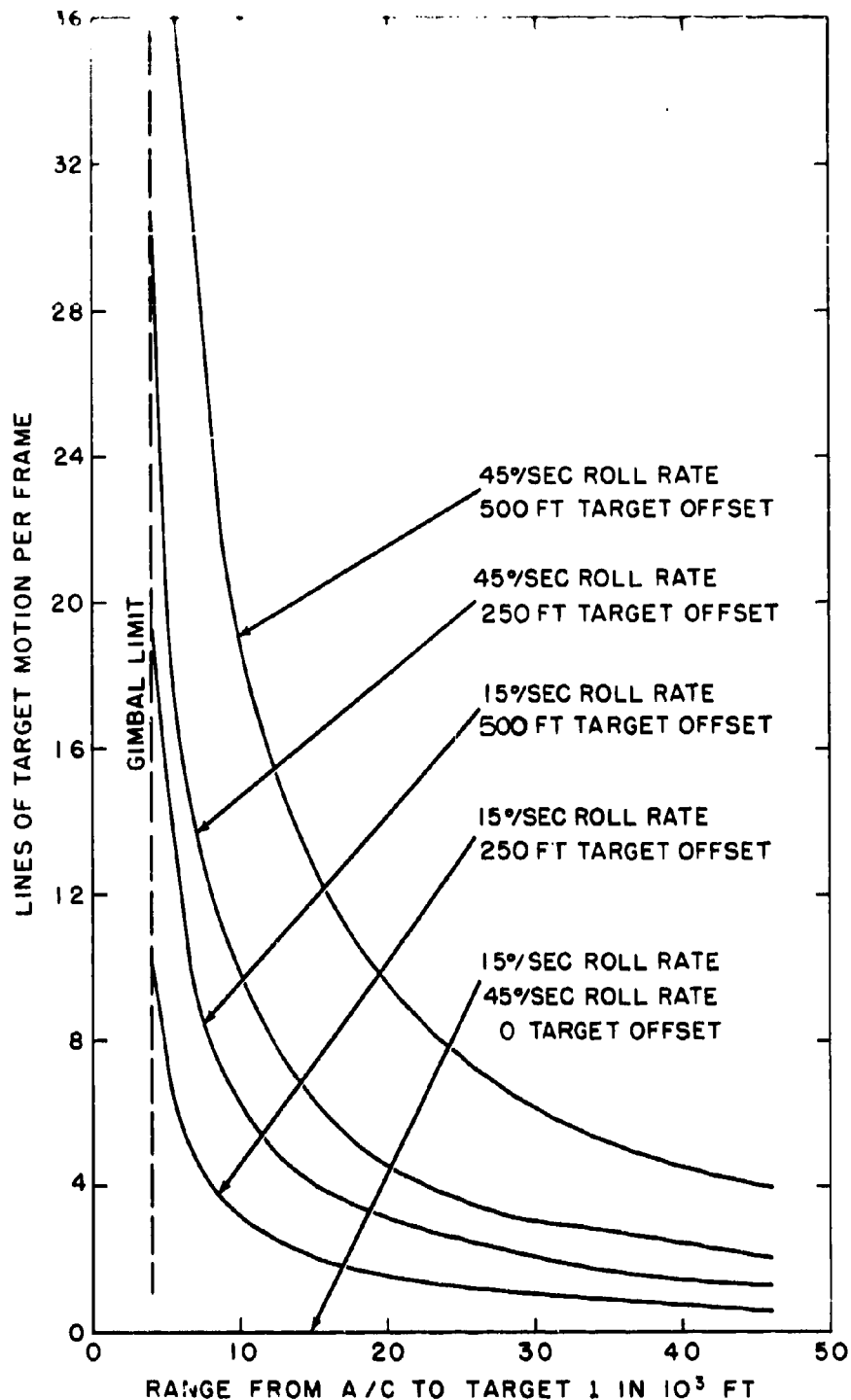


FIGURE 30 - TARGET MOTION PER FRAME AS A FUNCTION OF RANGE
TACTIC B GROUND LOCK MODE, TV SENSOR
15°/SEC AND 45°/SEC ROLL RATES (U)

SECRET

SECRET

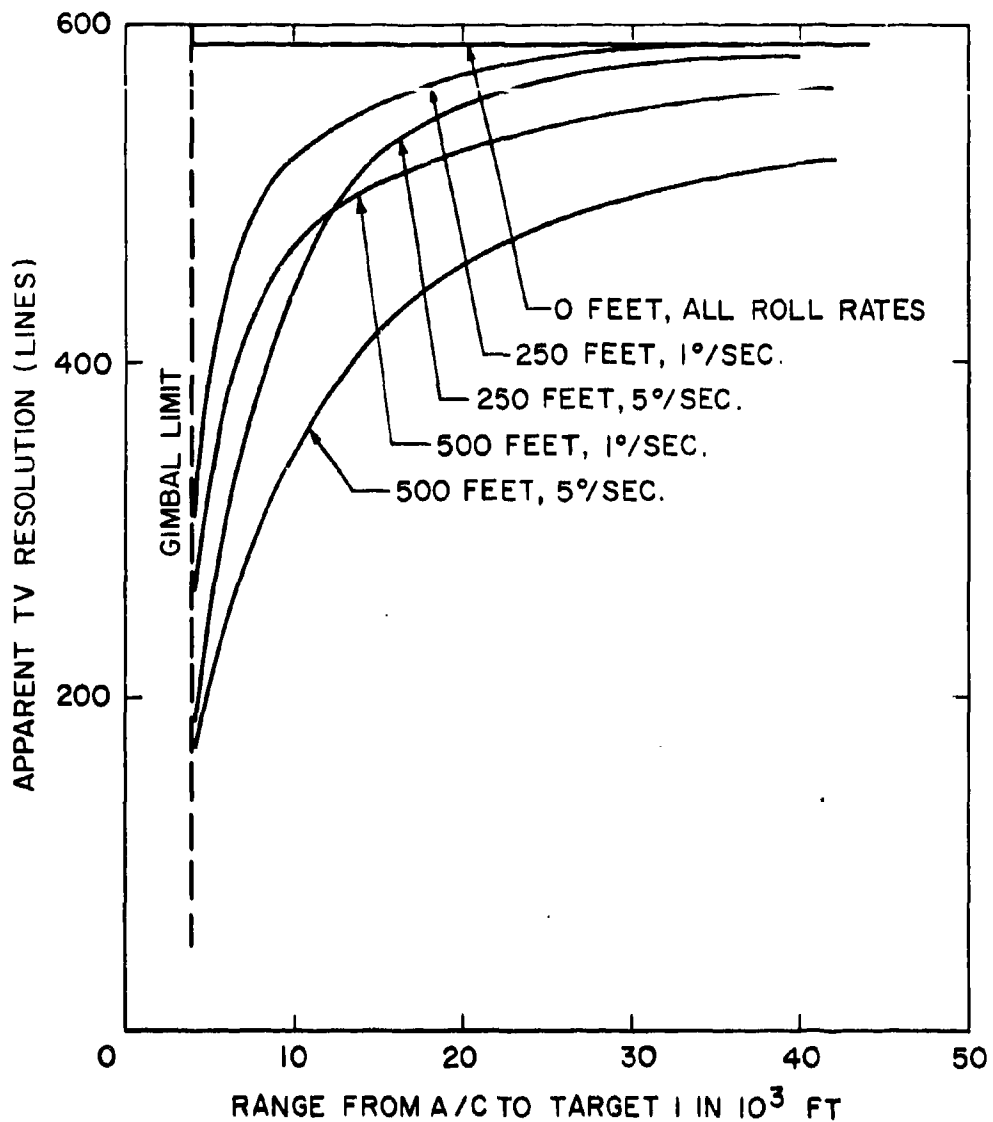


FIGURE 31 - APPARENT TV RESOLUTION AS A FUNCTION OF RANGE
TACTIC B GROUND LOCK MODE, TV SENSOR
 $1^\circ/\text{SEC}$ AND $5^\circ/\text{SEC}$ ROLL RATES (U)

SECRET

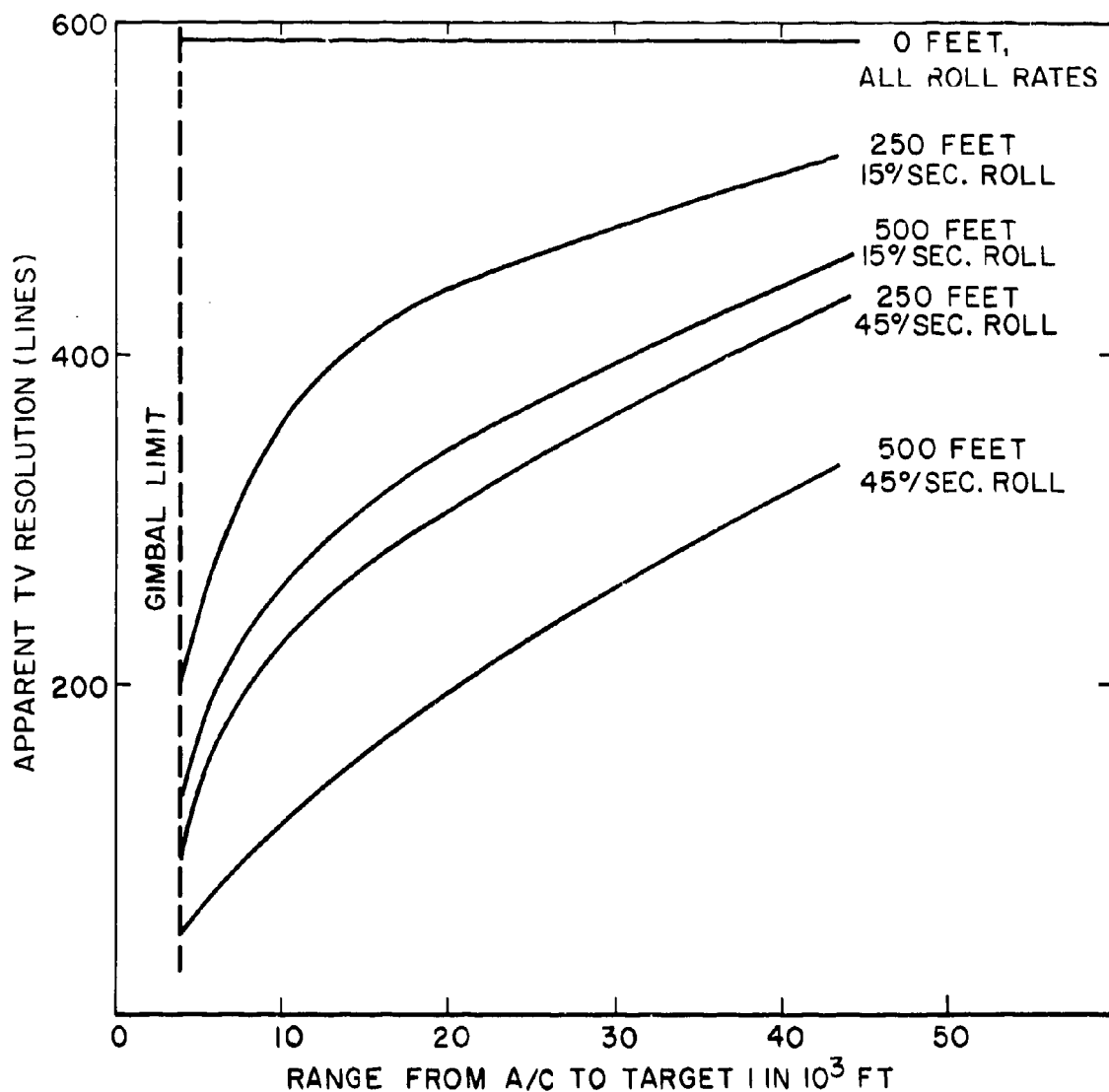


FIGURE 32 - APPARENT TV RESOLUTION AS A FUNCTION OF RANGE
TACTIC B GROUND LOCK MODE, TV SENSOR
15°/SEC AND 45°/SEC ROLL RATES (U)

SECRET

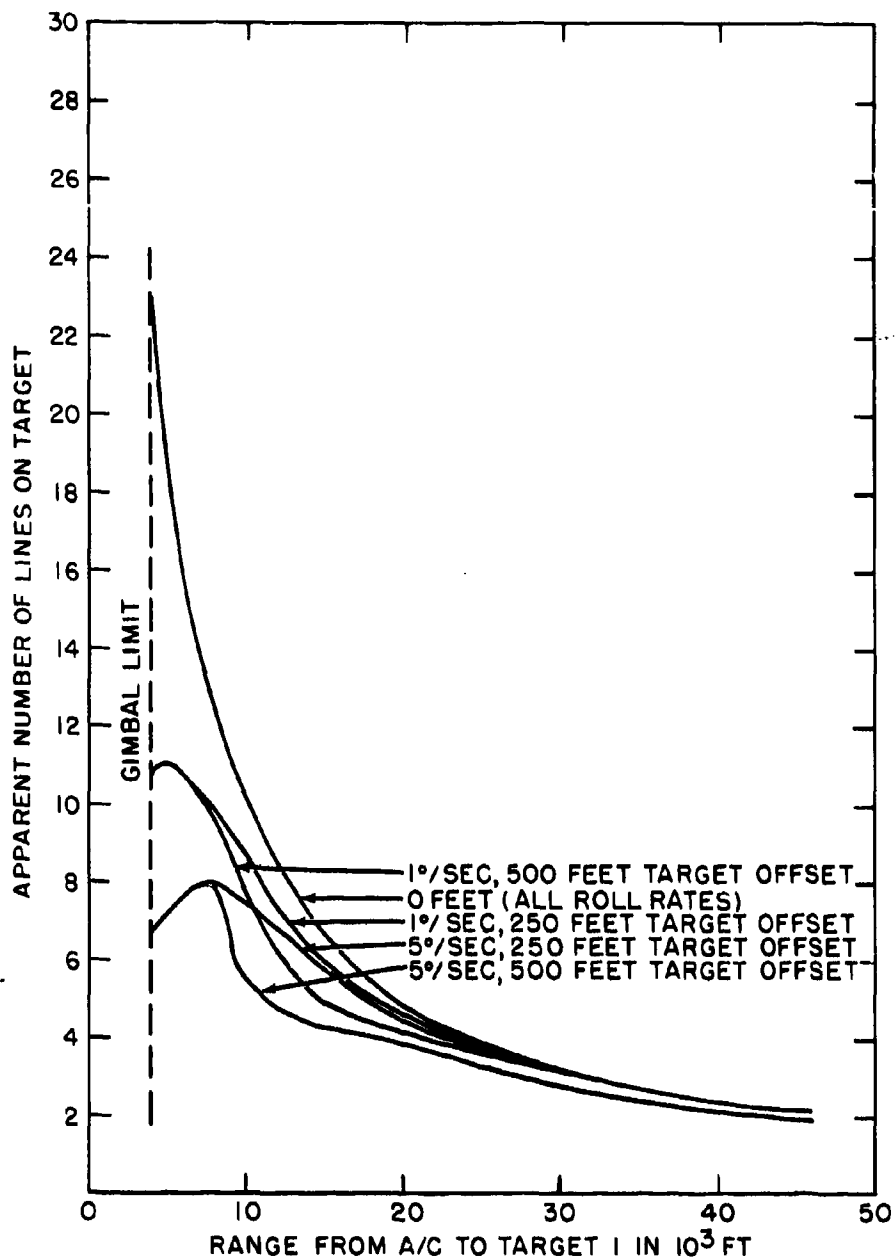


FIGURE 33 - APPARENT LINES ON TARGET AS A FUNCTION OF RANGE
TACTIC B GROUND LOCK MODE, TV SENSOR
1°/SEC AND 5°/SEC ROLL RATES (U)

REF.

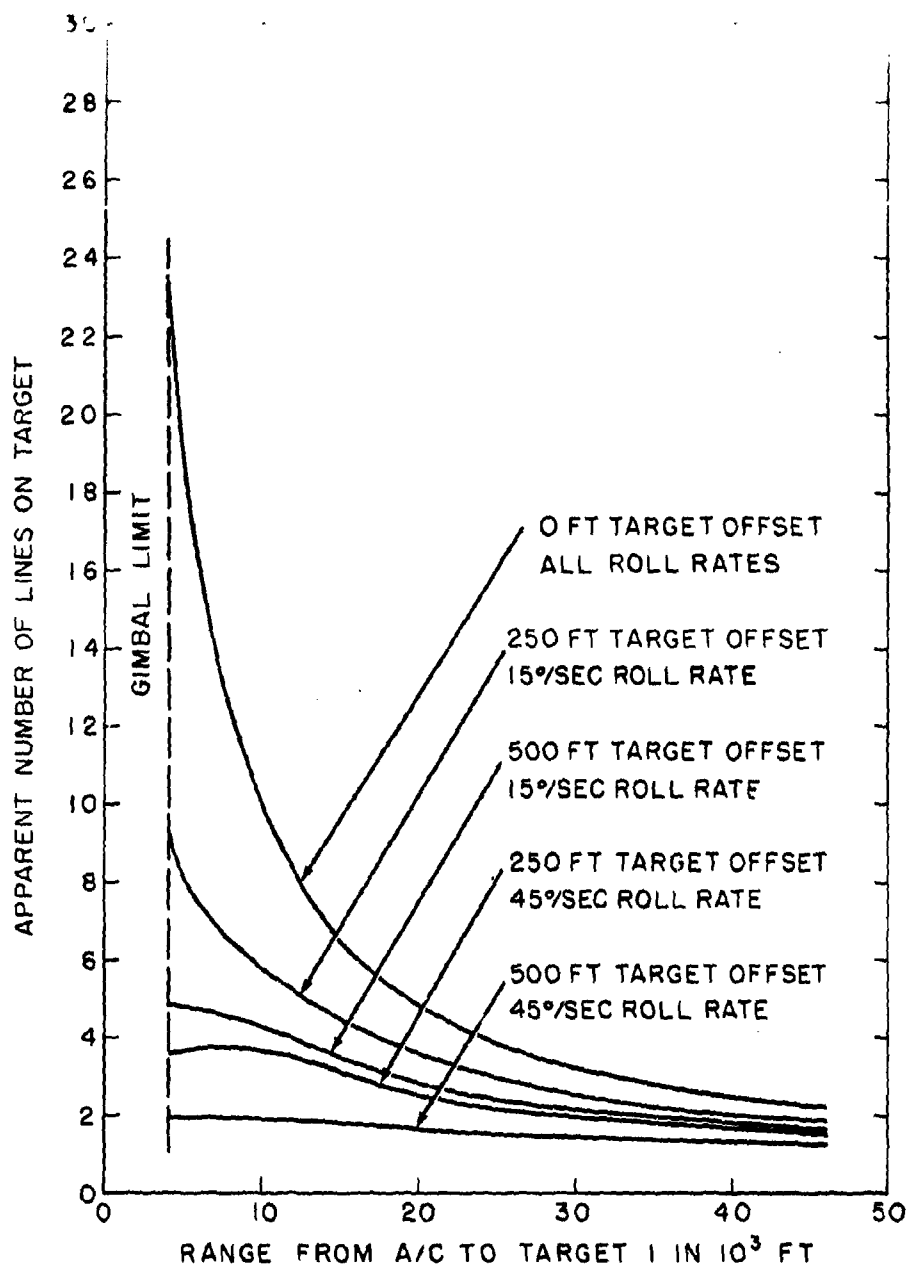


FIGURE 34 - APPARENT LINES ON TARGET AS A FUNCTION OF RANGE
TACTIC B GROUND LOCK MODE, TV SENSOR
15°/SEC AND 45°/SEC ROLL RATES (U)

SECRET

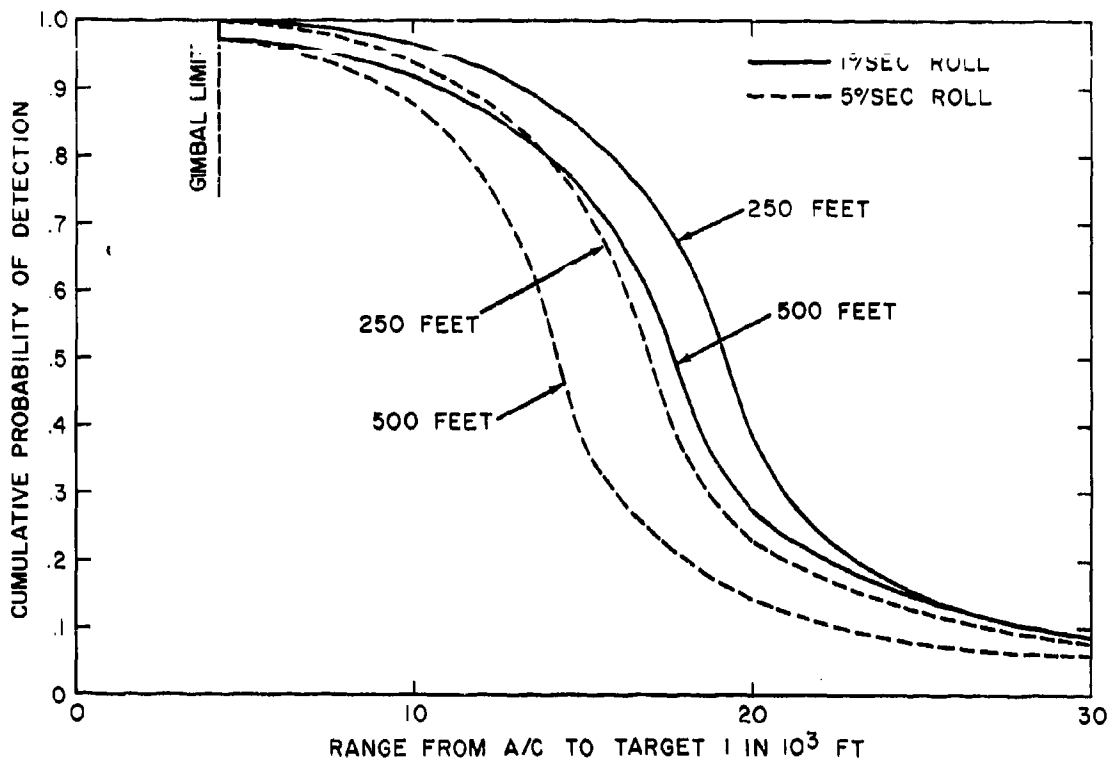


FIGURE 35 - CUMULATIVE PROBABILITY OF DETECTION AS A FUNCTION OF RANGE
TACTIC B GROUND LOCK MODE, TV SENSOR
1°/SEC AND 5°/SEC ROLL RATES (U)

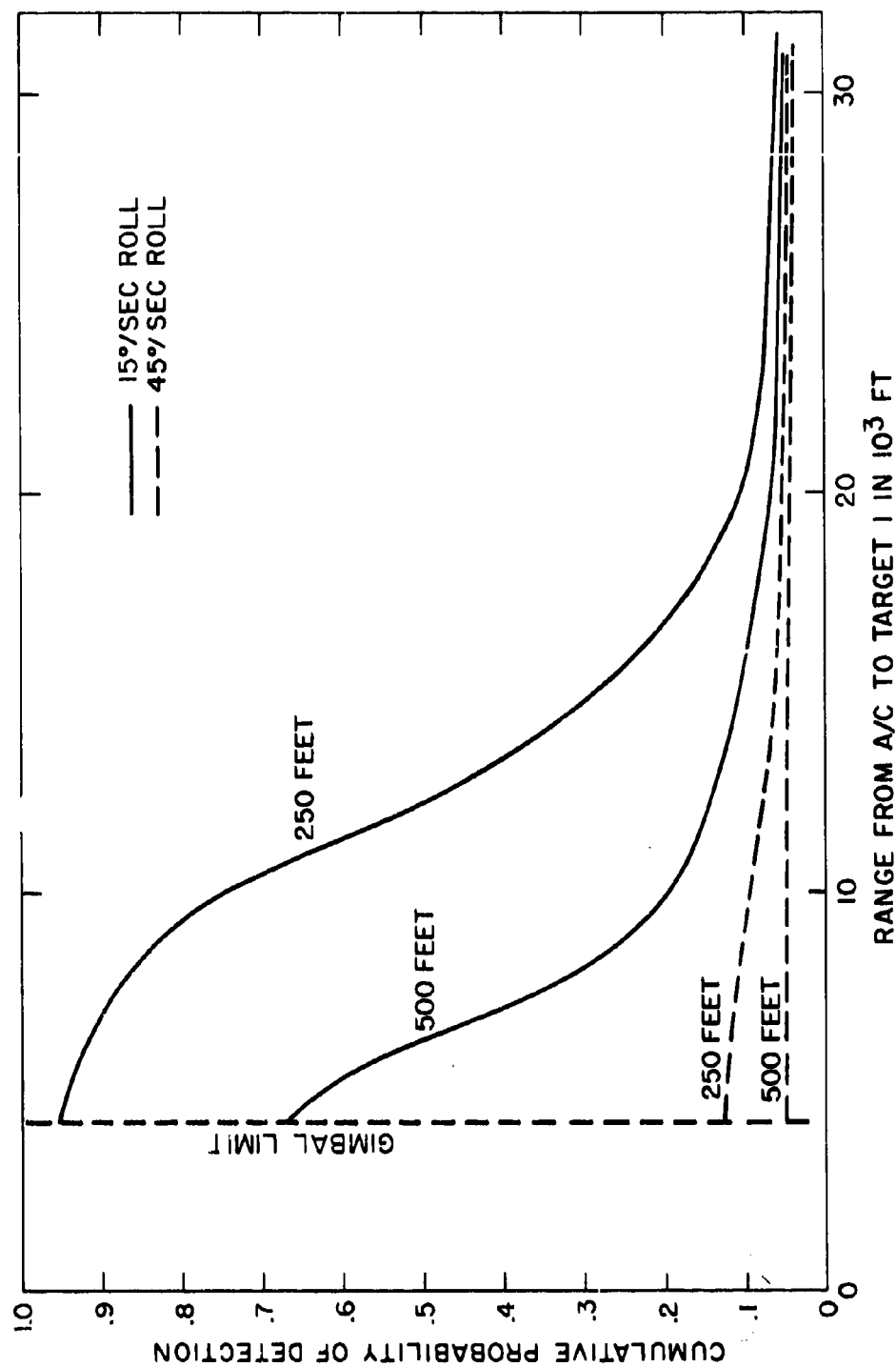


FIGURE 36 - CUMULATIVE PROBABILITY OF DETECTION AS A FUNCTION OF RANGE
TACTIC B GROUND LOCK MODE, TV SENSOR
15°/SEC AND 45°/SEC ROLL RATES (U)

SECRET

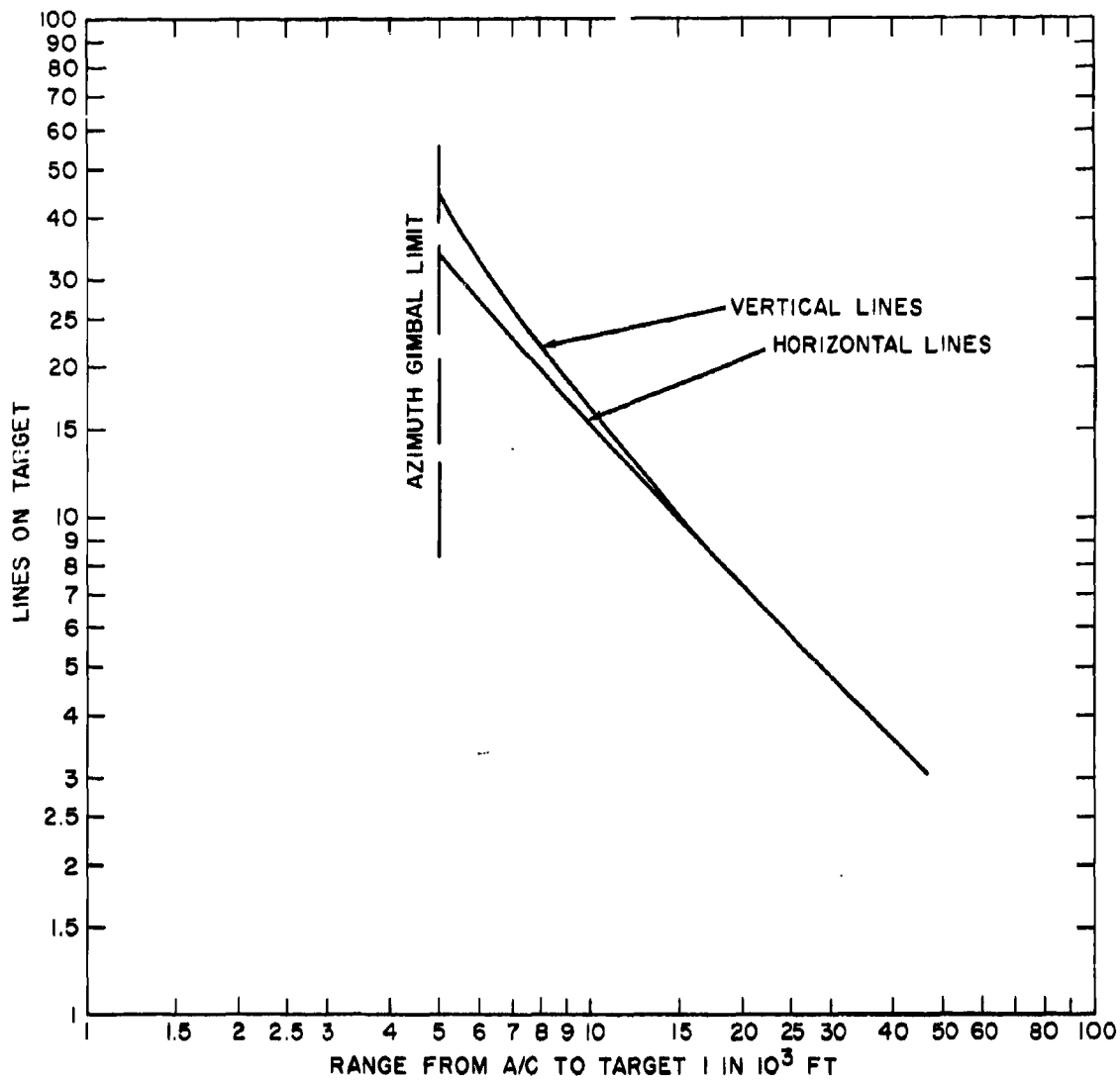


FIGURE 37 NUMBER OF LINES ON TARGET (10' x 20' x 10') AS A FUNCTION OF RANGE FOR 2500, 2750, AND 3000 FEET TARGET OFFSETS TACTIC C AND D (TV SENSOR) (U)

SECRET

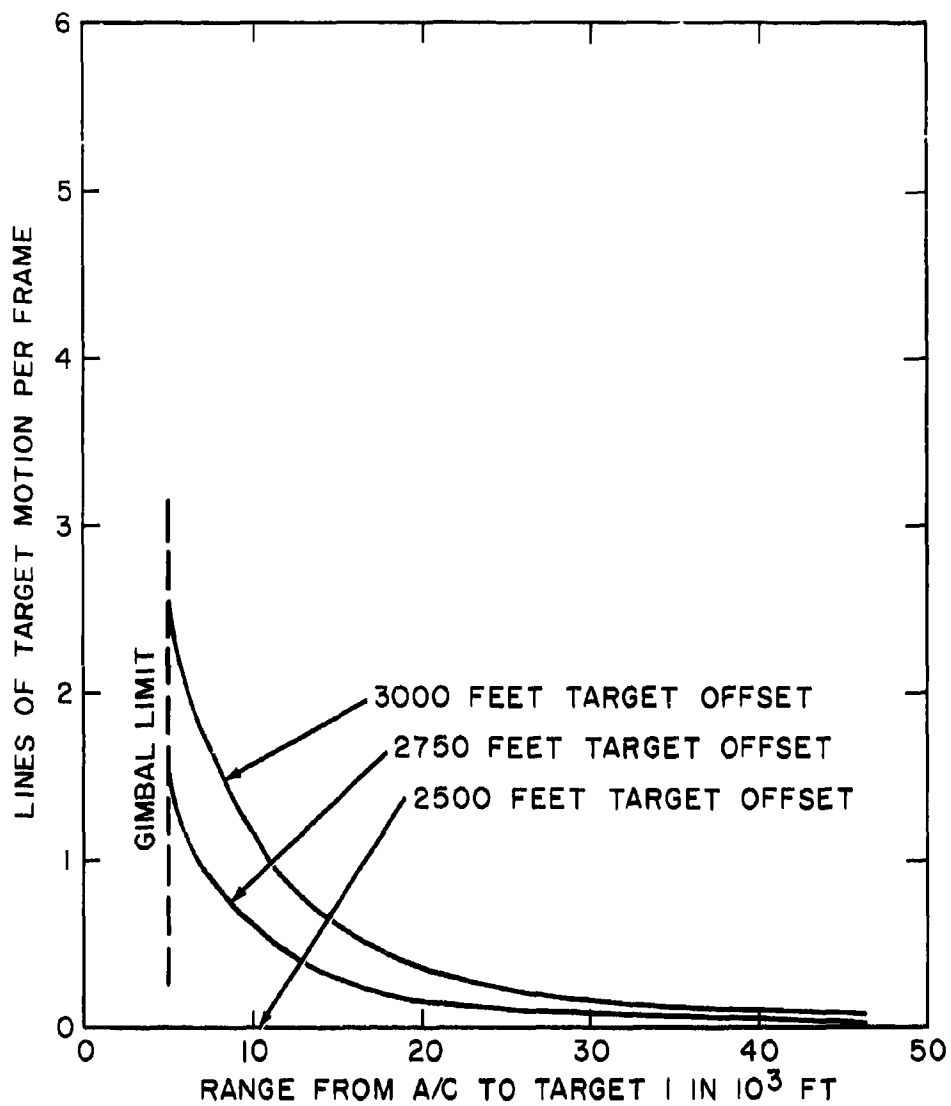


FIGURE 38 - TARGET MOTION PER FRAME AS A FUNCTION
OF RANGE
TACTIC C GROUND LOCK MODE, TV SENSOR
2500, 2750, AND 3000 FEET TARGET OFFSET (U)

SECRET

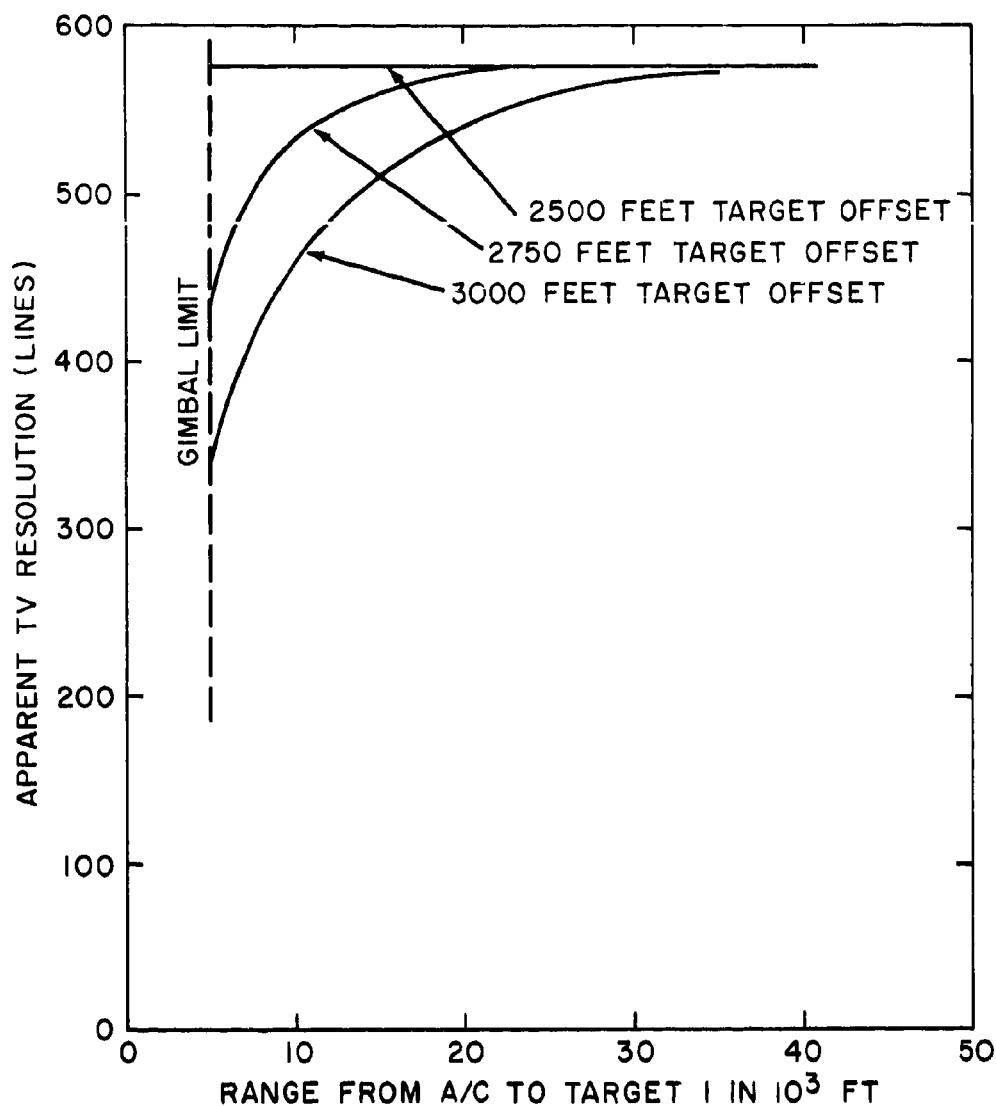


FIGURE 39 - APPARENT TV RESOLUTION AS A FUNCTION OF RANGE
TACTIC C GROUND LOCK MODE, TV SENSOR
2500, 2750, AND 3000 FEET TARGET OFFSET (U)

SECRET

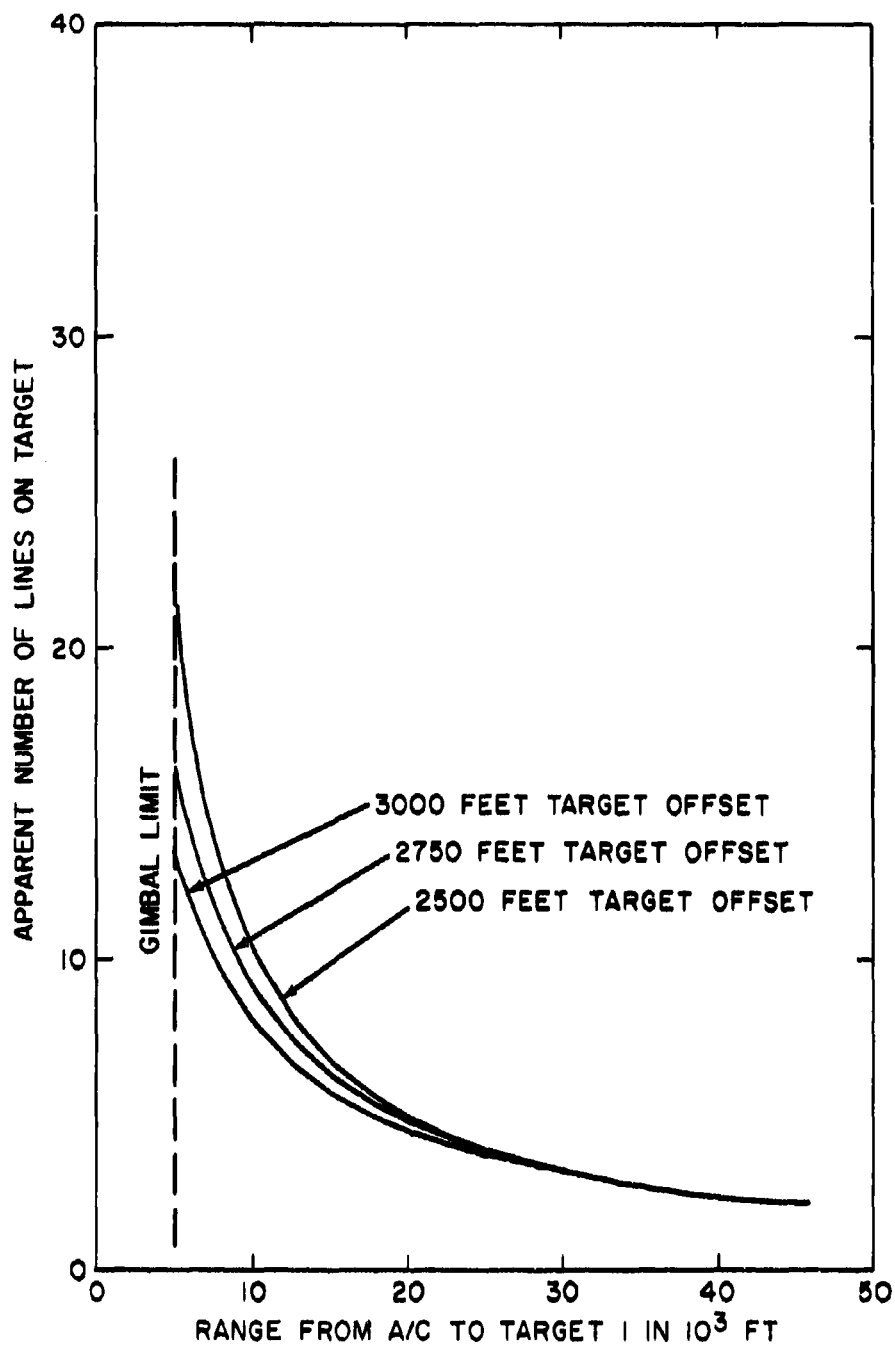


FIGURE 40 - APPARENT LINES ON TARGET AS A FUNCTION OF RANGE
TACTIC C GROUND LOCK MODE, TV SENSOR
2500, 2750, AND 3000 FEET TARGET OFFSETS (U)

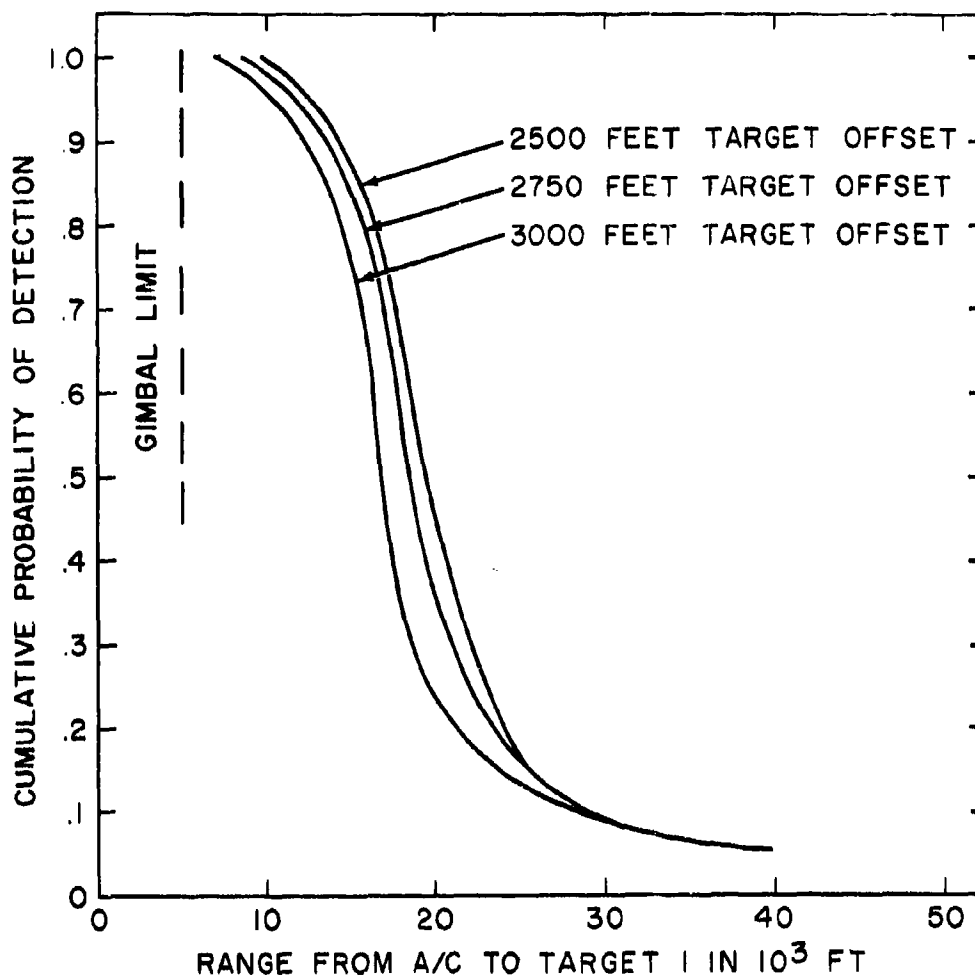


FIGURE 41 - CUMULATIVE PROBABILITY OF DETECTION AS A
FUNCTION OF RANGE
FOR TACTIC C GROUND LOCK MODE, TV SENSOR
2500, 2750, AND 3000 FEET TARGET OFFSETS (U)

SECRET

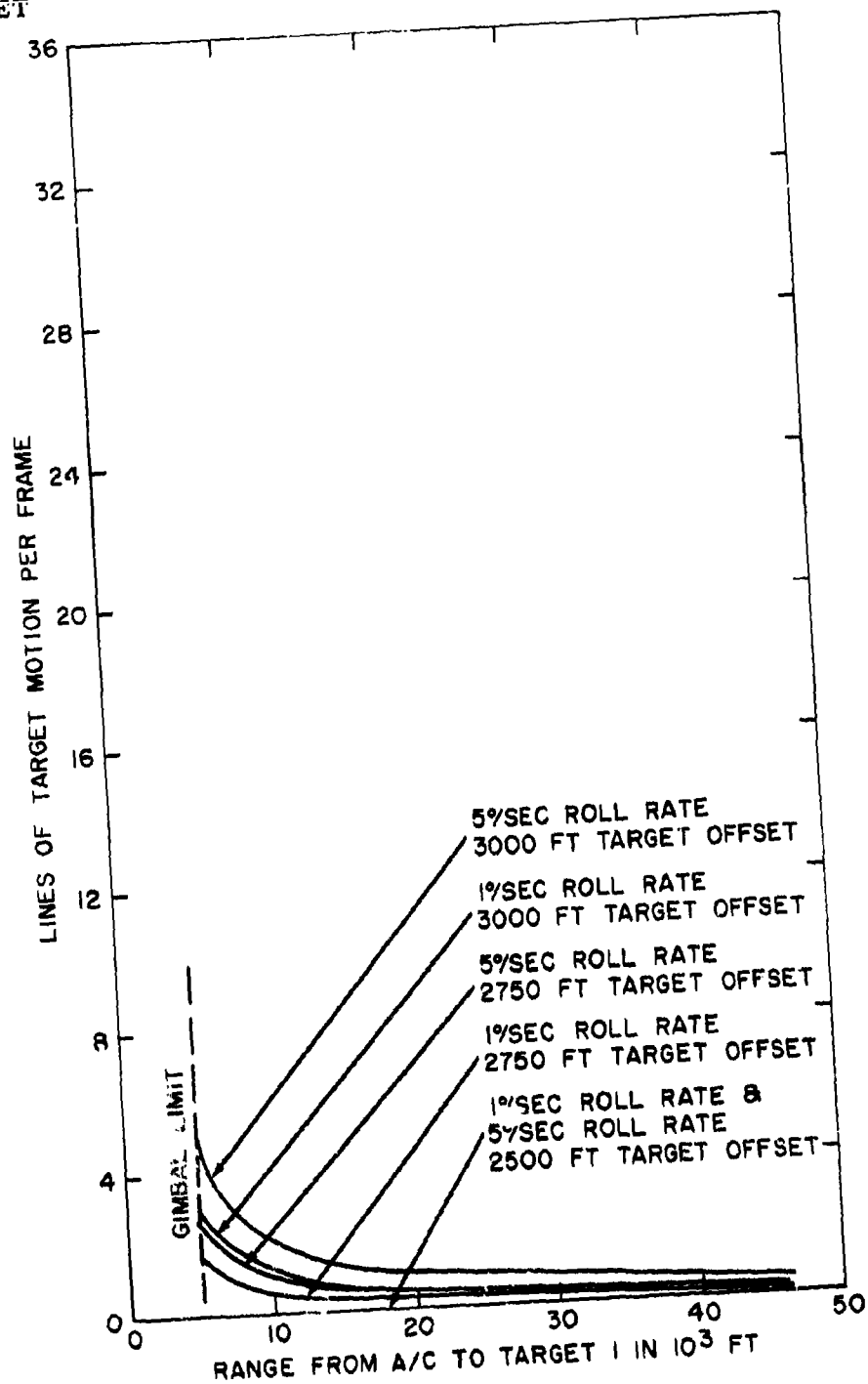


FIGURE 42 - TARGET MOTION PER FRAME AS A FUNCTION OF RANGE TACTIC D GROUND LOCK MODE, TV SENSOR 1°/SEC AND 5°/SEC ROLL RATES (U)

SECRET

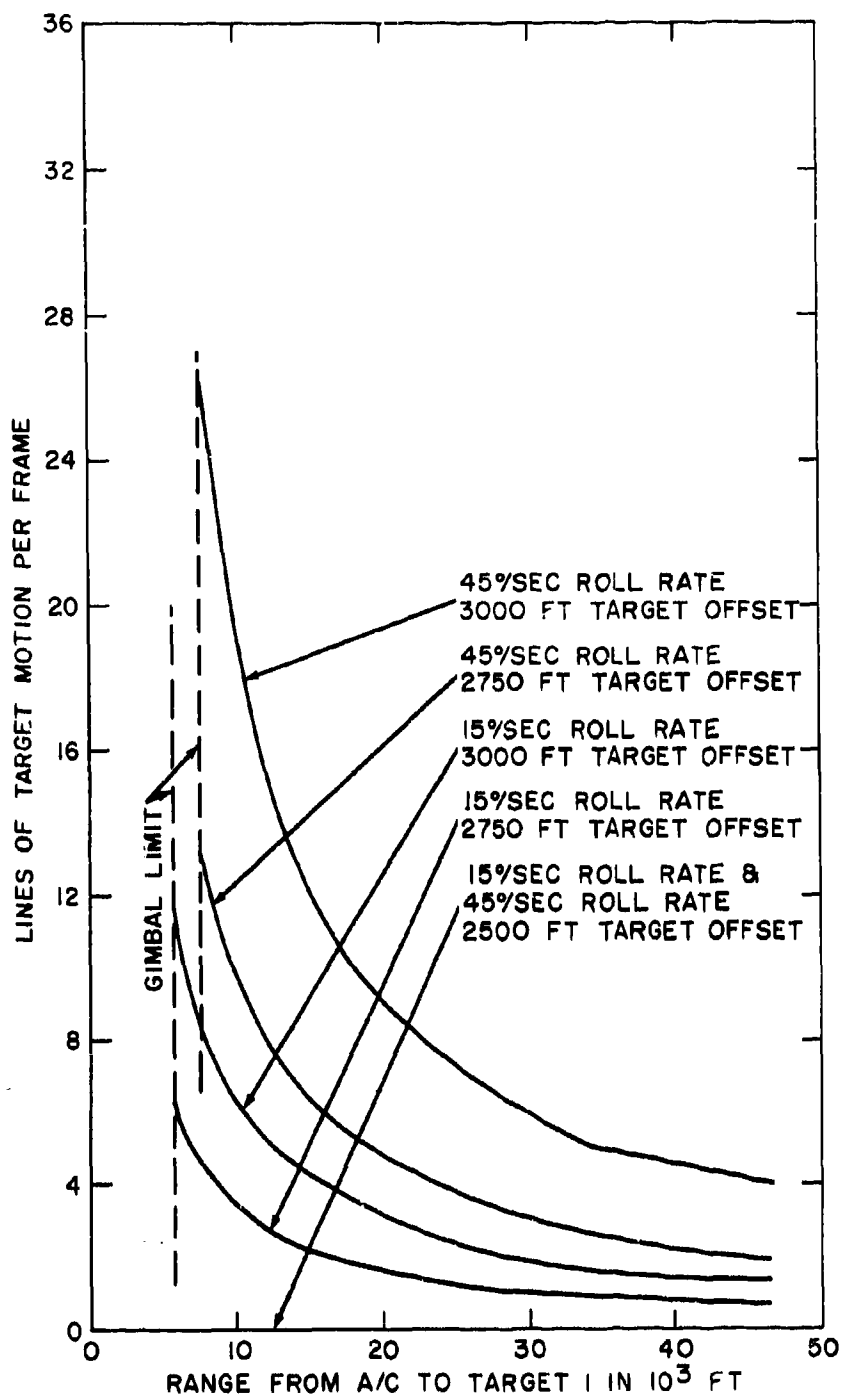


FIGURE 43 - TARGET MOTION PER FRAME AS A FUNCTION OF RANGE TACTIC D GROUND LOCK MODE, TV SENSOR 15°/SEC AND 45°/SEC ROLL RATES (U)

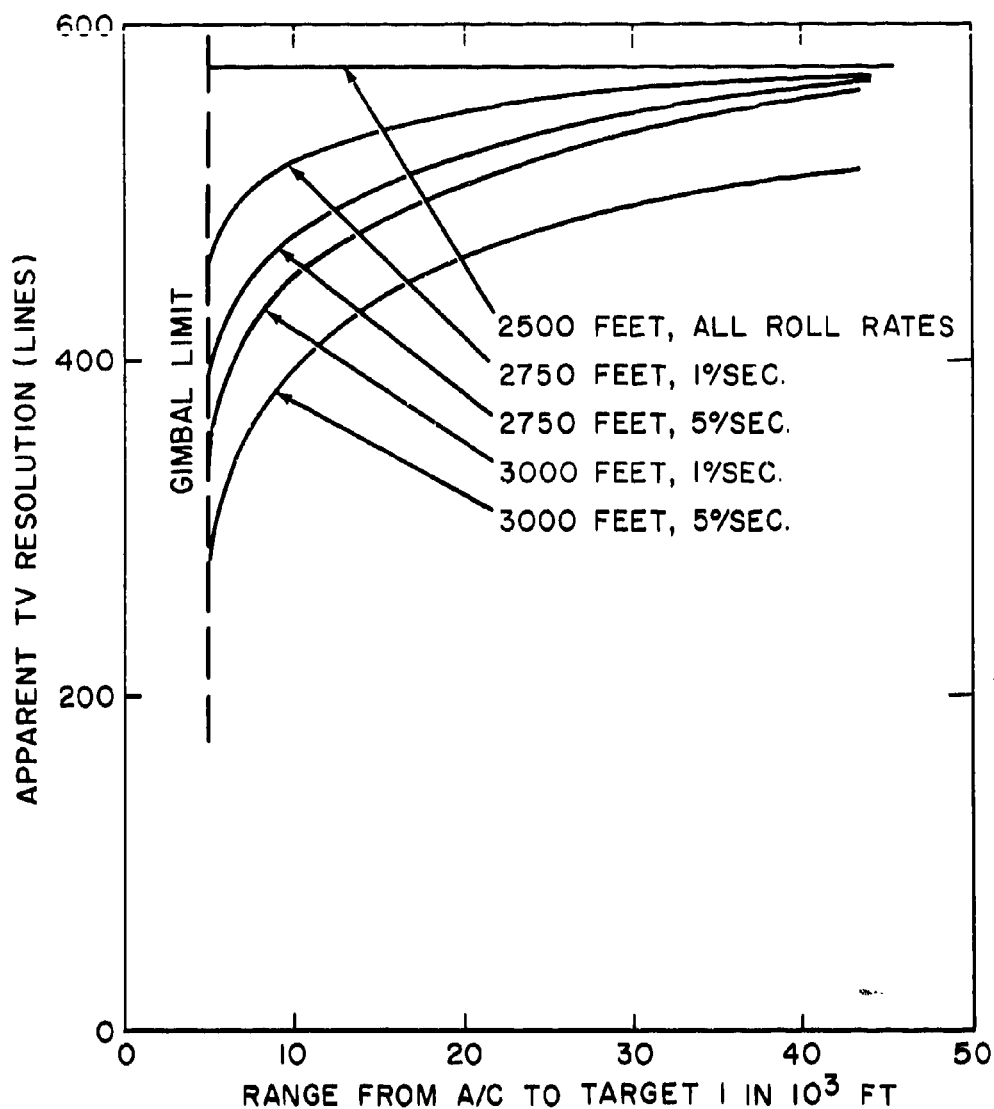


FIGURE 44 - APPARENT TV RESOLUTION AS A FUNCTION OF RANGE TACTIC D GROUND LOCK MODE, TV SENSOR $1^\circ/\text{SEC}$ AND $5^\circ/\text{SEC}$ ROLL RATES (U)

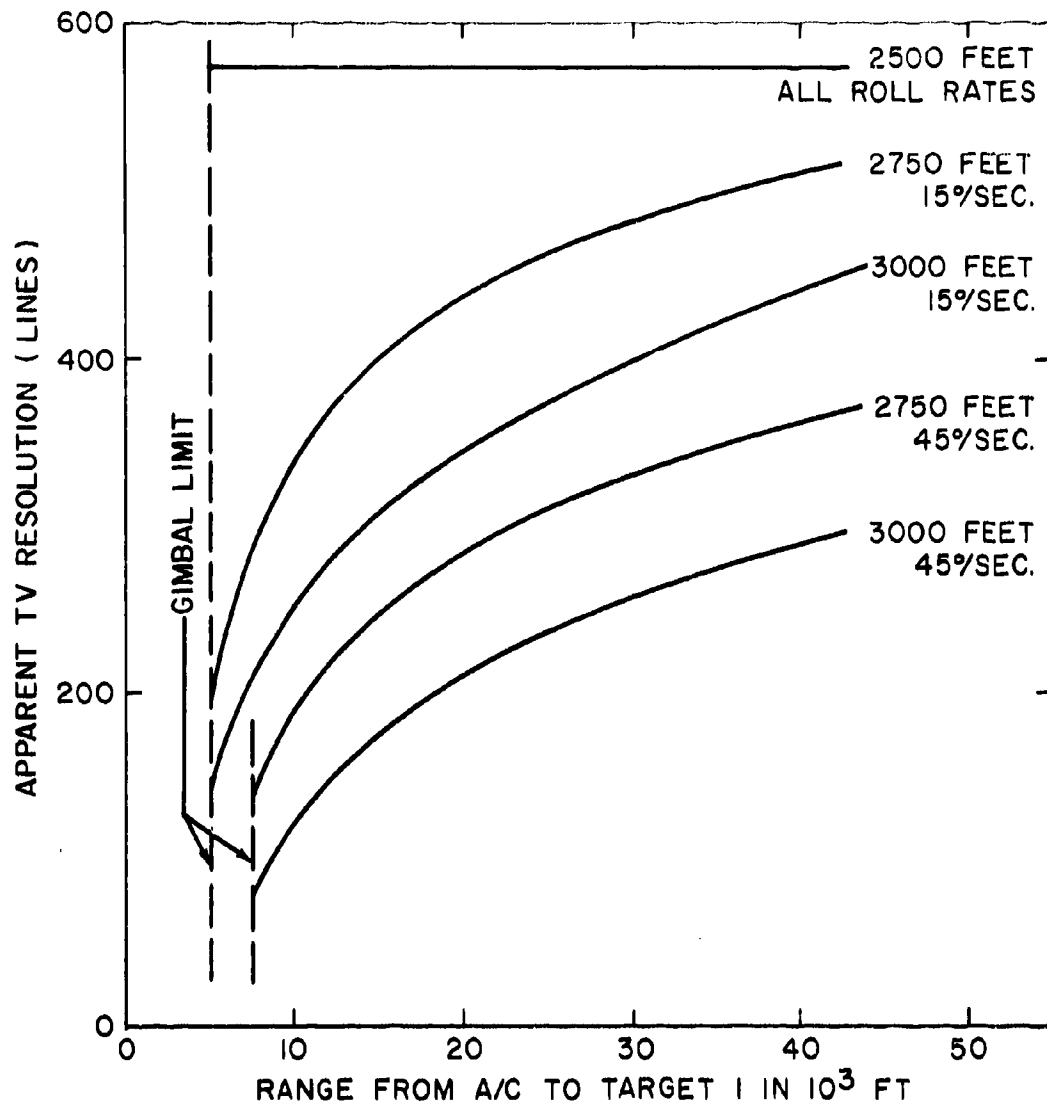


FIGURE 45 - APPARENT TV RESOLUTION AS A FUNCTION OF RANGE TACTIC D GROUND LOCK MODE, TV SENSOR 15°/SEC AND 45°/SEC ROLL RATES (U)

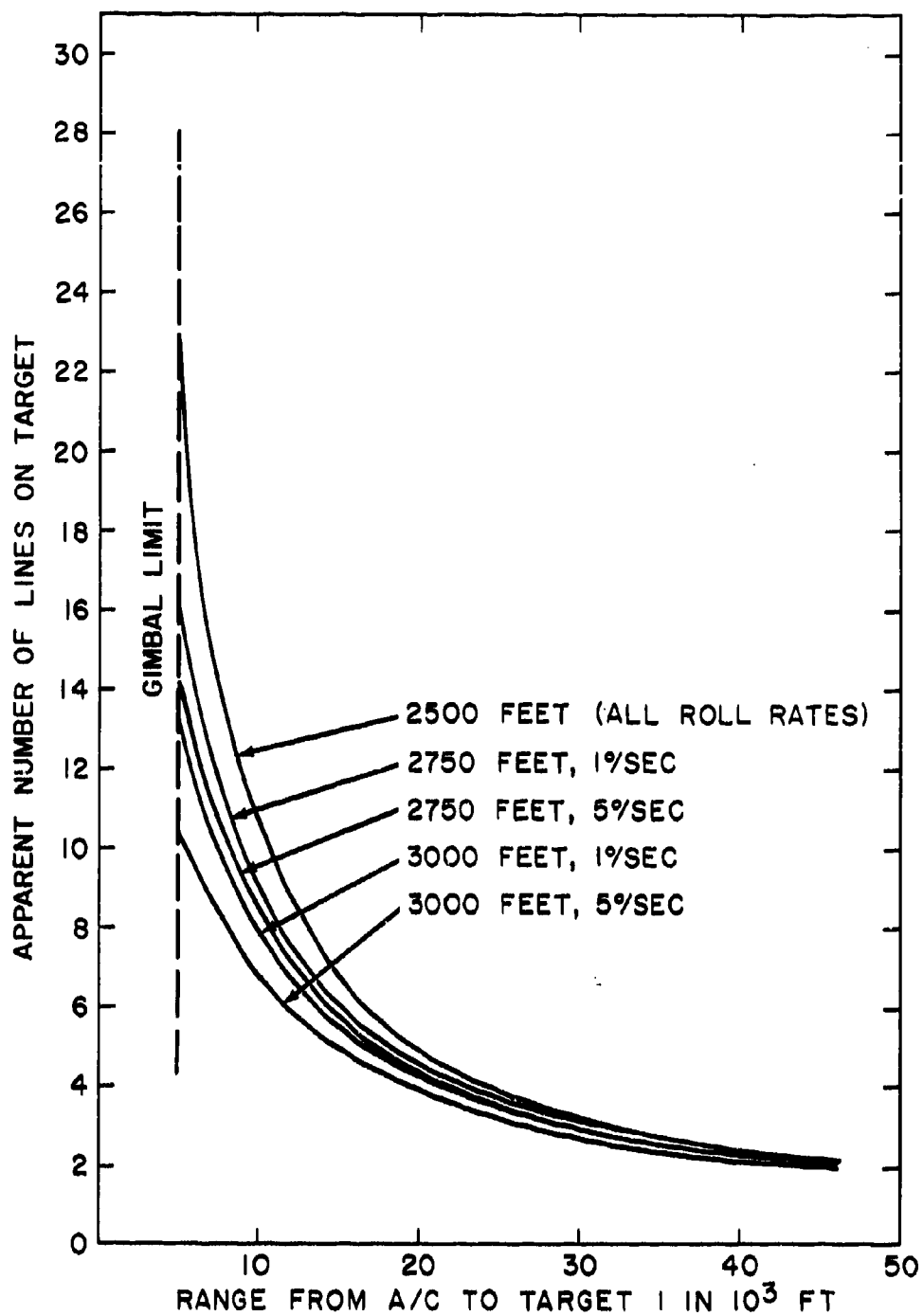


FIGURE 46 - APPARENT LINES ON TARGET AS A FUNCTION OF RANGE TACTIC D GROUND LOCK MODE, TV SENSOR 1°/SEC AND 5°/SEC ROLL RATES (U)

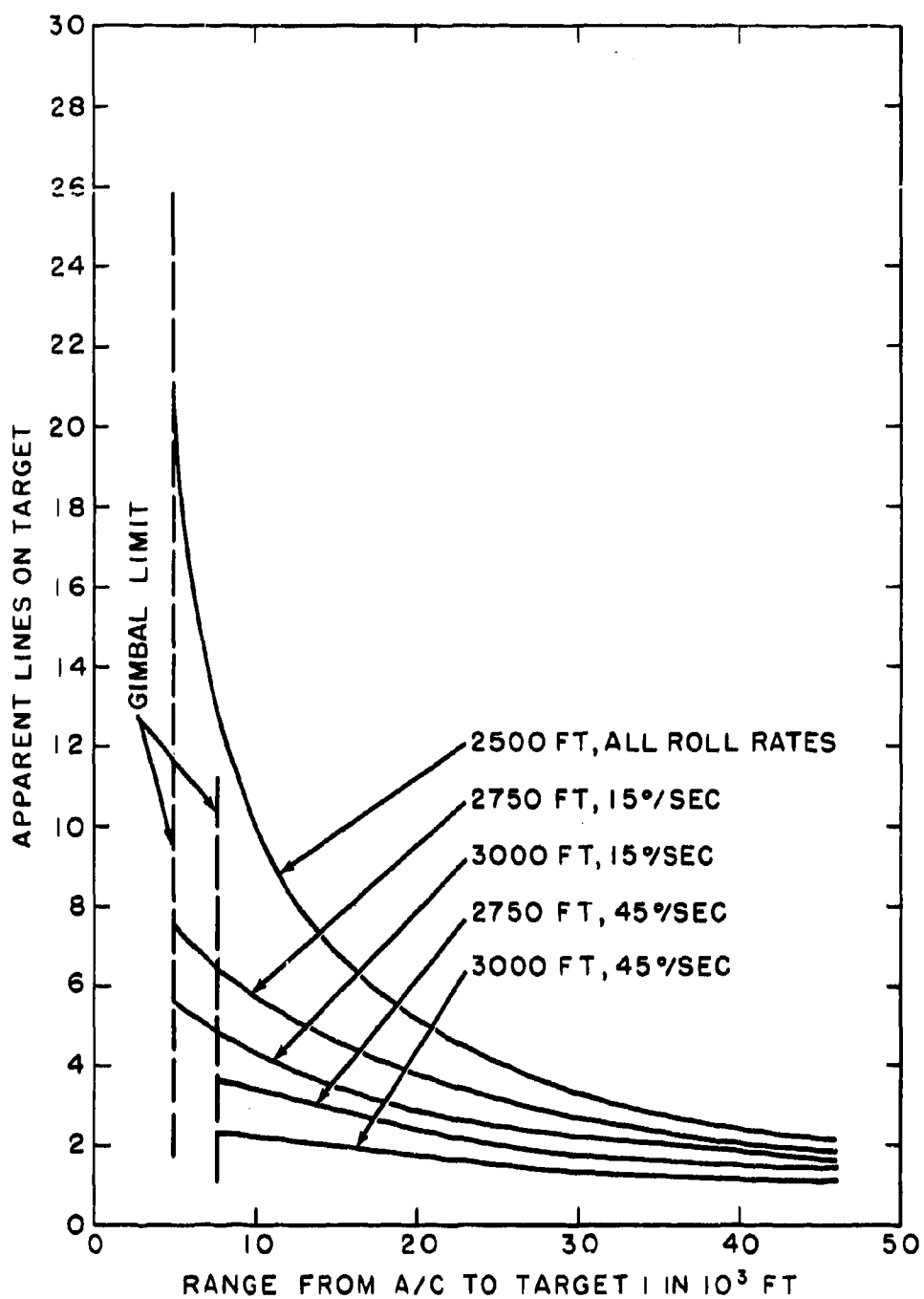


FIGURE 47 - APPARENT LINES ON TARGET AS A FUNCTION OF RANGE TACTIC D GROUND LOCK MODE, TV SENSOR 15°/SEC AND 45°/SEC ROLL RATES (U)

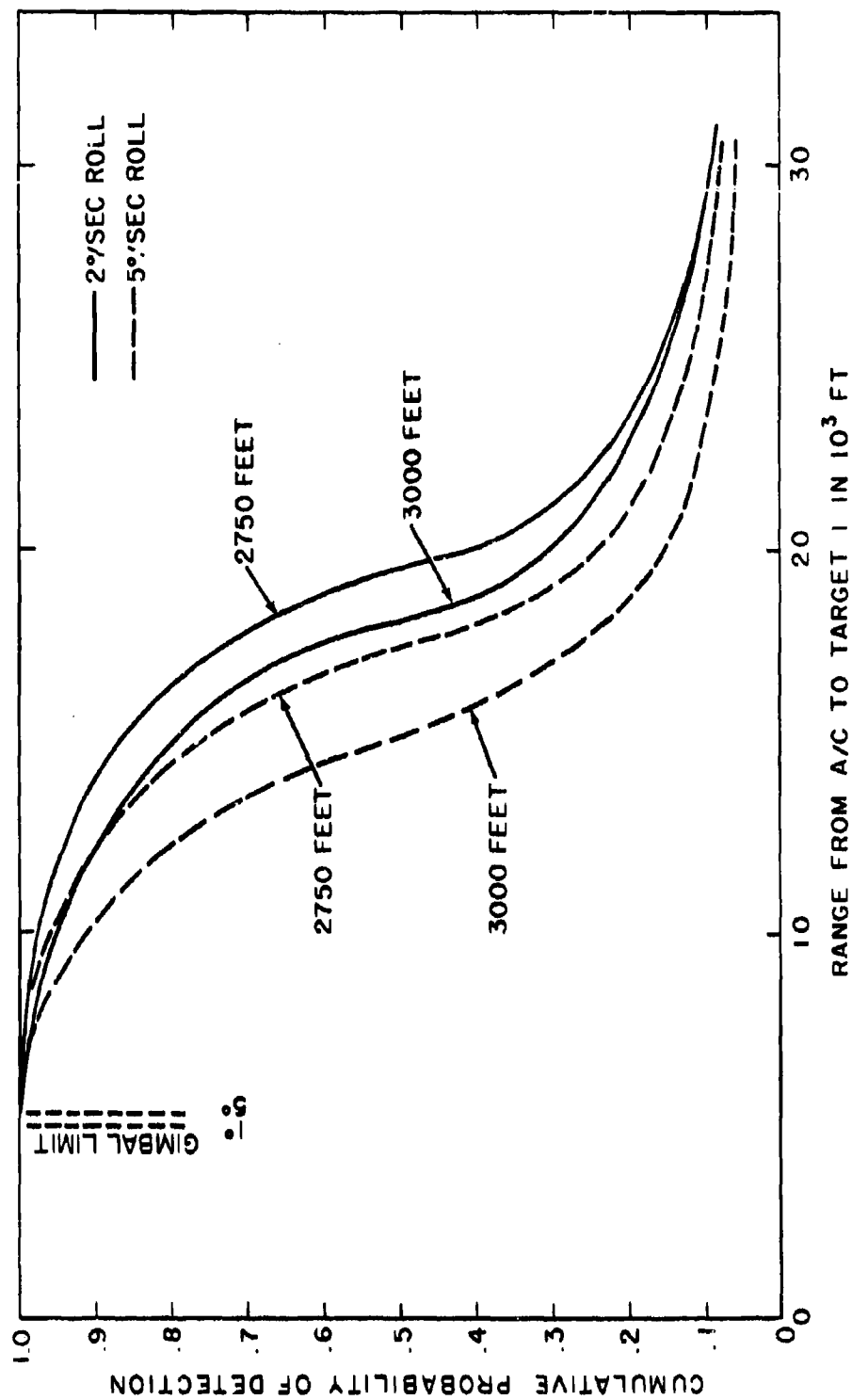


FIGURE 48 - CUMULATIVE PROBABILITY OF DETECTION AS A FUNCTION OF RANGE TACTIC D GROUND LOCK MODE, TV SENSOR $1^\circ/\text{SEC}$ AND $5^\circ/\text{SEC}$ ROLL RATES (U)

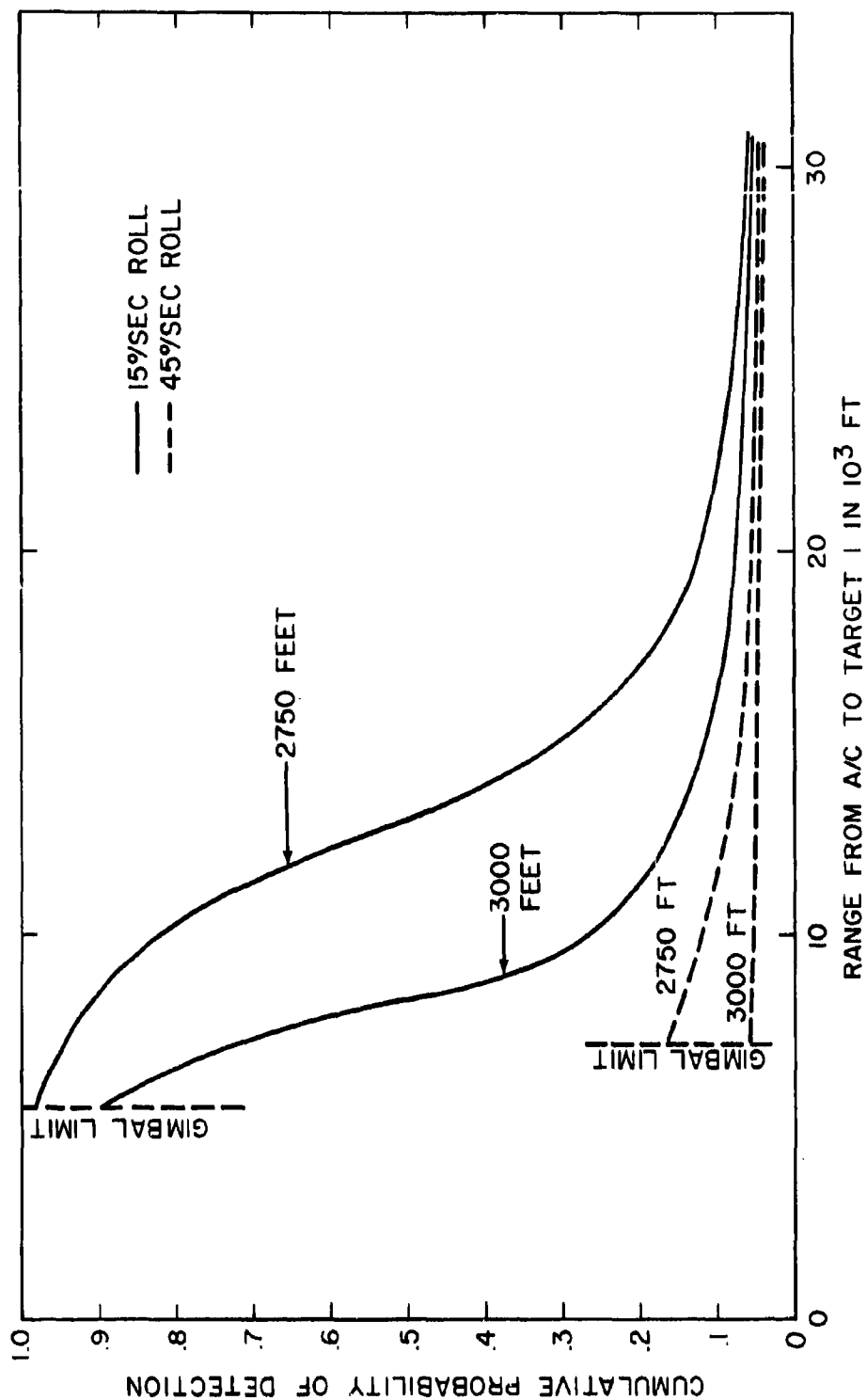


FIGURE 49 - CUMULATIVE PROBABILITY OF DETECTION AS A FUNCTION OF RANGE TACTIC D, GROUND LOCK MODE, TV SENSOR 15°/SEC AND 45°/SEC ROLL RATES (U)

SECRET

a target centered in its field of view. The only resolution degradation of this target due to the rolling of the aircraft would appear about the edges of the target. This degradation was found to be small, and was neglected.

(U) Target detection ranges, R_{DET} , and target acquisition ranges, R_{ACQ} , were determined from Figs. 28, 35, 36, 41, 48 and 49 for Tactics A, B, C and D respectively and listed in Table 2. Detection was assumed to occur at a cumulative probability of 0.5, and acquisition was assumed to occur at cumulative probability of 0.95.

(U) The resolution degradation due to motion was also investigated for the FLIR. Since the FLIR is not an integrating system, it was believed that the resolution degradation would be negligible. In fact, the only integrating portion of the system is the eye. An extreme tactic was investigated for the FLIR to verify that the resolution degradation is small.

(U) Similar calculations were performed for the FLIR as were performed for the LLLTV. The results of these calculations for an aircraft executing the maneuvers of Tactic D appear in Figs. 50-53.

7.0 CONCLUSIONS

1) (U) It is observed, from Table 2, that the targets in Tactics C and D, which have large offsets from the flight path generally have larger detection ranges than the targets in Tactics A and B, which are along the flight path.

(As the aircraft approaches the target in Tactics C and D, high angular line of sight rates tend to degrade the image resolution faster than in Tactics A and B. Therefore, this increased resolution degradation tends

TABLE 2

Target Detection and Acquisition Ranges for Tactics A and B (U)

| Tactic A (Simulates Roll Stabilized) | AO (Ft) | $\dot{\theta}$ (°/sec) | R _{DET} (Ft) | R _{ACQ} (Ft) | E/O Sensor Locked on this Target E/O Sensor Not Locked on this Target " " " " |
|---|---------|------------------------|-----------------------|-----------------------|---|
| Tactic B (Simulates Not- Roll Stabilized) | 0 | 0 | 19,300 | 12,200 | " |
| | 250 | 0 | 19,250 | 10,600 | " |
| | 500 | 0 | 17,750 | --- | " |
| | 0 | 1 | 19,300 | 12,200 | " |
| | 0 | 5 | 19,300 | 12,200 | " |
| | 0 | 15 | 19,300 | 12,200 | " |
| | 0 | 45 | 19,300 | 12,200 | " |
| | 250 | 1 | 19,250 | 10,600 | " |
| | 250 | 5 | 17,000 | 9,550 | " |
| | 250 | 15 | 12,200 | ----- | " |
| | 250 | 45 | --- | --- | " |
| | 500 | 1 | 17,750 | 7,800 | " |
| | 500 | 5 | 14,300 | 7,500 | " |
| | 500 | 15 | 6,300 | --- | " |
| | 500 | 45 | --- | --- | " |
| | 500 | | | | " |

AO = Target Offset Distance from Aircraft Flight Path

 $\dot{\theta}$ = Aircraft Roll Rate in Degrees/SecR_{DET} = Slant Range from Aircraft to Target at Point of DetectionR_{ACQ} = Slant Range from Aircraft to Target at Point of Acquisition

TABLE 2 (Cont'd)

Target Detection and Acquisition Ranges for Tactics C and D (U)

| Tactic C (Simulates Roll Stabilized) | AO (Ft) | $\dot{\theta}$ ($^{\circ}$ /sec) | R _{DET} (Ft) | R _{ACQ} (Ft) | E/O Sensor Locked on this Target E/O Sensor Not Locked on this Target " " " " " " |
|--|---------|-----------------------------------|-----------------------|-----------------------|---|
| Tactic D (Simulates Not Roll Stabilized) | 2500 | 0 | 19,750 | 12,750 | " " " " " " |
| | 2750 | 0 | 19,700 | 11,700 | " " " " " " |
| | 3000 | 0 | 18,250 | 10,000 | " " " " " " |
| | 2500 | 1 | 19,750 | 12,750 | " " " " " " |
| | 2500 | 5 | 19,750 | 12,750 | " " " " " " |
| | 2500 | 15 | 19,750 | 12,750 | " " " " " " |
| | 2500 | 45 | 19,750 | 12,750 | " " " " " " |
| | 2570 | 1 | 19,700 | 11,700 | " " " " " " |
| | 2570 | 5 | 17,500 | 10,300 | " " " " " " |
| | 2570 | 15 | 13,000 | 6,800 | " " " " " " |
| | 2570 | 45 | --- | --- | " " " " " " |
| | 3000 | 1 | 18,250 | 10,000 | " " " " " " |
| | 3000 | 5 | 15,200 | 8,500 | " " " " " " |
| | 3000 | 15 | 8,400 | --- | " " " " " " |
| | 3000 | 45 | --- | --- | " " " " " " |

AO = Target Offset Distance from Aircraft Flight Path

 $\dot{\theta}$ = Aircraft Roll Rate in Degrees/SecR_{DET} = Slant Range from Aircraft to Target at Point of DetectionR_{ACQ} = Slant Range from Aircraft to Target at Point of Acquisition

SECRET

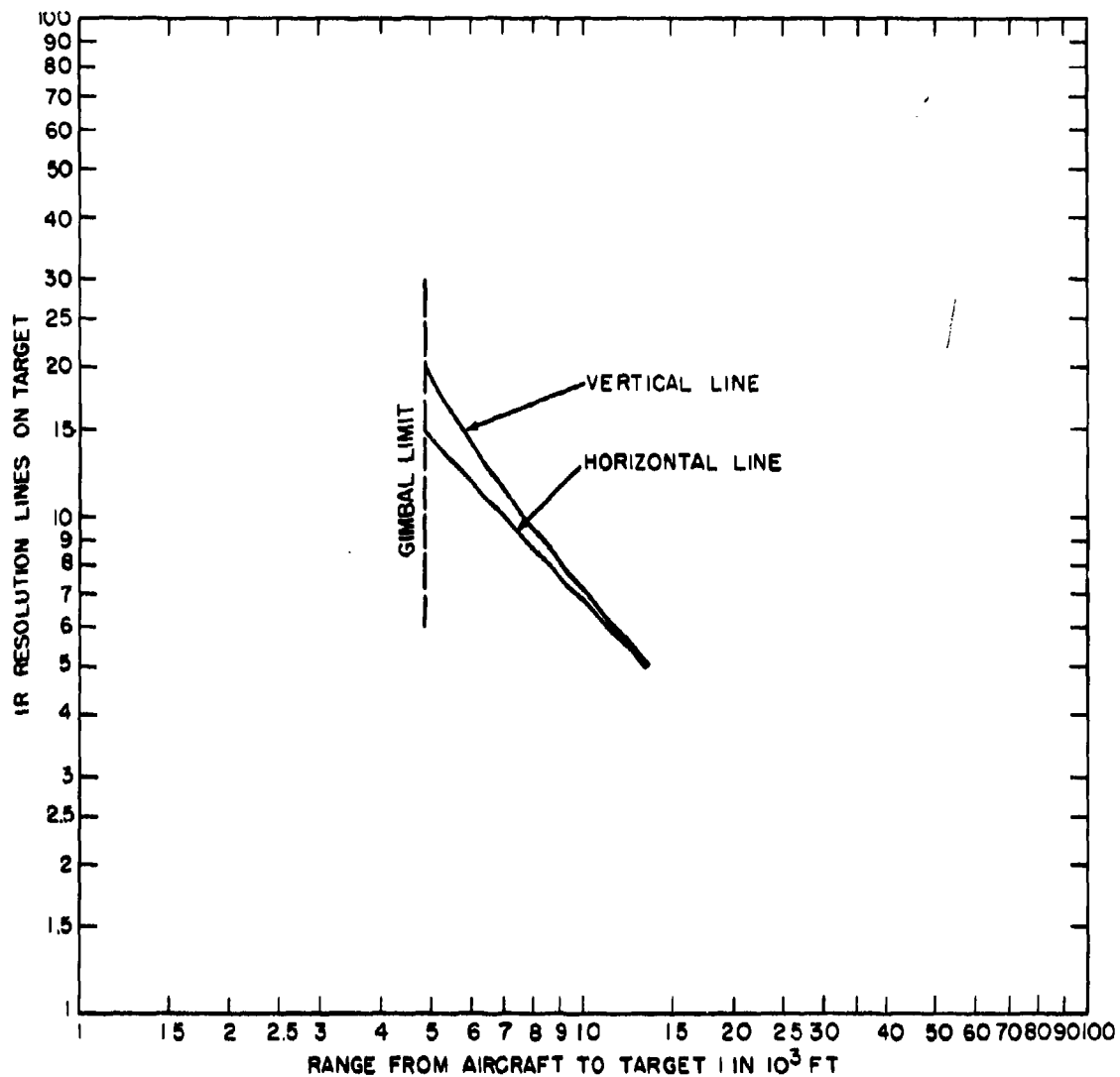


FIGURE 50 - RESOLUTION LINES ON TARGET AS A FUNCTION OF RANGE
TACTIC C & D GROUND LOCK MODE, FLIR SENSOR
TARGET OFFSET 2500, 2750, AND 3000 FEET (U)

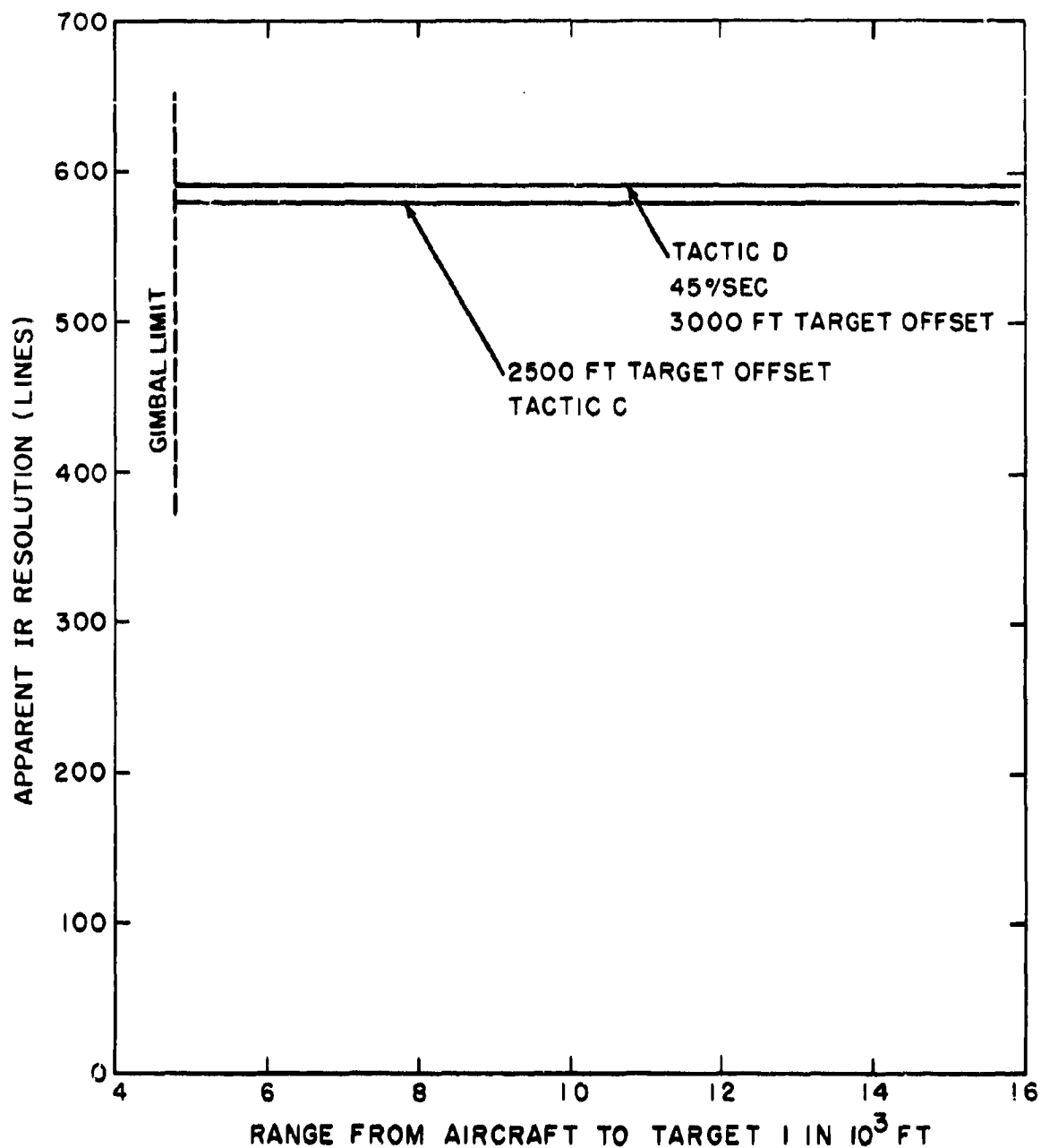


FIGURE 51 - APPARENT IR RESOLUTION AS A FUNCTION OF RANGE
TACTIC C & D GROUND LOCK MODE
FLIR SENSOR TARGET OFFSET 2500, 2750, AND
3000 FEET (U)

SECRET

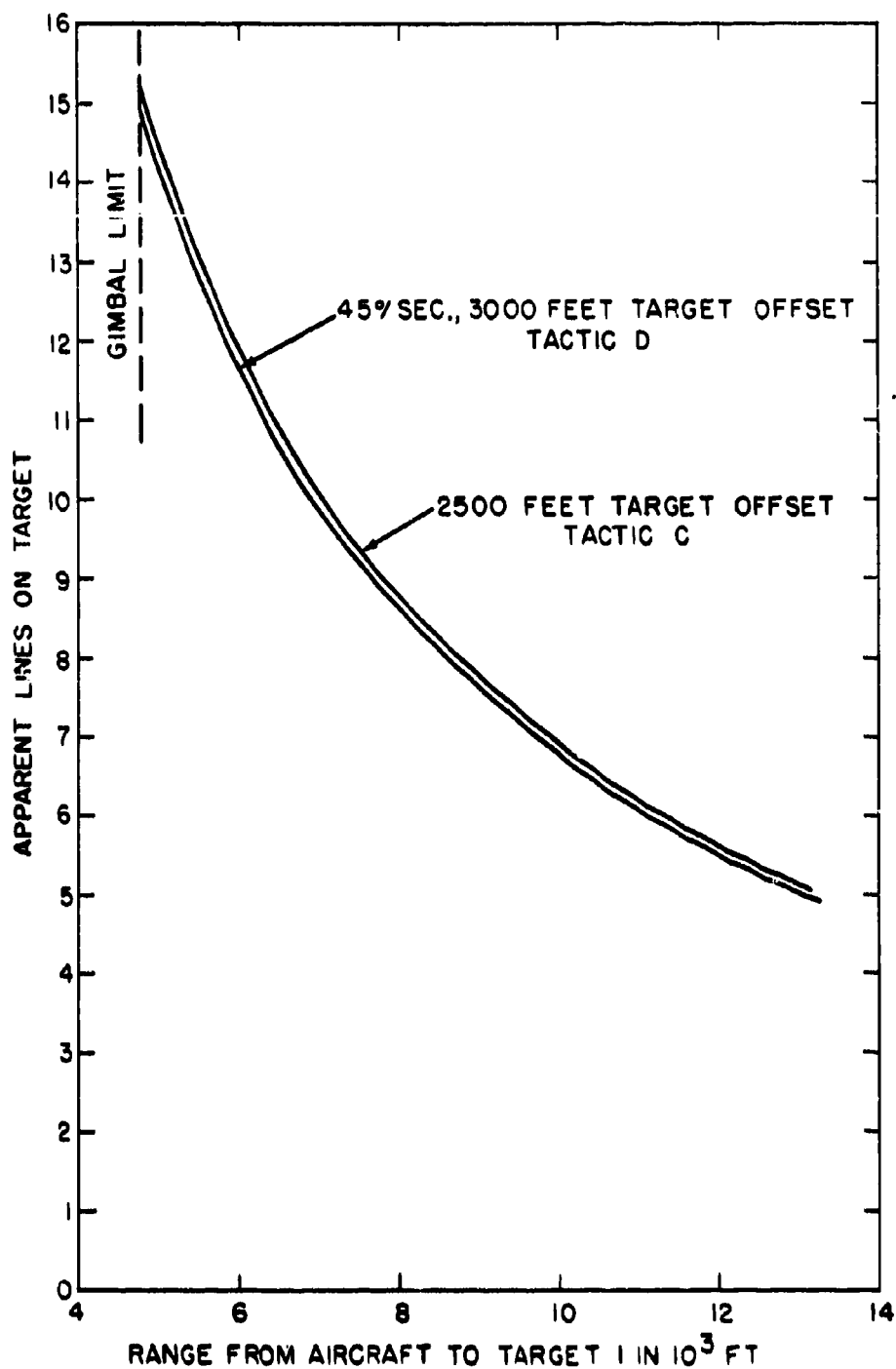


FIGURE 52 - APPARENT LINES ON TARGET AS A FUNCTION OF RANGE TACTIC C AND D GROUND LOCK MODE, FLIR SENSOR (U)

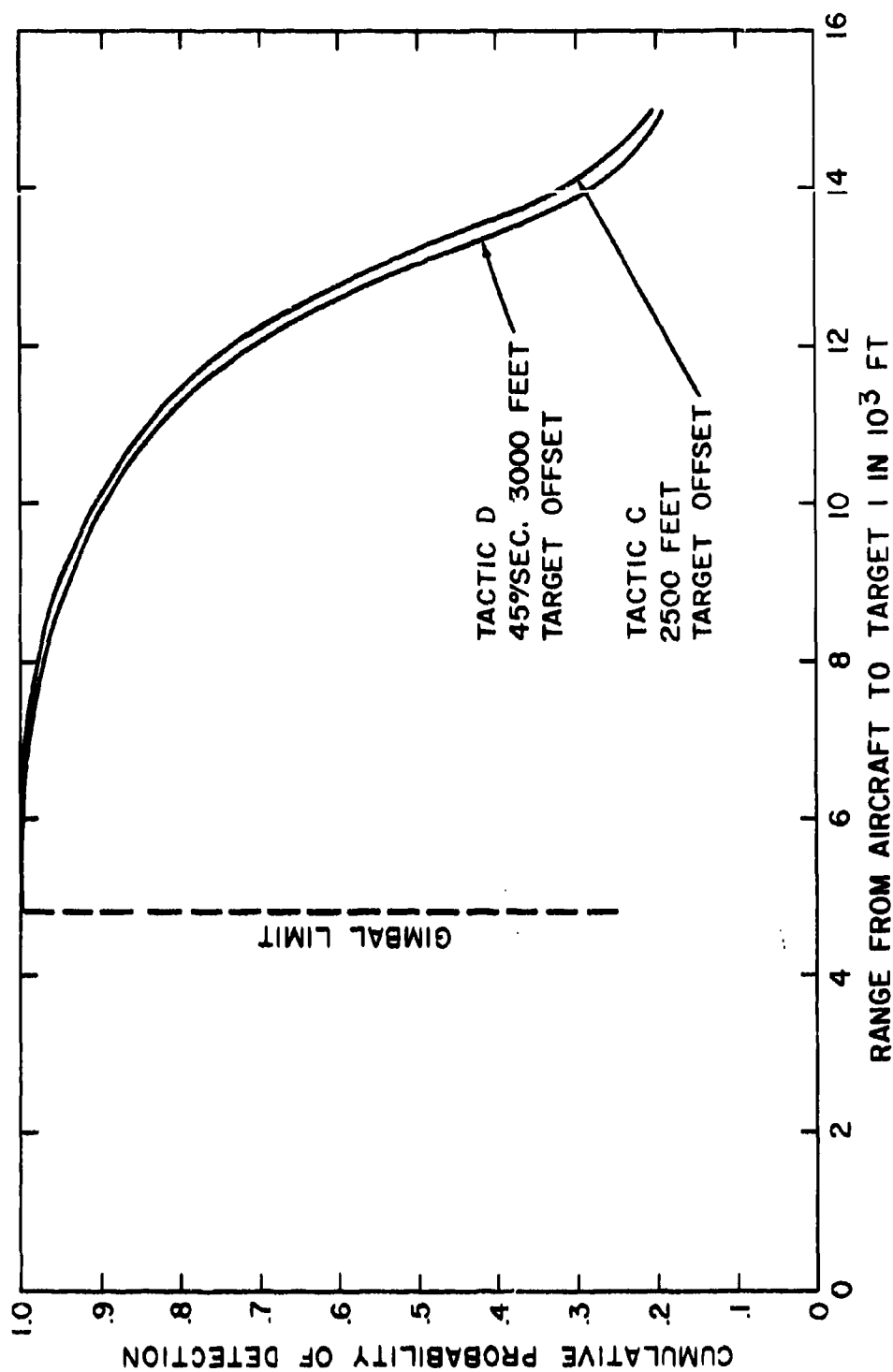


FIGURE 53 - CUMULATIVE PROBABILITY OF DETECTION AS A FUNCTION OF RANGE GROUND LOCK MODE, FLIR SENSOR (U)

to nullify the advantage of increased image size which occurs at larger target offsets.)

2) (U) Detection and acquisition ranges for the targets locked in the center of the electro-optical sensor's field of view are the same for the roll-stabilized and the unstabilized cases.

(The only resolution degradation due to aircraft roll in the unstabilized case is about the edge of the target. This degradation was found to be small and subsequently neglected.)

3) (S) Targets offset from the ground lock point are extremely sensitive to aircraft roll.

(Moderate roll rates up to $5^{\circ}/\text{sec}$ are generally acceptable depending on the type of air to ground weapons used. However, the more excessive rate of 15 to $45^{\circ}/\text{sec}$ tend to make target detection and acquisition extremely difficult if not impossible.)

4) (U) The resolution degradation due to image motion is negligible for the FLIR. This is shown in Fig. 53 which is a plot of cumulative probability of detection versus range. A roll-stabilized case of Tactic C is compared with a $45^{\circ}/\text{sec}$ roll rate in the non roll-stabilized Tactic D.

(S) Some caution should be exercised in interpreting the data given here. The extreme case of resolution degradation due to roll was investigated in this analysis, since in order to simplify the calculations, it was assumed that the friendly aircraft rolled continuously during the target detection and acquisition phases of its mission. It was also assumed that the targets initially offset from the ground

SECRET

lock point would remain there. In reality, the E/N has the ability to update the system, and he will continually attempt to keep the target close to the center of the sensor's field of view.

8.0 ACKNOWLEDGEMENTS (U)

The author wishes to acknowledge the help of Mr. T. Spink and Mr. L. Kuchinski in the preparation of this report.

SECRET

9.0 REFERENCES (U)

- (1) Trott, Timothy, "The Effects of Motion on Resolution,"
Photogrammetric Engineering, December 1960.
- (2) Spink, T. E., "Motion Picture Reporting Jiggle Study Results",
Westinghouse Electric Corporation, August 10, 1966.
- (3) Donelon, E. J., "The Effects of Image Motion on System Resolution,"
SATM #547, G. O. 53399, December 1965.
- (4) Coltman, J. "The Specifications of Image Properties by Response to
a Sine Wave," Journal of the Optical Society of America, Vol. 44, No. 6,
June 1954.
- (5) Fox, Roy H., RCA, Butlington, Massachusetts.
- (6) Project Blackspot Test Data.

SECRET

Distribution List: (U)

| | |
|---------------------|--|
| Lt. John Glaser | NASC, Washington, D. C. |
| Mr. Don Armbruster | NASC, Washington, D. C. |
| Lt. Tom Furness | Wright Patterson Air Force Base, Ohio |
| Dr. Harry Schnieder | Boeing, Seattle, Washington |
| Mr. R. D. Thompson | NAVAIRTEST CENTER, Patuxent River, Maryland |
| Mr. T. Spink | Westinghouse Aerospace Division, Friendship, Md. |

Best Available Copy

SECRET

Security Classification

DOCUMENT CONTROL DATA - R & D

(Security classification of title, body of abstract and indexing annotation must be entered when the overall report is classified)

| | | | |
|---|--|--|-----------------------------|
| 1. ORIGINATING ACTIVITY (Corporate author) Naval Research Laboratory Washington, D.C. 20390 | | 2a. REPORT SECURITY CLASSIFICATION SECRET | |
| | | 2b. GROUP 3 | |
| 3. REPORT TITLE EFFECTS OF AIRCRAFT ROLL ON TARGET ACQUISITION USING ELECTRO-OPTICAL SENSORS (U) | | | |
| 4. DESCRIPTIVE NOTES (Type of report and inclusive dates) A final report on one phase of a continuing problem. | | | |
| 5. AUTHOR(S) (First name, middle initial, last name) John A. Pavcc | | | |
| 6. REPORT DATE June 1970 | | 7a. TOTAL NO. OF PAGES 90 | 7b. NO. OF REFS 4 |
| 8a. CONTRACT OR GRANT NO. NRL Problem D01-03.318 | | 9a. ORIGINATOR'S REPORT NUMBER(S) NRL Memorandum Report 2139 | |
| b. PROJECT NO. A 05-510-151/652-1/W11-63-000 | | 9b. OTHER REPORT NO(S) (Any other numbers that may be assigned this report) | |
| c. | | | |
| d. | | | |
| 10. DISTRIBUTION STATEMENT In addition to security requirements which apply to this document and must be met, each transmittal outside the Department of Defense must have prior approval of Director, Naval Research Laboratory, Washington, D.C. 20390. | | | |
| 11. SUPPLEMENTARY NOTES | | 12. SPONSORING MILITARY ACTIVITY Naval Air Systems Command Department of the Navy Washington, D.C. 20360 | |

13. ABSTRACT

(SECRET)

The effects of aircraft roll on ground locked electro-optical sensors has been investigated with emphasis on the detection and acquisition phases of the mission. It was found that roll rates up to 5°/sec were generally acceptable.

Best Available Copy

Security Classification

14.

KEY WORDS

LINK A

LINK B

LINK C

[illegible]

WT

[illegible]

WT

ROLE

WT

TRIM

Best Available Copy

**Naval Research Laboratory
Technical Library
Research Reports Section**

DATE: August 22, 2002
FROM: Mary Templeman, Code 5227
TO: Code 5300 Paul Hughes
CC: Tina Smallwood, Code 1221.1 *to 8/19/03*
SUBJ: Review of NRL Reports

Dear Sir/Madam:

Please review NRL Memo Reports 2139, 2150, 2170, 2297, 2360, 2425, 2426 and 2429 for:

- ☒ Possible Distribution Statement
- ☒ Possible Change in Classification

Thank you,

Mary Templeman
Mary Templeman
(202)767-3425
maryt@library.nrl.navy.mil

The subject report can be:

- ☒ Changed to Distribution A (Unlimited)
- ☒ Changed to Classification _____
- ☐ Other:

Paul K. Hughes IV 8/18/2003
Signature Date

-- 1 OF 1
-- 1 - AD NUMBER: 510384
-- 2 - FIELDS AND GROUPS: 15/6, 17/5, 25/3
-- 3 - ENTRY CLASSIFICATION: UNCLASSIFIED
-- 5 - CORPORATE AUTHOR: NAVAL RESEARCH LAB WASHINGTON D C
-- 6 - UNCLASSIFIED TITLE: EFFECTS OF AIRCRAFT ROLL ON TARGET
-- ACQUISITION USING ELECTRO-OPTICAL SENSORS.
-- 8 - TITLE CLASSIFICATION: UNCLASSIFIED
-- 9 - DESCRIPTIVE NOTE: FINAL REPT.,
--10 - PERSONAL AUTHORS: PAVCO,JOHN A. ;
--11 - REPORT DATE: JUN 1970
--12 - PAGINATION: 89P MEDIA COST: \$ 7.00 PRICE CODE: AA
--14 - REPORT NUMBER: NRL-MR-2139
--16 - PROJECT NUMBER: A05-510-151/652-1/W11-63-000, NRL-53D01-03.318
--20 - REPORT CLASSIFICATION: CONFIDENTIAL
--22 - LIMITATIONS (ALPHA): DISTRIBUTION: DOD ONLY: OTHERS TO DIRECTOR,
-- NAVAL RESEARCH LAB., WASHINGTON, DC 20375.
--23 - DESCRIPTORS: (*TARGET ACQUISITION, *ELECTROOPTICS), ROLL,
-- ROTATION, DETECTORS, SIMULATION
--24 - DESCRIPTOR CLASSIFICATION: UNCLASSIFIED
--29 - INITIAL INVENTORY: 20
--32 - REGRADE CATEGORY: C
--33 - LIMITATION CODES: 4

-
--34 - SOURCE SERIES: F
--35 - SOURCE CODE: 251950
--36 - ITEM LOCATION: DTIC
--38 - DECLASSIFICATION DATE: OADR
--40 - GEOPOLITICAL CODE: 1100
--41 - TYPE CODE: N
--43 - IAC DOCUMENT TYPE:
--49 - AUTHORITY FOR CHANGE: S TO C GP-3

APPROVED FOR PUBLIC
RELEASE - DISTRIBUTION
UNLIMITED